

Publication No. 02-023-051

**SEPARATION OF DOLOMITE FROM THE
SOUTH FLORIDA PHOSPHATE ROCK—VOL 2**



Prepared by

University of Florida

Department of Materials Science and Engineering

under a grant sponsored by the

Florida Institute of Phosphate Research

Bartow, Florida

February, 1987

FLORIDA INSTITUTE OF PHOSPHATE RESEARCH



SEPARATION OF DOLOMITE FROM THE SOUTH FLORIDA PHOSPHATE ROCK

VOLUME II

Research Project FIPR #82-02-023

Final Report- February 1986

Prepared by

Principal Investigator

Dr. Brij M Mudgil

Co-Investigators

Dr. Frank N. Blanchard

Dr. Dinesh O. Shah

Dr. George Y. Onoda

Dr. E. Dow Whitney

Submitted to

Center for Research in Mining and Mineral Resources

Department of Materials Science and Engineering

University of Florida

Gainesville, Florida 32611

Florida Institute of Phosphate Research

Bartow, Florida

DISCLAIMER

The contents of this report are reproduced herein as received from the contractor.

The opinions, findings and conclusions expressed herein are not necessarily those of the Florida Institute of Phosphate Research, nor does mention of company names or products constitute endorsement by the Florida Institute of Phosphate Research.

ACKNOWLEDGEMENTS

The authors wish to thank Dr. J. L. Lawver, formerly Technical Director at International Minerals and Chemical Corp., Mr. Bernard L. Mirowchick and Mr. Robert E. Snow, also of IMC, Dr. Steven W Clark of Brewster Phosphates, and the late Mr. Ralph B. Hall of Gardinier, Inc., for helpful discussions. The following organizations are acknowledged for providing materials and chemicals, and other assistance during the course of this investigation.

Agrico Chemical Co.

Amax Chemical Corp.

American Cyanamid Co.

Brewster Phosphates

Carpco, Inc.

Estech General Chemical Corp.

Freeport Minerals

Gardinier, Inc.

International Minerals & Chemical Corp.

Mobil Chemical Co.

W R. Grace & Co.

Westvaco

Financial support of this work by the Florida Institute of Phosphate Research (Contract #82-02-023) and the EIES-College of Engineering (COE Funds) University of Florida, is also acknowledged.

Any opinions, findings, and conclusions or recommendations expressed in this report are those of the authors and do not necessarily reflect the views of the Florida Institute of Phosphate Research.

TABLE OF CONTENTS

	<u>Page</u>
List of Figures.....	i
List of Tables.....	xi
Conclusions.....	xvii

VOLUME II

Chapter VI. Apatite-Dolomite Flotation with Fatty Acid after Conventional Conditioning

Experimental.....	240
Materials.....	240
Mineral Preparation.....	240
Mineral Characterization.....	241
Methods.....	244
Flotation and Oleate Adsorption Experiments.....	244
Electrokinetic Measurements.....	245
Chemical Analyses.....	246
Transmission IR Spectroscopy.....	246
Results and Discussion.....	247
Conventional Conditioning.....	247
Flotation Studies.....	247
Oleate Adsorption Results.....	254
Loss of Selectivity in the Alkaline pH Range.....	254
Summary.....	274

TABLE OF CONTENTS (Cont'd)

Chapter VII. The Two Stage Conditioning Process

Introduction.....	275
Basic Studies.....	275
Results and Discussion.....	279
Flotation After Reconditioning Without Changing Collector Concentration.....	279
Flotation After Reconditioning With Reduced Collector Concentration.....	285
Mechanism of Selective Flotation by Two-Stage Conditioning.....	285
Relevance of Two-Stage Conditioning Process to Current Processing Schemes.....	297
Bench Scale Flotation Tests.....	300
Materials.....	301
Apatite.....	301
Dolomite.....	301
Chemicals.....	303
Methods.....	303
Chemical Analysis.....	303
Flotation.....	303
Results and Discussion.....	305
Single Minerals.....	305
Agrico Dolomite-Agrico Apatite Mixture.....	312
Amax Apatite and New Jersey Dolomite Mixture.....	318
Agrico Apatite and IMC Four Corners Dolomite Mixture.....	318
Agrico Apatite-Perry Dolomite Mixture.....	323
Summary.....	337

TABLE OF CONTENTS (Cont'd)

Chapter VIII. Selective Flocculation

Introduction.....338

Experimental.....339

 Materials.....339

 Minerals.....339

 Polymers.....340

 Methods.....340

 Flocculation.....340

 Separation of Floccs.....341

 Analysis of Floccs and Fines.....341

 Polymer Adsorption.....341

Results and Discussion.....342

 Single Mineral Flocculation.....342

 Mixed Mineral Flocculation Studies.....342

 Reasons for Poor Recoveries.....345

Summary.....346

References.....349

VOLUME I

Chapter I. Introduction.....1

Chapter II. Materials and Methods

 Introduction.....4

 Experimental.....4

TABLE OF CONTENTS (Cont'd)

Sample Preparation.....	4
P ₂ O ₅ Analysis.....	4
Materials.....	4
Apparatus.....	4
Reagents.....	10
Methods.....	10
Insols Analysis.....	11
Procedure.....	11
Ca, Mg, Fe and Al Analysis.....	11
Chapter III. <u>Mineralogical Studies</u>	
Introduction.....	3
Qualitative X-ray Diffraction Analysis.....	16
General Statements and Methods.....	16
Results.....	18
Magnesium as a Substituent in Carbonate Fluorapatite.....	21
General Statements.....	21
Quantitative XRD.....	22
Calculated Calibration Curves.....	23
Selection of Instrumental Conditions.....	23
Preparation of Standards.....	24
Measurement of Standards.....	26
Intensity Correction Factor.....	26
Calibration Curve and Equation.....	31

TABLE OF CONTENTS (Cont'd)

Results and Interpretations for Quantitative XRD.....	34
Infrared Absorption Analysis.....	49
Introduction.....	49
Results.....	53
Calculated X-ray Powder Diffraction Patterns.....	59
Introduction.....	59
Methods.....	59
Results.....	60
X-ray Diffraction, Polarizing Microscope and Scanning Electron Microscope Studies of the Color Fractions Comprising the Phosphorite Samples.....	63
General Statements and Methods.....	63
X-ray Diffraction Studies.....	65
Polarizing Microscope Studies.....	65
Scanning Electron Microscope Studies.....	66
Results.....	68
Description of Grains in the K-29 Fraction.....	69
Weight Percent of Color Fractions in Each Sample.....	72
X-ray Diffraction Studies.....	72
Polarizing Microscope Studies.....	77
Scanning Electron Microscope and X-ray Spectrometer Studies.....	104
Studies of Samples K-1, K-18 and K-5.....	104
Studies of Sample K-2.....	120
Polarizing Microscope, Scanning Electron Microscope and X-ray Spectrometer Studies of Agrico Dolomitic Matrix.....	127
General Statements and Methods.....	127

TABLE OF CONTENTS (Cont'd)

Results.....	129
Studies of Size Fractions of Phosphorite Samples.....	150
General Statements and Methods.....	150
Studies of Larger Size Fractions.....	150
Studies of Smaller Size Fractions.....	151
Results.....	152
Studies of Larger Size Fractions.....	152
Studies of Smaller Size Fractions.....	162
Dolomite Studies.....	166
General Statements and Materials.....	166
Comparison of Gross Characterisitcs of IMC Dolomite, Agrico Bottom 8's Dolomite and Agrico Dolomitic Matrix....	166
Comparison of Grain Slides of Agrico Bottom 8's Dolomite, IMC Dolomite, IMC 4-Corners Dolomite and Agrico Dolomitic Matrix.....	167
Studies of Interlocked Grains of Agrico Dolomite Matrix in Feed Float and Fractions.....	168
Studies Using the -65x150 Mesh Size Fraction.....	168
Studies Using the -35x150 Mesh Size Fraction.....	170
X-ray Diffraction Studies of Eight Dolomite Samples.....	170
Dolomite Grinding Tests.....	172
Results.....	172
Comparison of Grain Slides of Agrico Bottom 8's Dolomite, IMC Dolomite, IMC 4-Corners Dolomite and Agrico Dolomitic Matrix.....	176
Studies of Interlocked Grains of Agrico Dolomitic Matrix in Feed, Float and Sink Fractions.....	177
Studies Using the -65x150 Mesh Size Fraction.....	177
Studies Using the -35x150 Mesh Size Fraction.....	182

TABLE OF CONTENTS (Cont'd)

X-ray Diffraction Studies of Eight Dolomite Samples.....182

Dolomite Grinding Tests.....194

 X-ray Diffraction Studies.....194

 Scanning Electron Microscope Studies.....197

X-ray Diffraction, Scanning Electron Microscope and X-ray
Spectrometer Studies of Agrico High-Grade Apatite.....206

 General Statements and Methods.....206

 Results.....207

Summary and Conclusions.....212

 Qualitative X-ray Diffraction Analysis.....212

 Quantitative X-ray Diffraction Analysis.....212

 Other Approaches to Estimating Mg-Substitution
 in Apatite.....213

 X-ray Diffraction, Polarizing Microscope and
 Scanning Electron Microscope Studies of the Color
 Fraction Comprising the Phosphorite Samples.....213

 Polarizing Microscope, Scanning Electron
 Microscope and X-ray Spectrometer Studies of
 Agrico Dolomitic Matrix.....214

 Studies of the Size Fractions of Phosphorite Samples.....215

 Dolomite Studies.....216

 X-ray Diffraction, Scanning Electron Microscope
 and X-ray Spectrometer Studies of Agrico High-Grade
 Apatite.....217

Chapter IV. Aging Studies

 Experimental.....218

 Results and Discussion.....218

 Aging at Natural pH.....218

TABLE OF CONTENTS (Cont'd)

Effect of Ionic Strength.....	221
Aging at Acidic pH.....	221
Aging at Alkaline pH.....	224
Effect of Particle Size and Pulp Density.....	224
Summary.....	224
Chapter V. <u>Flotation Kinetics of Apatite and Dolomite</u>	
Experimental.....	231
Materials.....	231
Flotation Procedure.....	231
Results and Discussion.....	233
Summary.....	239

LIST OF FIGURES

<u>Figure No.</u>	<u>Description</u>	<u>Page</u>
<u>Chapter III. Mineralogical Studies</u>		
1	Diffractogram of sample B-1 showing most intense peaks for quartz (Q), apatite (A), feldspar (F), crandallite (C), dolomite (D), and wavellite (W).	17
2	Comparison of dolomite (104) peaks of SRM 88a and Steinhatchee dolomite in an X-ray diffractogram.	30
3	Negative intensity measurements.	32
4	Plot of chemically determined MgO against MgO contributed by dolomite (determined by quantitative XRD) for 18 samples of phosphorite. Error bars represent a 1:1 ratio. The fact that all the points lie to the right of the line indicates that there is more MgO than can be accounted for by dolomite contained in the phosphorite. Most of this excess (an average of 0.57%) believed to represent Mg substituting in the apatite structure.	46
5	Infrared absorption spectrum of Steinhatchee dolomite.	50
6	Infrared absorption spectrum of SRM 120b.	51
7	Infrared absorption spectrum of a mixture of SRM 120b and Steinhatchee dolomite (30:1 by weight).	52
8	Infrared absorption calibration curve.	54
9	Calculated X-ray diffractogram of fluorapatite.	55
10	Half-ground grains of the K-29 black color fraction showing the internal appearances of the phosphate grains. 1 cm = 0.23 mm.	56
11	Half-ground grains of the K-29 color fraction. The numbered grains are described in the text. 1 cm = 0.23 mm.	70
12	Grain of pure dolomite (left) and pure apatite (right) shown in plane light (a) and between crossed polars (b). 1 cm = 0.065 mm.	84
13	Grain of apatite containing a moderate amount of dolomite, shown in plane light (a) and between crossed polars (b). Arrow indicates grain. 1 cm = 0.065 mm.	85

<u>Figure No.</u>	<u>Description</u>	<u>Page</u>
14	Grain of apatite containing a large amount of dolomite, shown in plane light (a) and between crossed polars (b). Arrow indicates grain. 1 cm = 0.065 mm.	86
15	Grain with apatite rim, but with interior almost entirely dolomite (left arrow) and grain of apatite containing a small amount of dolomite and a quartz inclusion (right arrow). Shown in plane light (a) and between crossed polars (b). 1 cm = 0.065 mm.	87
16	Two apatite grains from the green color fraction of the K-2 sample. Bottom grain is surrounded by a dolomite rim. Shown in plane light (a) and between crossed polars (b). 1 cm = 0.25 mm.	88
17	Two apatite grains from the white color fraction of the K-2 sample. The top grain has a thin dolomite rim and the bottom grain has a thick dolomite rim. Shown in plane light (a) and between crossed polars (b). 1 cm = 0.25 mm.	89
18	Apatite grain from the gray color fraction of the K-2 sample. Grain shown a dolomite rim (ground away on upper portion) and an interior composed of pseudomorphs of apatite after dolomite. Shown in plane light (a) and between crossed polars (b). 1 cm = 0.065 mm.	90
19	X-ray emission spectra obtained by collecting X-rays from the entire exposed surfaces of K-1 white (a), brown (b) and black (c) grains.	105
20	X-ray emission spectra obtained by collecting X-rays from the entire exposed surfaces of K-18 white (a), gray (b) and black (c) grains.	106
21	X-ray emission spectra obtained by collecting X-rays from the entire exposed surfaces of K-5 white (a), gray (b) and black (c) grains.	107
22	(a) Diffractogram of the K-1 white fraction. (b) Diffractogram of the K-5 white fraction.	110
23	SEM photograph of K-1 white grain. Areas 1 and 2 are enlarged in Figure 24.	112
24	SEM photographs of K-1 white grain showing enlargements of area 1 (a) and area 2 (b) in Figure 23.	113

<u>Figure No.</u>	<u>Description</u>	<u>Page</u>
25	X-ray emission spectra obtained by collecting X-rays from the area in Figure 24a (area 1 in Figure 23) (a) and the area in Figure 24b (area 2 in Figure 23) (b).	114
26	SEM photograph of K-1 black grain. Area in box is enlarged in Figure 27a.	115
27	(a) SEM photograph of K-1 black grain showing enlargement of area designated by box in Figure 26. Arrows indicate quartz particles. (b) X-ray emission photograph showing the distribution of silicon radiation from the area shown in (a).	116
28	(a) SEM photograph of K-18 white grain. Area in box is enlarged in (b). (b) Area 1 is composed of apatite. Particle 2 is composed of calcite.	118
29	X-ray emission spectra obtained by collecting X-rays from area 1 (a) and area 2 (b) in Figure 21b.	119
30	(a) SEM photograph of a section of a K-2 gray grain. Black dots indicate dolomite particles. (b) X-ray emission spectrum obtained by collecting X-rays from particle 1 in (a).	121
31	SEM photograph of K-2 grain washed in dilute HCl. Area in box A is enlarged in Figure 32.	123
32	(a) SEM photograph of K-2 grain showing enlargement of area designated by box A in Figure 31. Area in box B is enlarged in (b).	124
33	(a) X-ray emission spectrum obtained by collecting X-rays from the area in Figure 32a (area in box A in Figure 31). (b) X-ray emission spectrum obtained by collecting X-rays from the area in Figure 32b (area in box B in Figure 32a).	125
34	X-ray emission spectra obtained by collecting X-rays from Steinhatchee dolomite (a) and Agrico high grade apatite (b).	126
35	X-ray emission spectra obtained by collecting X-rays from the entire exposed surfaces of K-36 grains composed of pure dolomite (a), apatite containing a large amount of dolomite (b) and apatite containing a moderate amount of dolomite (c).	130

<u>Figure No.</u>	<u>Description</u>	<u>Page</u>
36	X-ray emission spectra obtained by collecting X-rays from the entire exposed surfaces of K-36 grains composed of apatite containing a small amount of dolomite (a) and pure apatite (b).	131
37	K-36 grain containing a small amount of dolomite. Shown in plane light (a) and between crossed polars (b). Areas 1, 2, and 3 and areas indicated by black dots contain dolomite. Area 4 is composed of pure apatite. SEM photograph of this grain is shown in Figure 38. 1 cm = 0.065 mm.	132
38	SEM photograph of K-36 grain containing a small amount of dolomite (see Figure 37). Areas 2 and 3 are composed of dolomite. Area 4 is composed of apatite.	133
39	X-ray emission spectra obtained by collecting X-rays from area 3 (a) and (b) in Figures 37b and 38.	134
40	K-36 grain containing a moderate amount of dolomite. Shown in plane light (a) and between crossed polars (b). Black dots in (b) indicate areas which contain dolomite. SEM photograph of this grain is shown in Figure 41a. 1 cm = 0.09 mm.	135
41	(a) SEM photograph of K-36 grain containing a moderate amount of dolomite (see Figure 40). Area in box A is enlarged in (b). Area in box B is enlarged in Figure 43. (b) Particles 1, 2 and 3 are composed of dolomite. Areas 4 and 5 are composed of apatite.	136
42	X-ray emission spectar obtained by collecting X-rays from area 1 (a) and area 5 (b) in Figure 41b.	137
43	Enlargement of area designated by box B in Figure 41a. Particle 1 is composed of dolomite. Area 2 is composed of apatite.	138
44	X-ray emission spectra obtained by collecting X-rays from particle 1 (a) and area 2 (b) in Figure 43.	139
45	K-36 grain containing a large amount of dolomite. Shown in plane light (a) and between crossed polars (b). Areas of high birefringence in (b) contain dolomite. SEM photograph of this grain is shown in Figure 46. 1 cm = 0.065 mm.	140

<u>Figure No.</u>	<u>Description</u>	<u>Page</u>
46	(a) SEM photograph of K-36 grain containing a large amount of dolomite (see Figure 45). Area in box A is enlarged in (b). (b) Area in box B is enlarged in Figure 47.	141
47	K-6 +35 mesh size fraction (a) and K-6 48 x 65 mesh size fraction (b). Both size fractions contain grains of apatite (1), quartz (2) and dolomite (3). Particles are shown between crossed polars. 1 cm = 0.25 mm.	142
48	IMC dolomite 270 x 352 mesh size fraction. Box 1 designates dolomite rhomb of pure dolomite grain and box 2 designates dolomite rhomb enclosed in apatite grain. Particles are shown between crossed polars. 1 cm = 0.023 mm.	143
49	(a) Agrico Bottom 8's dolomite showing apatite (1), quartz (2) and iron oxide (3) inclusions. Shown in crossed polars. 1 cm = 0.25 mm. (b) Agrico Bottom 8's dolomite showing coarsely crystalline dolomite matrix. Shown in plane light. 1 cm = 0.065 mm.	173
50	(a) IMC dolomite showing finely crystalline dolomite matrix with dark-center rhombs which make up a large percentage of this sample. 1 cm = 0.065 mm. (b) Enlarged view of light center (1) and dark center (2) rhombs of IMC dolomite. 1 cm = 0.023 mm. Both shown in plane light.	175
51	K-36 dolomite 65 x 150 mesh size feed fraction. The feed fraction contains dolomite grains (1), quartz grains (2), and apatite grains containing various amounts of dolomite (3). Shown in plane light (a) and between crossed polars (b). 1 cm = 0.25 mm.	178
52	K-36 dolomite 65 x 150 mesh size float fraction. The float fraction is composed mostly of dolomite grains (1), but also contains a few apatite grains (2). Shown in plane light (a) and between crossed polars (b). 1 cm = 0.25 mm.	179
53	K-36 dolomite 65 x 150 mesh size sink fraction. The sink fraction is composed mostly of apatite grains containing various amounts of dolomite (1), but also contains a few dolomite grains (2) and a few quartz grains (3). Shown in plane light and between crossed polars (b). 1 cm = 0.25 mm.	180

<u>Figure No.</u>	<u>Description</u>	<u>Page</u>
54	K-36 dolomite 35 x 150 mesh size feed fraction. The feed fraction contains dolomite grains (1), quartz grains (2), and apatite grains containing various amounts of dolomite (3). Shown in plane light (a) and between crossed polars (b). 1 cm = 0.25 mm.	183
55	Diffraction diagram of IMC 4-Corners dolomite.	185
56	Diffraction diagram of IMC dolomite.	186
57	Diffraction diagram of Agrico Bottom 8's dolomite.	187
58	Diffraction diagram of Agrico dolomite matrix (sample K-36).	188
59	Diffraction diagram of Florida Rock #89 dolomite.	189
60	Diffraction diagram of Aglime dolomite.	190
61	Diffraction diagram of Pondscreenings dolomite.	191
62	Diffraction diagram of Steinhatchee dolomite.	192
63	Diffraction diagrams of Steinhatchee dolomite ground for 1, 2, 4, and 16 hours.	198
64	Diffraction diagrams of IMC 4-Corners dolomite ground for 1, 2, 4, and 8 hours.	199
65	SEM photographs of Steinhatchee dolomite ground for 1 hour (a) and 2 hours (b).	203
66	SEM photographs of Steinhatchee dolomite ground for 4 hours (a) and 8 hours (b).	204
67	SEM photographs of Steinhatchee dolomite ground for 1 hour (a) and 2 hours (b).	205
68	Diffraction diagram of Agrico high-grade apatite.	208
69	X-ray emission obtained by collecting X-rays from Agrico high-grade apatite.	209
70	SEM photographs of Agrico high-grade apatite (a and b) showing feathery surface texture of grains.	210
71	SEM photographs of Steinhatchee dolomite ground for 4 hours (a) and 8 hours (b).	211

<u>Figure No.</u>	<u>Description</u>	<u>Page</u>
Chapter IV. Aging Studies		
1	Aging behavior under natural pH conditions	220
2	Aging behavior at 35 wt % pulp density, and target pH = 4.0.	223
3	Aging behavior at 35 wt % pulp density, and target pH = 9.0	225
4	Effect of aging on pH of 1 wt % apatite slurry (size fraction 65 x 100 mesh).	226
5	Effect of aging on pH of 1 wt % apatite slurry (size fraction -325 mesh).	227
6	Effect of aging on pH of 1 wt % dolomite slurry (size fraction 65 x 100 mesh).	228
7	Effect of aging on pH of 1 wt % dolomite slurry (mineral size fraction -325 mesh).	229
Chapter V. Flotation Kinetics of Apatite and Dolomite		
1	Plot of $-\ln(1 - x)$ vs t for apatite	237
2	Plot of $-\ln(1 - x)$ vs. t for dolomite.	238
Chapter VI. Apatite-Dolomite Flotation with Fatty Acid After Conventional Conditioning		
1	Flotation of apatite and dolomite as a function of conditioning pH (single and 1:1 apatite:dolomite mixture) using 1.87×10^{-4} kmol/m ³ sodium oleate concentration.	248
2	Flotation of 95:5 apatite:dolomite mixture as a function of conditioning pH using 1.87×10^{-4} kmol/m ³ sodium oleate concentration.	249
3	Flotation of apatite and dolomite as a function of conditioning pH (single, 1:1 and 95:5 apatite:dolomite mixture) using 9.35×10^{-5} kmol/m ³ sodium oleate concentrate.	250
4	Flotation of apatite and dolomite as a function of sodium oleate concentration at pH 10 (single and 1:1 apatite:dolomite mixture).	251

<u>Figure No.</u>	<u>Description</u>	<u>Page</u>
5	Flotation of apatite and dolomite as a function of sodium oleate concentration at pH 10 (single and 95:5 apatite:dolomite mixture).	252
6	Amount of oleate adsorbed on apatite and dolomite as a function of conditioning pH.	255
7	Amount of oleate adsorbed on apatite and dolomite as function of collector concentration at pH 10.	256
8	Correlation between amount floated and oleate adsorbed as a function of conditioning pH for apatite.	257
9	Correlation between amount floated and oleate adsorbed as a function of collector concentration.	258
10	Correlation between amount floated and oleate adsorbed as a function of collector concentration at pH 10 for apatite.	259
11	Correlation between amount floated and oleate adsorbed as a function of collector concentration at pH 10 for dolomite.	260
12	Flotation of apatite as a function of dissolved ion concentration at pH 10.	262
13	Effect of calcium on the zeta potential of apatite.	263
14	Effect of magnesium ions on the zeta potential of apatite.	264
15	Effect of carbonate ions on the zeta potential of apatite.	265
16	Effect of Ca^{+2} ions on the amount of oleate adsorbed on apatite as a function of collector concentration.	269
17	Effect of Mg^{+2} ions on the amount of oleate adsorbed on apatite as a function of collector concentration.	270
18	Zeta potential of apatite as a function of pH.	271
19	Zeta potential of dolomite as a function of pH.	272

Chapter VII. The Two Stage Conditioning Process

1	Effect of pH on the amount of cations dissolved from apatite and dolomite (65 x 100 mesh) 1 wt % slurry.	277
---	--	-----

<u>Figure No.</u>	<u>Description</u>	<u>Page</u>
2	Flotation of apatite and dolomite after reconditioning at pH 4.2 as a function of initial collector concentration.	280
3	Flotation of apatite and dolomite as a function of reconditioning pH using 1.87×10^{-4} kmol/m ³ sodium oleate concentration.	281
4	Flotation of 95:5 apatite:dolomite mixture as a function of reconditioning pH using 1.87×10^{-4} kmol/m ³ sodium oleate concentration.	282
5	Flotation of apatite and dolomite as a function of reconditioning time (single and 1:1 mineral mixture).	283
6	Flotation of 95:5 apatite:dolomite mixture as a function of reconditioning time.	284
7	Flotation of apatite and dolomite as a function of reconditioning pH, with supernatant replaced with water.	286
8	Flotation of 95:5 apatite:dolomite mixture as a function of reconditioning pH, with 70% supernatant replaced with water.	287
9	Amount of oleate adsorbed on apatite and dolomite as a function of reconditioning and conditioning pH.	288
10	Amount of oleate adsorbed on apatite as a function of collector concentration after conditioning at pH 10.0 and reconditioning at pH 4.2.	289
11	Amount of oleate adsorbed on dolomite as a function of collector concentration after conditioning at pH 10 and reconditioning at pH 4.2.	290
12	Amount of oleate adsorbed on apatite and dolomite as a function of reconditioning time.	291
13	Flotation of apatite as a function of amount of oleate adsorbed after conditioning at pH 10 and reconditioning at pH 4.2.	293
14	Flotation of dolomite as a function of amount of oleate adsorbed after conditioning at pH 10 and reconditioning at pH 4.2.	294
15	Transmission IR spectra of calcium oleate, magnesium oleate and oleic acid.	295

<u>Figure No.</u>	<u>Description</u>	<u>Page</u>
16	Transmission IR spectra of apatite, after conditioning at pH 10 and after two-stage conditioning.	296
17	Effect of Ca ⁺² ions on the amount of oleate adsorbed on apatite as a function of collector concentration.	298
18	Effect of Mg ⁺² ions on the amount of oleate adsorbed on apatite as a function of collector concentration.	299
19	Apatite (left) and dolomite (right) particles from Agrico dolomite feed (65 x 150 mesh). (a) Backscattered electron image. (b) Calcium distribution map. (c) Magnesium distribution map. (d) Phosphorous distribution map.	316
20	Agrico dolomite, 65 x 150 mesh float fraction (apatite particle is in center). (a) Backscattered electron image. (b) Calcium distribution map. (c) Magnesium distribution map. (d) Phosphorous distribution map.	317
21	Agrico dolomite, 65 x 150 mesh sink fraction. (a) Back-scattered electron image. (b) Calcium distribution map. (c) Magnesium distribution map. (d) Phosphorous distribution map.	319

LIST OF TABLES

<u>Table No.</u>	<u>Description</u>	<u>Page</u>
Chapter II. <u>Materials and Methods</u>		
1	Master List of Samples and Chemical Analyses.	5
Chapter III. <u>Mineralogical Studies</u>		
1	Results of Qualitative Diffraction Analysis.	19
2	X-ray Diffraction Standards and Calibration Curve Data.	25
3	Test for Precision of Intensity Measurement (Integrated Area) Using Sample K2.	27
4	Test for Precision of Intensity Measurement (Peak Height) Using Sample K2.	28
5	Comparison of Dolomite Intensities and the Intensity Correction Factor.	29
6	Mass Absorption Coefficients.	33
7	Results of Quantitative X-ray Diffraction.	35
8	Summary of Chemical Analysis.	36
9	Weight Percent Dolomite and Weight Percent MgO.	44
10	Unit Cell Parameters of Carbonate-Fluorapatite and Dolomite.	45
11	Comparison of MgO Contributed by Dolomite with Total MgO.	47
12	Infrared Absorption Calibration Curve Data.	57
13	Variation of Diffraction Intensity Ratio (200)/(111) in Fluorapatite with Magnesium Substitution for Calcium.	61
14	(200)/(111) Carbonate-Fluorapatite Peak Intensity Ratios.	62
15	Dolomite Content of the Phosphorite Samples Used in the Color Fraction Studies.	64
16	Weight Percent of the Color Fractions.	73

<u>Table No.</u>	<u>Description</u>	<u>Page</u>
17	Dolomite X-ray Diffraction Data for the Color Fractions.	74
18	Apatite X-ray Diffraction Data for the Color Fractions.	76
19	Weight Percent of Grains in Each Color Fraction Containing Various Amount of Dolomite. Sample K-1 (13.5% Dolomite)	78
20	Weight Percent of Grains in Each Color Fraction Containing Various Amounts of Dolomite. Sample K-29 (11.8% Dolomite)	79
21	Weight Percent of Grains in Each Color Fraction Containing Various Amounts of Dolomite Sample K-2 (6.13% Dolomite)	80
22	Weight Percent of Grains in Each Color Fraction Containing Various Amounts of Dolomite. Sample K-27 (2.42% Dolomite)	81
23	Weight Percent of Grains in Each Color Fraction Containing Various Amounts of Dolomite Sample K-18 (2.06% Dolomite)	82
24	Weight Percent of Grains in Each Color Fraction Containing Various Amounts of Dolomite. Sample K-5 (0.87% Dolomite)	83
25	Total Weight Percent Dolomite Compared with Weight Percent of Grains Composed of Pure Dolomite.	92
26	Weight Percent of Grains Composed of Apatite Interlocked with Dolomite.	93
27	Projected Number of Grains in the White Color Fraction Containing Various Amounts of Dolomite.	95
28	Projected Number of Grains in the Gray Color Fraction Containing Various Amounts of Dolomite.	96
29	Projected Number of Grains in the Brown Color Fraction Containing Various Amounts of Dolomite.	97
30	Projected Number of Grains in the Green Color Fraction Containing Various Amounts of Dolomite.	98
31	Projected Number of Grains in the Black Color Fraction Containing Various Amounts of Dolomite.	99

<u>Table No.</u>	<u>Description</u>	<u>Page</u>
32	Average Diameter of the Grains (measured in mm).	100
33	Comparison Between Weight Percent Grains in Each Category and Projected Number (out of 100) of Grains in Each Category.	101
34	Comparison of Number of Pure Dolomite Grains from Light Color Fractions with Weight Percent Dolomite	102
35	Comparison of Total Number of Pure and Interlocked Grains.	103
36	Percent of Grains in Each Size Fraction Containing Various Amounts of Dolomite. Sample K-6	153
37	Percent of Grains in Each Size Fraction Containing Various Amounts of Dolomite. Sample K-42	154
38	Percent of Grains in Each Size Fraction Containing Various Amounts of Dolomite. Sample K-44	155
39	Percent of Grains in Each Size Fraction Containing Various Amounts of Dolomite. Sample K-36	156
40	Dolomite X-ray Diffraction Data for the Size Fraction.	158
41	Chemical Composition of Size Fractions of Sample K-6.	159
42	Chemical Composition of Size Fractions of Sample K-42.	160
43	Chemical Composition of Size Fractions of Sample K-44.	161
44	Chemical Composition of Size Fractions of IMC Dolomite.	164
45	Comparison of Number of Pure and Interlocked Grains in Different Dolomite Samples.	169
46	Comparison of K-36 -65 +150 Mesh Size Feed, Float, and Sink Fractions.	181
47	Comparison of K-36 -65 +150 Mesh and K-36 -35 +150 Mesh Size Fractions.	184
48	Mineral Composition of Different Dolomite Samples.	193
49	Grinding Time Results for Steinhatchee Dolomite.	195

<u>Table No.</u>	<u>Description</u>	<u>Page</u>
50	Grinding Time Results for IMC 4-Corners Dolomite.	196
51	Comparison of Peak Widths for Steinhatchee Dolomite.	200
52	Comparison of Peak Widths for IMC 4-Corners Dolomite.	201
Chapter IV. Aging Studies		
1	List of Samples Selected for Aging Studies	219
2	Effect of Ionic Strength on Aging Behavior	222
Chapter V. Kinetics Studies		
1	Recovery Versus Time for Apatite, Dolomite and Synthetic Mixture Flotation	234
2	Recovery Versus Time for Different Size Fractions of Apatite and Dolomite	235
3	Flotation Rates for Different Size Fractions of Apatite and Dolomite	236
Chapter VI. Apatite-Dolomite Flotation		
1	Chemical Analysis	242
2	Amount of Dissolved Calcium and Magnesium Ions	243
3	Depletion of Oleate Ions Due to Ca^{+2} , Mg^{+2} Complexation	267
Chapter VII. Two Stage Conditioning		
1	Chemical Analysis	276
2	Amount of Dissolved Calcium and Magnesium Ions	278
3	Flotation of Apatite and Dolomite after Two-Stage Conditioning	307
4	Flotation of Apatite and Dolomite after Two-Stage Conditioning	308
5	Flotation of Apatite and Dolomite after Two-Stage Conditioning Using OA-5 as the Collector	309

<u>Table No.</u>	<u>Description</u>	<u>Page</u>
6	Flotation of Agrico Apatite and Dolomite after Two-Stage Conditioning	310
7	Flotation of Agrico Apatite and Dolomite after Conditioning at Lower Agitation Intensity	311
8	Flotation of 1:1 Agrico Apatite and Dolomite Mixture after Two Stage Conditioning	313
9	Comparision of Feed, Float and Sink Fractions from a Two Stage Conditioning Test Using Agrico Dolomite (-65 mesh)	314
10	Flotation of 95:5 Apatite and Dolomite Mixture after Two-Stage Conditioning	320
11	Flotation of 95:5 Apatite and Dolomite Mixture after Two Stage Conditioning Using OA-5 as the Collector	321
12	Flotation of a Synthetic Mixture of Agrico Apatite and IMC Four-Corners Dolomite After Two Stage Conditioning	322
13	Effect of Pulp Density on Flotation of 80:20 Agrico Apatite and Perry Dolomite 65 x 100 mesh	324
14	Effect of Pulp Density on Flotation of 80:20 Agrico Apatite and Perry Dolomite 35 x 65 mesh	325
15	Effect of Pulp Density on Flotation of 80:20 Agrico Apatite and Perry Dolomite 35 x 150 mesh	326
16	Effect of Collector Concentration on Flotation of 80:20 Agrico Apatite and Perry Dolomite	328
17	Flotation of 80:20 Agrico Apatite and Perry Dolomite after Two Stage Conditioning	330
18	Flotatin of 80:20 Agrico Apatite and Perry Dolomite after Two Stage Conditioning by Agitation	331
19	Flotation of Natural Agrico Feed after Two Stage Conditioning	332
20	Flotation of Natural Agrico Feed After Two Stage Conditioning	333
21	Flotation of Natural Feed after Two-Stage Conditioning	334

<u>Table No.</u>	<u>Description</u>	<u>Page</u>
22	Flotation of Natural Agrico Feed After Two-Stage Conditioning	335
23	Flotation of Natural Brewster Feed After Two-Stage Conditioning	336
Chapter VIII. Selective Flocculation		
1	Single Mineral Flocculation of Apatite and Dolomite	343
2	Flocculation of Apatite-Dolomite Mixtures	344
3	Saturation Adsorption of PEO on Apatite and Dolomite	347

CONCLUSIONS

The objectives of the proposed research are to establish the mode of existence of dolomite, specifically magnesium in Florida phosphate and to develop suitable techniques for separation of dolomite from apatite. Highlights of major accomplishments are briefly discussed below.

Mineralogical Studies

Quantitative X-ray diffraction analysis, combined with chemical analysis of a number of phosphate samples revealed that more MgO than accounted for by dolomite alone was associated with these samples. The amount of excess MgO, as Mg substituting in the apatite lattice, averaged about 0.57%, which is in agreement with values reported in the literature (0.41-0.49%).

X-ray diffraction analysis and microscopic observations of the color fractions constituting five phosphate samples demonstrated that a considerable amount of dolomite existed as discrete grains. However, samples containing more than two percent dolomite were found to contain a significant number of interlocked grains. It was also determined that more dolomite in such grains existed on the surface of the particles than in grains with fewer dolomite inclusions. It is envisioned that interlocked particles will have to be ground to extremely small size in order to achieve liberation of apatite from dolomite. Grinding, however, was determined to cause changes in the properties of dolomite samples which could influence separation behavior. It is to be noted that the amount of dolomite inclusions is best determined with a polarizing microscope while SEM techniques are more appropriate for studying the amount of dolomite on the apatite surface.

Study of size fractions of phosphorite samples revealed that most of the dolomite was preferentially segregated in the coarse and fine fractions.

Microscopic studies and X-ray analysis of a number of dolomite samples from Florida indicated that different dolomite samples had varying physical and compositional characteristics. This may be of significance in developing procedures to separate dolomite from apatite.

Apatite-Dolomite Separation Studies

Aging Studies: Aging behavior of selected samples was studied with the objective of establishing a procedure to achieve consistent pH during the flotation tests. The pH of the mineral suspension containing dolomite drifted toward an equilibrium pH of about 8.2 while the pH of the apatite suspension reached an equilibrium value in the range of 5.5 to 6.5.

Particle size and pulp density had a noticeable effect on the kinetics of the pH drift but only a minor effect on the final pH value. It was difficult to maintain suspensions containing dolomite at acidic pH values due to a rapid drift towards equilibrium pH at about 8.2.

Kinetics of Apatite-Dolomite Flotation: It has been reported in the past that separation of apatite and dolomite might be achieved because of differences in their rates of flotation. A systematic study of the flotation kinetics of apatite and dolomite indicated that the rate of flotation of the two minerals are similar, and under present experimental conditions, desired separation may not be achieved.

Conventional Conditioning: Flotation behavior of single and mixed mineral systems was investigated as a function of the collector concentration over a pH range varying from 3 to 11. Selectivity, predicted by single mineral

flotation tests at pH 7 to 10, was not observed in mixed minerals. This is attributed to the depletion of oleate by precipitation with cations dissolved from dolomite. At pH 11, the loss of selectivity in mixed mineral systems is due to possible modification of the apatite surface when in contact with dolomite.

Two Stage Conditioning Process: This process involves conditioning the feed at pH 10 followed by reconditioning at a lower pH before flotation. Selective flotation of dolomite from apatite was observed both for single and mixed minerals by reconditioning at pH 4. To understand the mechanisms of observed selective flotation, further studies involving electrokinetic behavior, oleate adsorption, infrared spectroscopy, and solubility of the minerals were conducted. Selective flotation of dolomite by reconditioning at pH 4 is attributed to the combined effect of higher oleate adsorption on dolomite and hydrolysis of the adsorbed oleate molecules to oleic acid at lower pH values.

The method has been tested at bench scale level with several dolomite-apatite mixtures and natural magnesium phosphate samples from the Florida phosphate field. Reductions of the MgO content of the samples from 1.8-4.0% MgO to below 1% MgO at recoveries of about 90% P₂O₅ in the sink fraction have been obtained in bench scale flotation tests. Reconditioning pH was determined to be one of the most important process parameters in this process.

Selective Flocculation Studies: Although exhaustive data about the nature and extent of interlocking of apatite and dolomite grains in the South Florida deposit is not available, limited mineralogical results suggest that certain phosphorites would need to be ground to fine sizes for complete liberation.

Selective flocculation is a promising technique for processing of mineral fines. Preliminary tests using PEO as a flocculant resulted in reducing the MgO levels below 1%, although recoveries were low. It is further indicated that adsorption of PEO on apatite needs to be reduced or eliminated to achieve higher recoveries.

Chapter VI

APATITE-DOLOMITE FLOTATION WITH FATTY ACID

AFTER CONVENTIONAL CONDITIONING

A study was conducted to establish the reasons for the lack of selectivity obtained during the flotation of apatite and dolomite using fatty acid after conventional conditioning.

EXPERIMENTAL

Materials

Mineral Preparation

Apatite: A flotation feed sample of 16 x 150 mesh size, free of any significant amounts of dolomite, was supplied by the International Minerals and Chemical Corp., Bartow, Florida. The silica grains in the feed sample were removed using the electrostatic separator at CarpcO, Inc., Jacksonville, Florida. The cleaned sample was identified by X-ray diffraction to be carbonate-fluorapatite (also called francolite). One batch of the sample was reduced in size to 65 x 100 mesh using an alumina mortar and pestle for flotation and oleate adsorption experiments. The sized sample was washed ten times with triple distilled water, dried at 50°C, and stored in a glass bottle. The second batch of the mineral was ground to -325 mesh in a rod mill for electrophoresis experiments. Iron impurities from the ground sample were removed by a hand magnet.

Dolomite: Hand picked dolomite pebbles (3/4 x 16 mesh) were also supplied by the International Minerals and Chemical Corp., Bartow, Florida. The mineral was identified by X-ray diffraction to be dolomite. The pebbles were first ground to a finer size in a rod mill and then in an alumina mortar and pestle

to 65 x 100 mesh size for flotation and oleate adsorption experiments. The ground material was washed ten times with triple distilled water, dried at 50°C and stored in a glass bottle. Another batch of -325 mesh powder was prepared for electrokinetic experiments by the same procedure as for apatite. Iron impurities from the ground samples were removed by a hand magnet.

Mineral Characterization

Chemical Analysis: Chemical analysis of the apatite and dolomite, conducted by Thornton Laboratories, Inc., Tampa, is reported in Table 1. It is clear from the data that MgO content of the phosphate sample and P₂O₅ content of the dolomite sample are not significant.

Surface Area Measurements: Surface area was measured by the BET technique using nitrogen gas as the adsorbate. It was determined to be 4.24 m²/g for dolomite and 18.62 m²/g for apatite. The surface area is relatively high considering the particle size. This can be attributed to the porosity of the samples as confirmed by scanning electron microscope micrograph. The high surface area of the minerals, however, made it possible to conduct flotation and oleate adsorption tests on minerals of the same size fraction.

Solubility of Minerals: Amounts of dissolved cations from apatite and dolomite were measured over the pH range 4.8 to 11. The solubility of single and mixed minerals (1:1 and 95:5 apatite:dolomite) is presented in Table 2. It is observed that the solubility of apatite is negligible at pH 11 and it increases as the pH decreases. Dolomite, on the other hand, is soluble even at pH 11 and its solubility increases exponentially as the pH decreases. It is clear from the data presented that the solubility of dolomite is almost an order of magnitude higher than that of apatite over the pH range examined.

Table 1
Chemical Analysis

Mineral	P ₂ O ₅ %	Fe ₂ O ₃ %	Al ₂ O ₃ %	Acid Insolubles	MgO %	CaO %	CO ₂ %	F %	Organic Matter, Carbon %
Apatite	36.78	0.42	0.93	3.34	0.12	50.35	1.68	3.82	0.19
Dolomite	1.67	0.94	0.96	5.11	17.58	32.33	42.16 (loss on ignition)	0.21	0.06

Table 2

Amount of Dissolved Calcium and Magnesium Ions

pH	Mineral	Ca ⁺² (ppm)	Mg ⁺² (ppm)
11.0	Apatite	0.1	0.0
	Dolomite	1.4	0.0
10.0 ± 0.3	Apatite	0.3	0.0
	Dolomite	1.2	0.4
	1:1 Mixture	0.9	0.3
	95:5 Mixture	0.3	0.0
7.0 ± 0.7	Apatite	0.6	0.2
	Dolomite	5.0	2.4
	1:1 Mixture	3.3	1.8
	95:5 Mixture	0.7	0.3
4.8 ± 0.3	Apatite	8.0	0.7
	Dolomite	70.0	32.0
	1:1 Mixture	50.0	15.0
	95:5 Mixture	10.0	1.4

Chemicals

Purified sodium oleate from Fisher Scientific Co. was used in this study.

ACS certified grade potassium hydroxide and nitric acid were used to modify the pH. Also, ACS grade calcium and magnesium nitrate standards, potassium carbonate, potassium phosphate and 99.999% potassium nitrate were used in this investigation.

Triple distilled water of less than 1.2 micromhos specific conductivity was used in the study.

Methods

Flotation and Oleate Adsorption Experiments

Conventional (One-Stage) Conditioning: One gram of the mineral was aged for two hours in 100 ml of triple distilled water at the desired pH. The aged sample was conditioned with the collector by tumbling at 27 RPM for five minutes. The pH of the conditioned slurry was measured and reported as conditioning pH. The reagentized feed was either floated or analyzed for residual oleate content as described below.

Flotation: The conditional slurry was transferred to the Hallimond cell, and floated for one minute with nitrogen gas at a flow rate of 48 ml/min.

Oleate adsorption: The supernatant of the conditioned slurry was transferred to a glass tube for oleate analysis. The amount of oleate adsorbed on the mineral surface was calculated from the oleate depletion in the bulk solution.

Two-Stage Conditioning: One gram of the mineral was aged for two hours as in the previous experiment. It was conditioned for 2.5 minutes at pH 10 with the

desired amount of the collector. The reagentized slurry was further conditioned (or reconditioned) for 2.5 minutes at a lower pH. In another series of experiments, the slurry was reconditioned at a lower pH with reduced collector concentration, which was obtained by replacing 70% of the supernatant with water. All of the variables mentioned above such as pH, ionic strength and temperature were kept constant unless otherwise stated.

Electrokinetic Measurements

Electrophoretic mobility was measured by a Rank Mark II electrophoresis apparatus. One gram of -325 mesh sample was suspended in 100 ml of water of desired pH and ionic strength in a glass cylinder. The container was inverted 10 times and the suspension was allowed to settle for 10 minutes. 60 ml of the supernatant, containing the fine particles, was further aged for two hours before electrophoretic mobility measurements were conducted. The pH of the slurry was determined before and after the measurements. Zeta potential was calculated from electrophoretic mobility values using the following equation:

$$\zeta = \frac{4 (U) \eta}{\epsilon}$$

where ζ = zeta potential

U = electrophoretic mobility

η = viscosity

ϵ = dielectric constant

Assuming $\epsilon = 78.5$ and $\eta = 0.89$ cps under the present experimental conditions the above relation would reduce to:

$$\zeta = 12.8 (U).$$

Chemical Analysis

Calcium and magnesium analysis were conducted using a Perkin-Elmer 6000 atomic adsorption spectrophotometer.

Oleate analysis was done by Gregory's method (1). It was observed that the analytical procedure yielded significantly lower than actual results when centrifugation was employed under acidic pH conditions. This was attributed to the separation of second phase oleic acid during centrifugation, which could cause difficulties in transferring a representative sample for further analysis. It should be mentioned that since the 65 x 100 mesh size fraction was used for adsorption measurements, centrifugation of the suspension was not necessary to achieve solid/liquid separation. It was also proven that any trace amounts of fines generated during conditioning did not interfere with the oleate analysis. However, under alkaline pH conditions, precipitation of Ca/Mg oleate was found to interfere with the oleate analysis. This problem was overcome by using EDTA for sequestering as recommended by Gregory. The above procedure was standardized by analyzing samples of known oleate solutions in the presence of Ca^{+2} and Mg^{+2} ions at different pH levels.

Transmission IR Spectroscopy

Transmission IR spectroscopy was conducted using -325 mesh mineral samples. Sample preparation technique was similar to that used by Peck (2), A brief description of the procedure employed is given below.

One gram of -325 mesh sample was suspended in 100 ml of water at the desired pH. The suspension was agitated by inverting the graduated cylinder ten times and then allowed to settle for 5 minutes. Eighty ml of the

supernatant containing the fine particles were reagentized with, 50 ml of 1.6×10^{-2} kmol/m³ sodium oleate solution at pH 10 and reconditioned at pH 4 to 5. Samples obtained during different stages of conditioning were centrifuged at 15,000 RPM for five minutes. The solid samples were dried for 2 days at 50°C in air. Then 0.01 g of apatite and 0.005 g of dolomite were mixed with 2.0 g of KBr. After drying the KBr sample mixture in a vacuum oven at 80°C, the powder was pressed into 0.5 cm diameter pellets for transmission IR spectroscopy.

RESULTS AND DISCUSSION

Conventional Conditioning

Flotation Studies

Individual and mixed mineral flotation behavior of apatite and dolomite as a function of conditioning pH at two levels of collector concentration are illustrated in Figures 1, 2 and 3. Flotation results as a function of collector concentration at pH 10 are presented in Figures 4 and 5.

Single mineral flotation: It is seen from the single mineral flotation test data that separation of the dolomite from apatite is possible under the following conditions:

- (i) In the alkaline pH range - Selective flotation of apatite is observed in the pH range of 7 to 10, using 9.4×10^{-5} kmol/m³ and 1.87×10^{-4} kmol/m³ of sodium oleate concentration. At pH 11, dolomite can be expected to float selectively with 1.87×10^{-4} kmol/m³ of sodium oleate.
- (ii) In the acidic pH range - Dolomite can be expected to float selectively at pH 5.5 with 1.87×10^{-4} kmol/m³ sodium oleate.

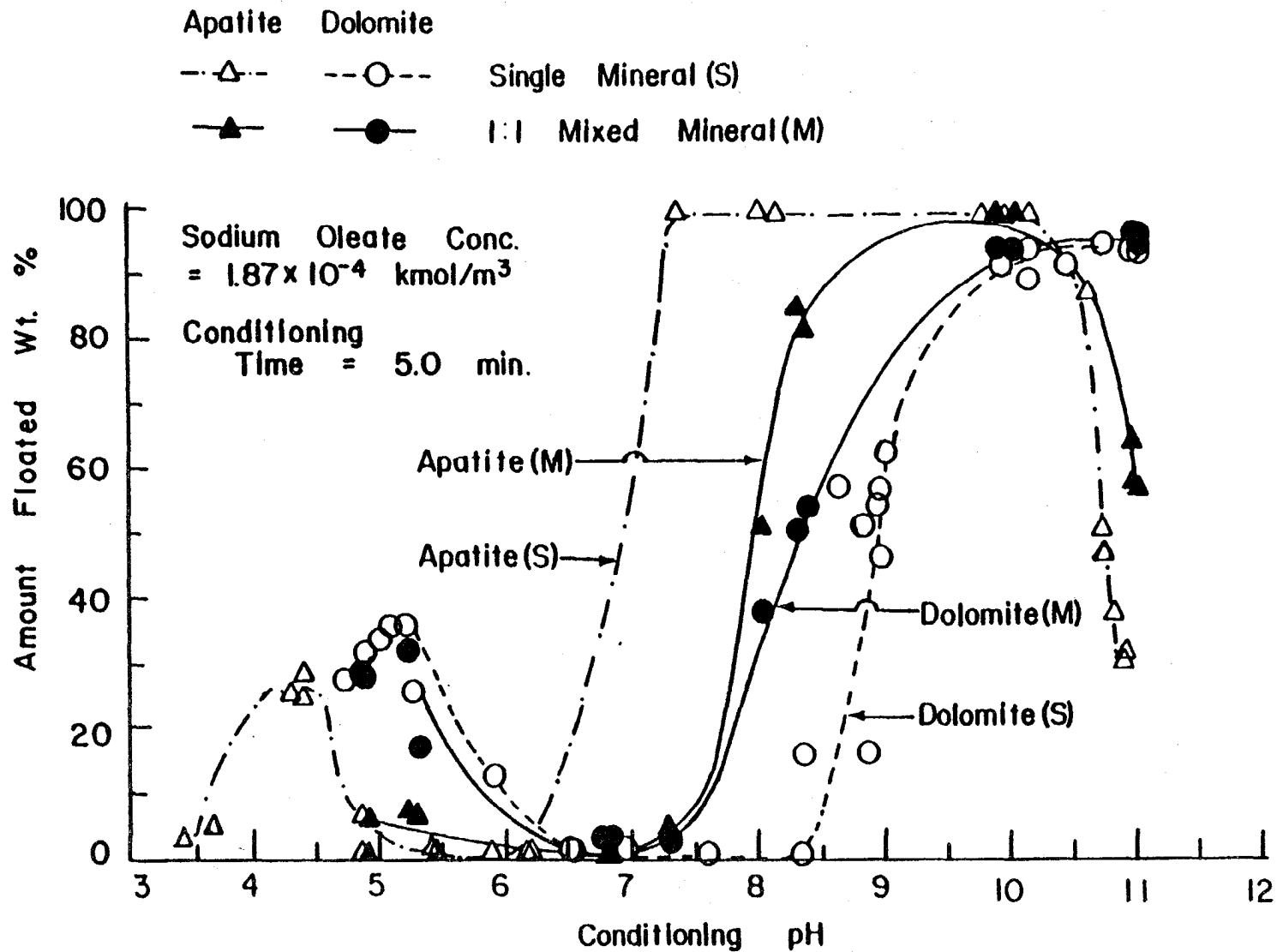


Figure 1. Flotation of apatite and dolomite as a function of conditioning pH (single and 1:1 apatite:dolomite mixture) using 1.87×10^{-4} kmol/m³ sodium oleate concentration.

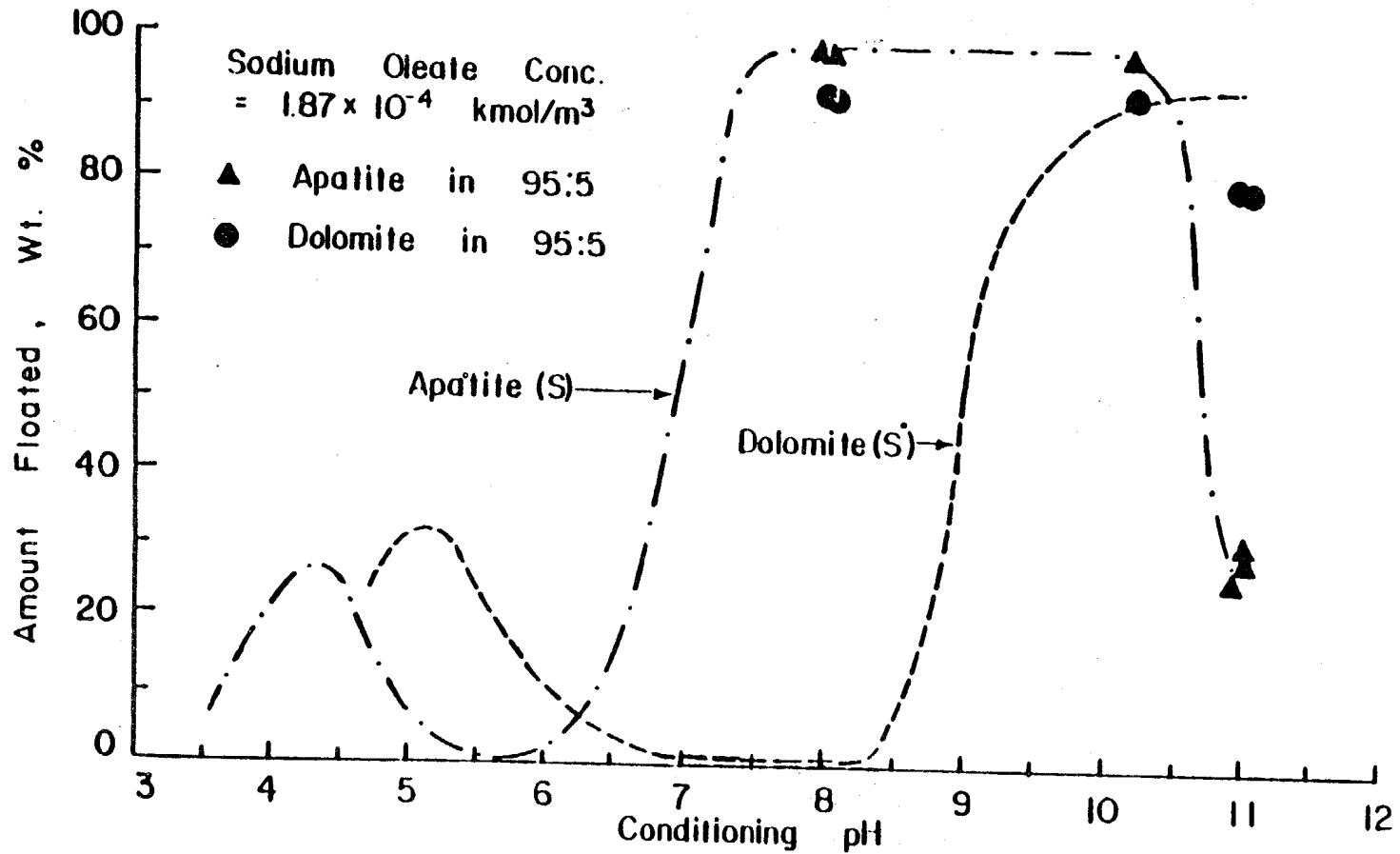


Figure 2. Flotation of 95:5 apatite:dolomite mixture as a function of conditioning pH using 1.87×10^{-4} kmol/m³ sodium oleate concentration.

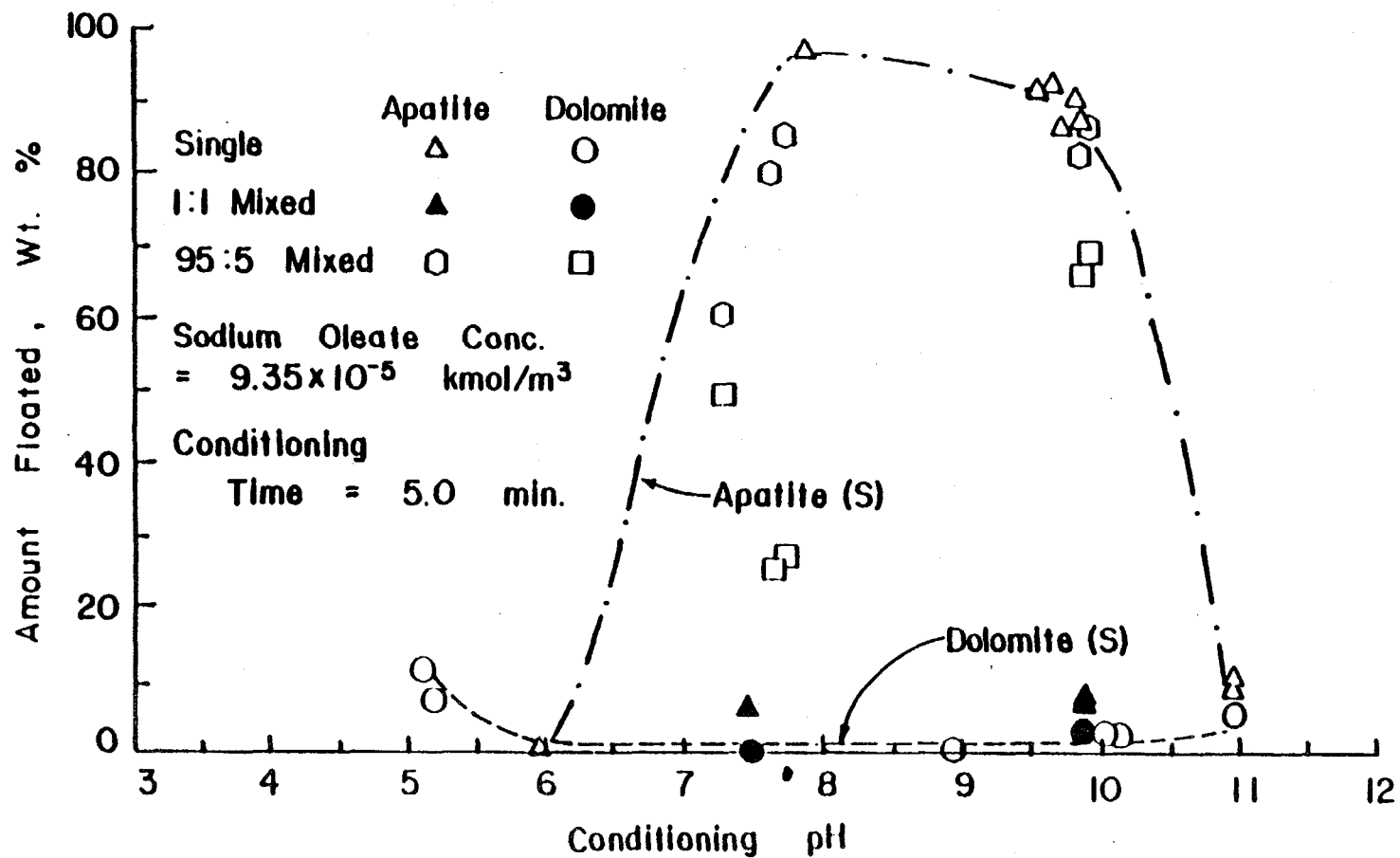


Figure 3. Flotation of apatite and dolomite as a function of conditioning pH (single, 1:1 and 95:5 apatite:dolomite mixture) using 9.35×10^{-5} kmol/m³ sodium oleate concentration.

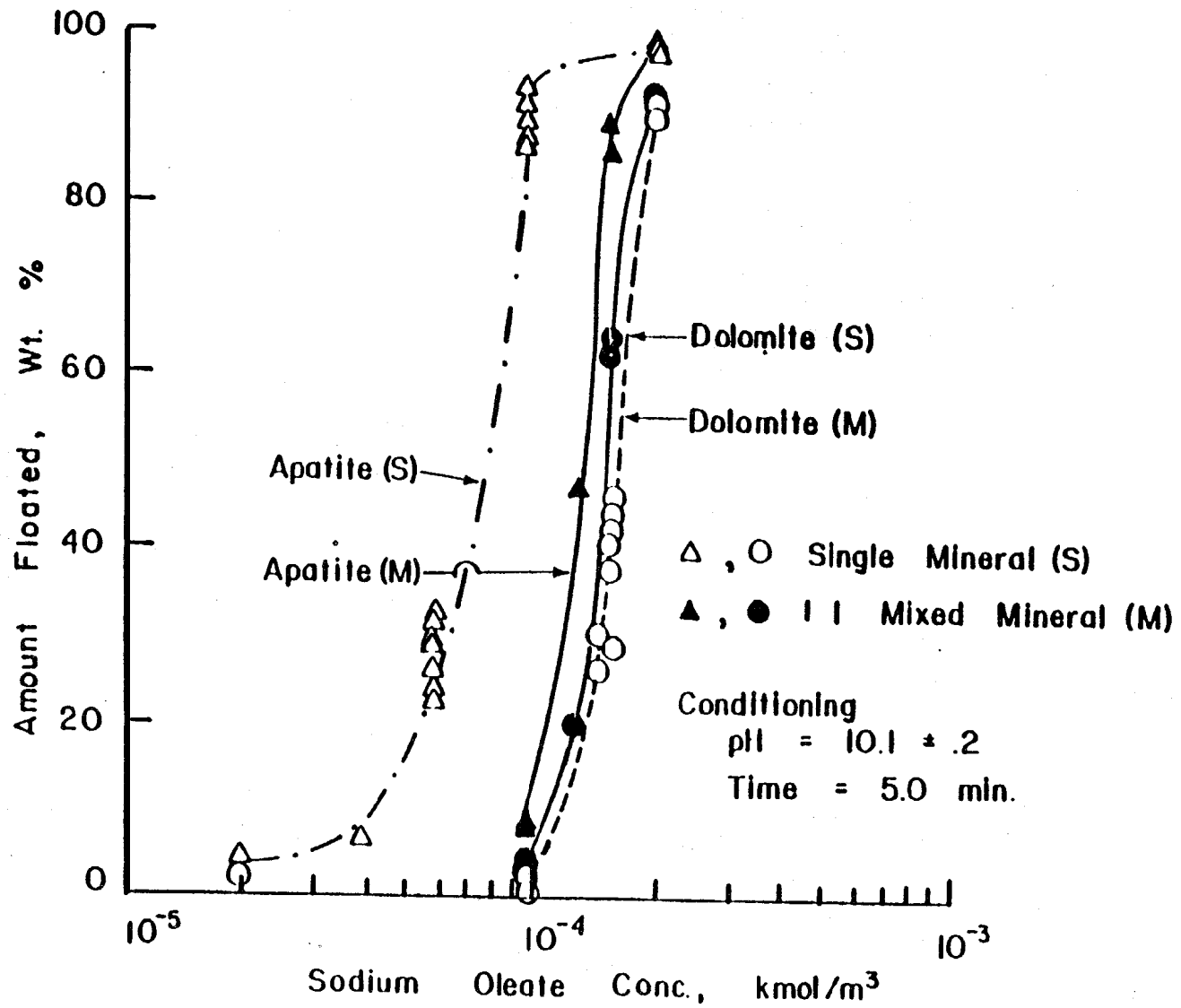


Figure 4. Flotation of apatite and dolomite as a function of sodium oleate concentration at pH 10 (single and 1:1 apatite:dolomite mixture).

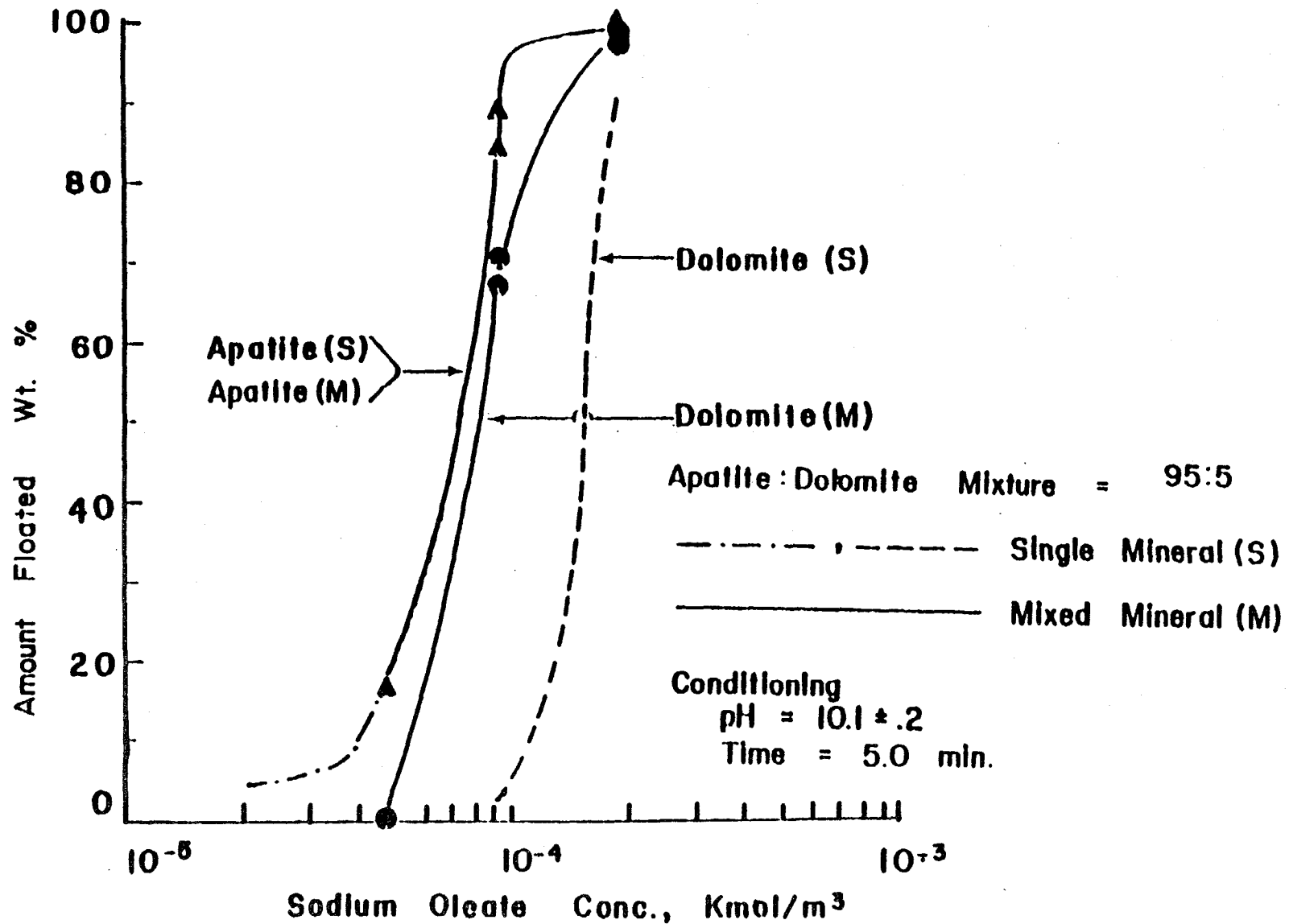


Figure 5. Flotation of apatite and dolomite as a function of sodium oleate concentration at pH 10 (single and 95:5 apatite:dolomite mixture).

1:1 apatite:dolomite mixture flotation: In the alkaline pH range, the selectivity predicted by the single mineral tests is not observed when both the minerals are floated together. In the pH range of 7 to 10, the loss of selectivity in the 1:1 mixed mineral system is due to a decrease in the apatite flotation and an increase in the dolomite flotation. At pH 11 the selectivity of dolomite flotation is reduced due to higher flotation of apatite as compared to that in the single mineral flotation tests. The reasons for the loss of selectivity under alkaline pH conditions are discussed in a later section.

At pH 5.5, both single and 1:1 mixed mineral flotation results indicate selective flotation of dolomite from apatite. Similar results have also been reported in the literature. It should, however, be noted that in the present study, as well as those reported in the past, recovery of the dolomite under acidic pH conditions is low. In some of the previous studies, attempts were made to further improve the dolomite recovery by adding larger amounts of the collector, but it resulted in a loss of selectivity. The use of surface modifying agents has also been investigated. The additional cost of the reagents, however, renders this process economically less attractive.

95:5 apatite:dolomite mixture flotation: As shown in Figures 2, 3 and 5, the selectivity is also lost for the 95:5 mixture. The flotation behavior of apatite in the mixture is determined to be similar to that in the individual mineral flotation tests. The flotation of dolomite, on the other hand, is significantly higher than in the single mineral flotation tests, thus causing a loss of selectivity.

Oleate Adsorption Results

Effect of pH and collector concentration: The adsorption of oleate on apatite and dolomite as a function of conditioning pH and collector concentration is presented in Figures 6 and 7. It should be noted that in the present study, a direct correlation of the adsorption and flotation data could be obtained, since both of these investigations were conducted using the same size material. A correlation between the two sets of data at different levels of pH and initial collector concentration is presented in Figures 8, 9, 10 and 11.

Loss of Selectivity in the Alkaline pH Range

The selectivity predicted on the basis of single mineral flotation tests is not obtained with 1:1 mixed minerals under alkaline pH conditions. In the pH range of 7 to 10, selectivity is lost due to a decrease in the apatite flotation (see Figures 4 and 6). The loss of selectivity at pH 11 can be attributed to an increase in the apatite flotation,

The loss in the apatite recovery in the 1:1 mixed mineral system can be attributed to (i), the presence of dolomite slimes (ii), the smearing of the dolomite on the apatite surface or (iii), the interference by the dissolved ions. The first possibility was examined by floating apatite in a supernatant of the dolomite. Both centrifuged and non-centrifuged supernatants were tested to determine the role of dolomite fines in the apatite flotation. The 'smearing' effect was investigated by conditioning both the apatite and the dolomite in the same container but separated by a -400 mesh copper wire net. Lower flotation of apatite in all these tests indicated that the dolomite fines in the bulk or the physical coating of the dolomite on apatite are not

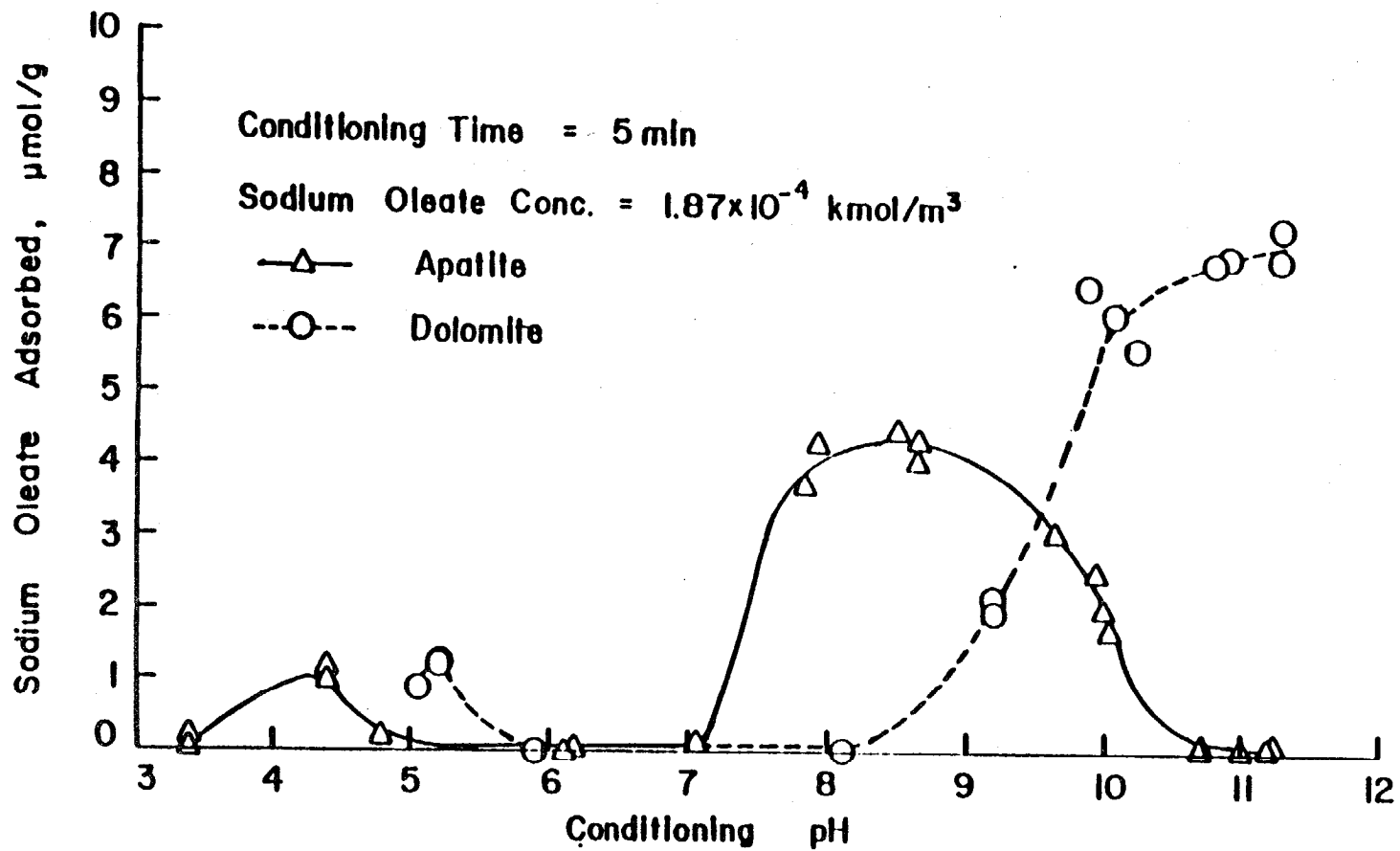


Figure 6. Amount of oleate adsorbed on apatite and dolomite as a function of conditioning pH.

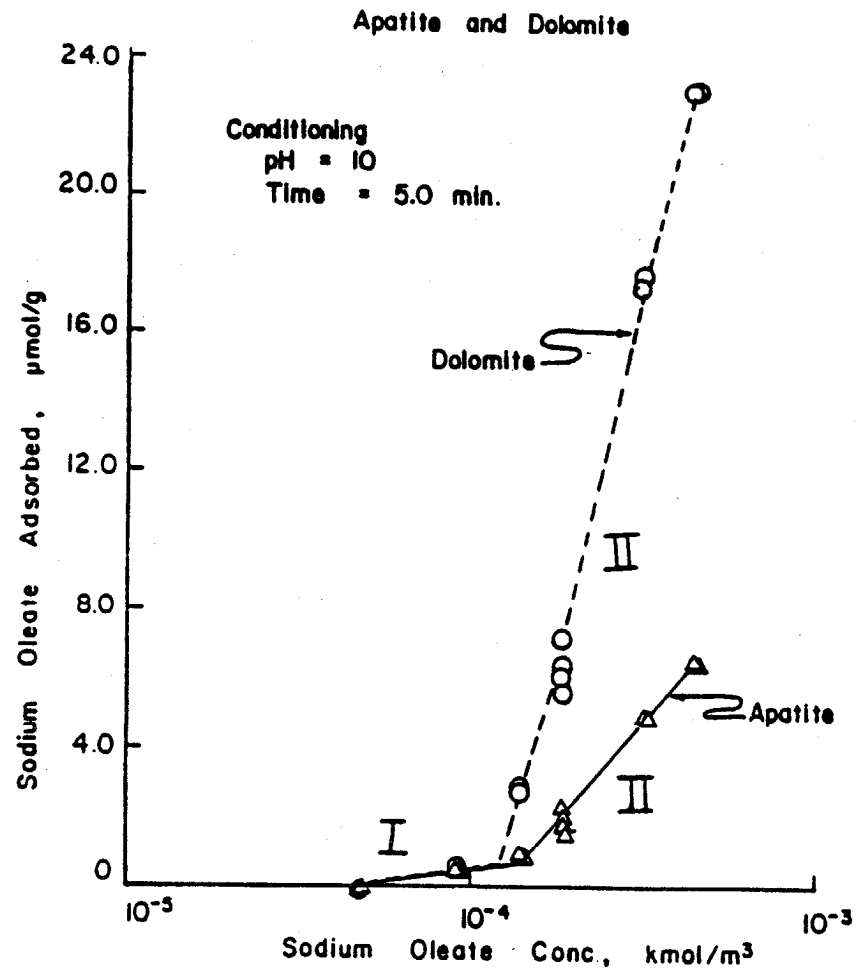


Figure 7. Amount of oleate adsorbed on apatite and dolomite as a function of collector concentration at pH 10.

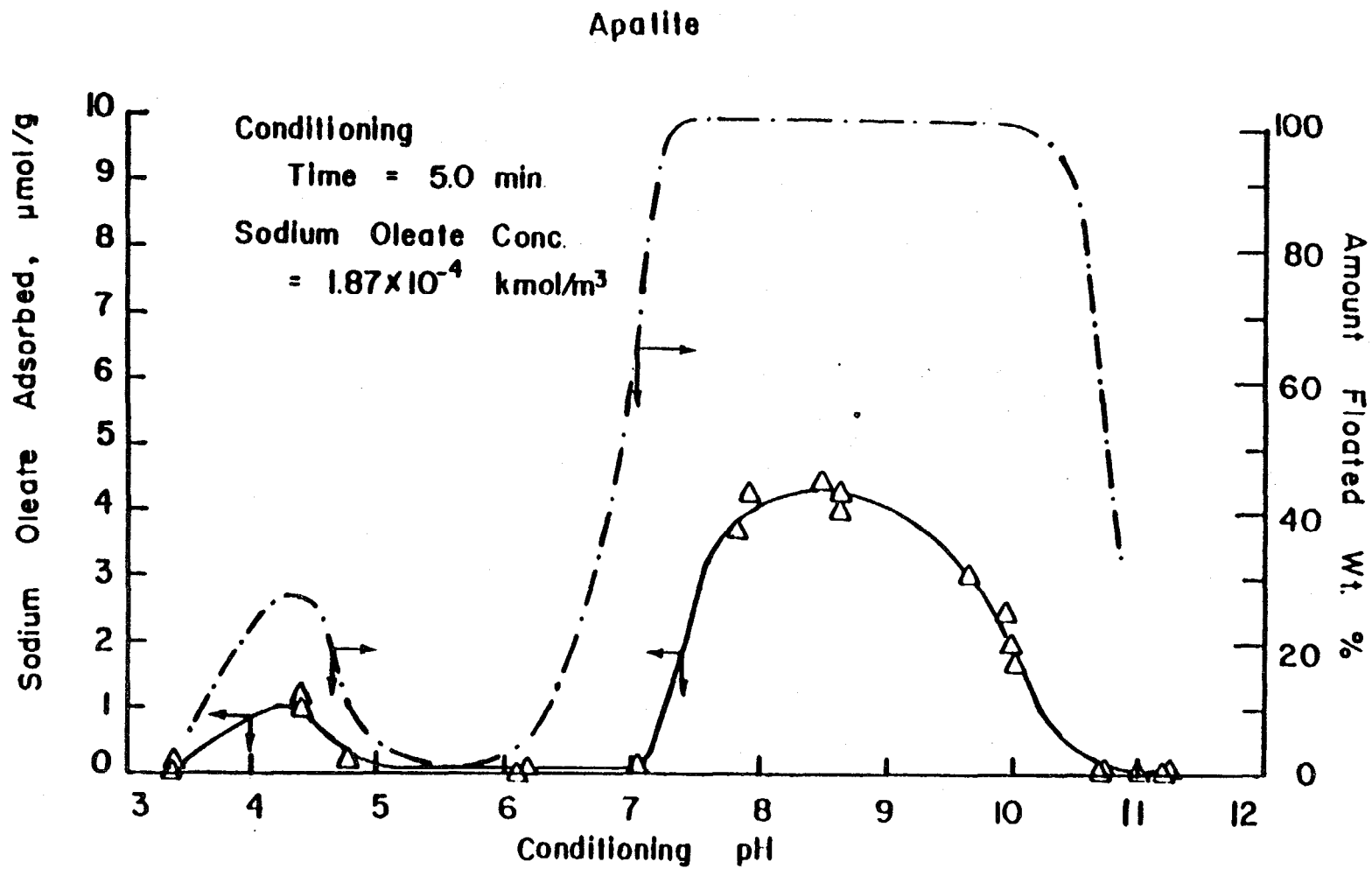


Figure 8. Correlation between amount floated and oleate adsorbed as a function of conditioning pH for apatite.

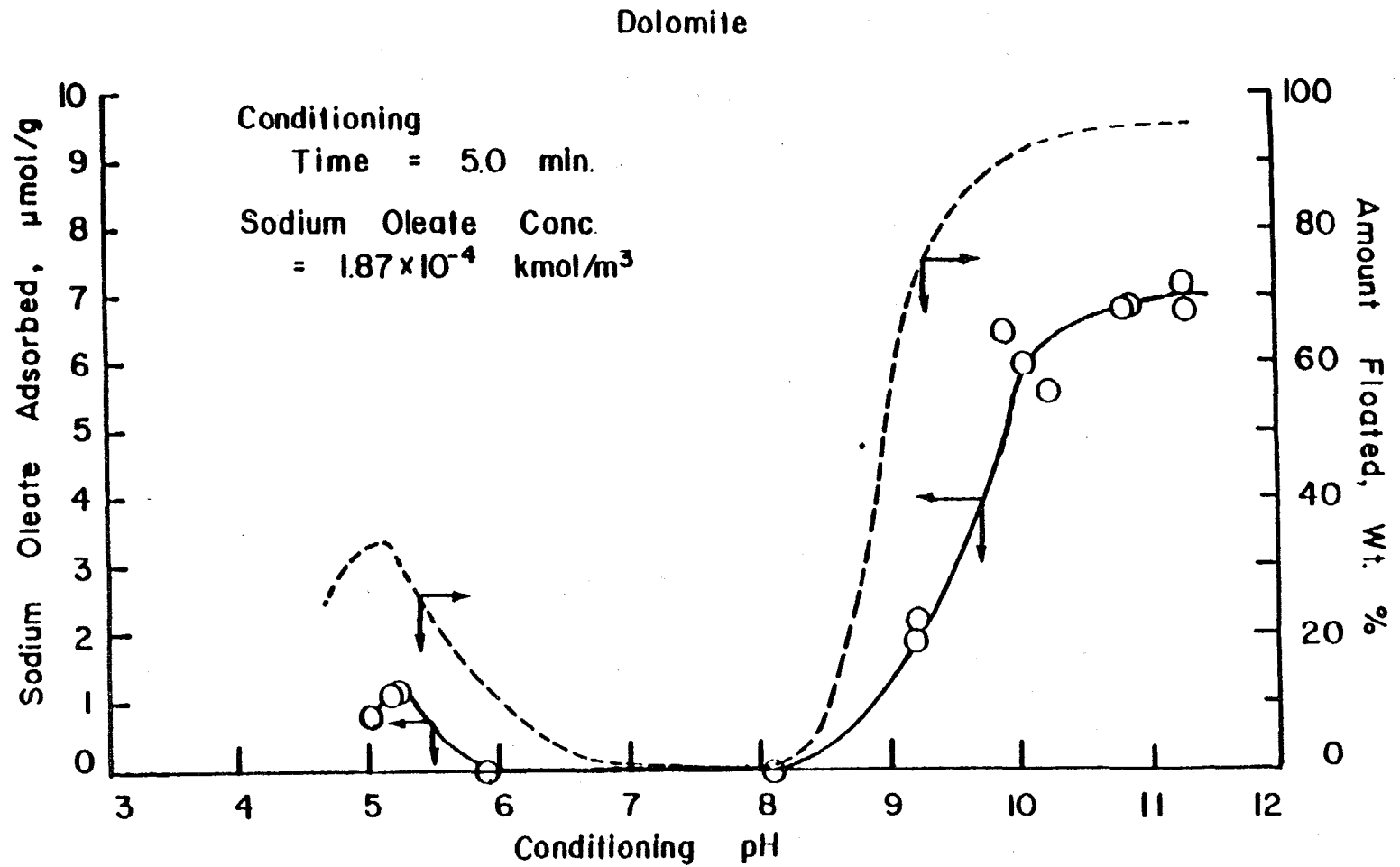


Figure 9. Correlation between amount floated and oleate adsorbed as a function of collector concentration.

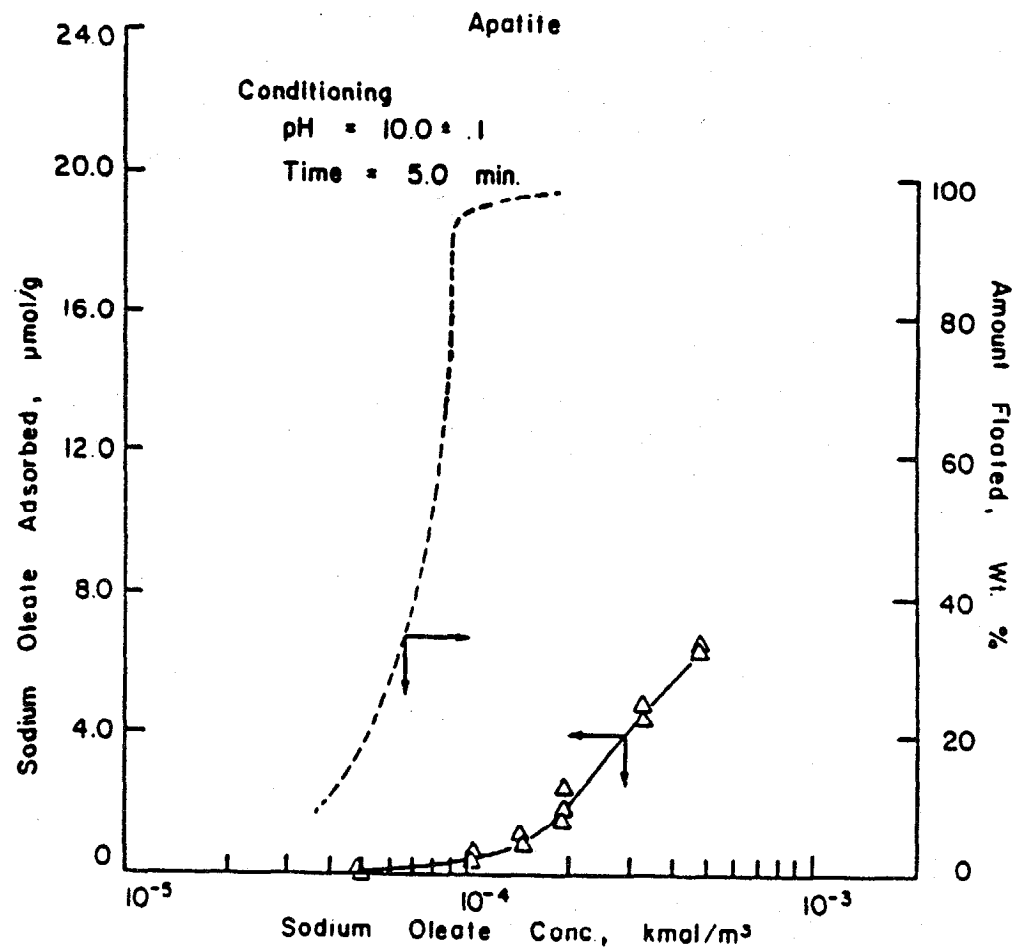


Figure 10. Correlation between amount floated and oleate adsorbed as a function of collector concentration at pH 10 for apatite.

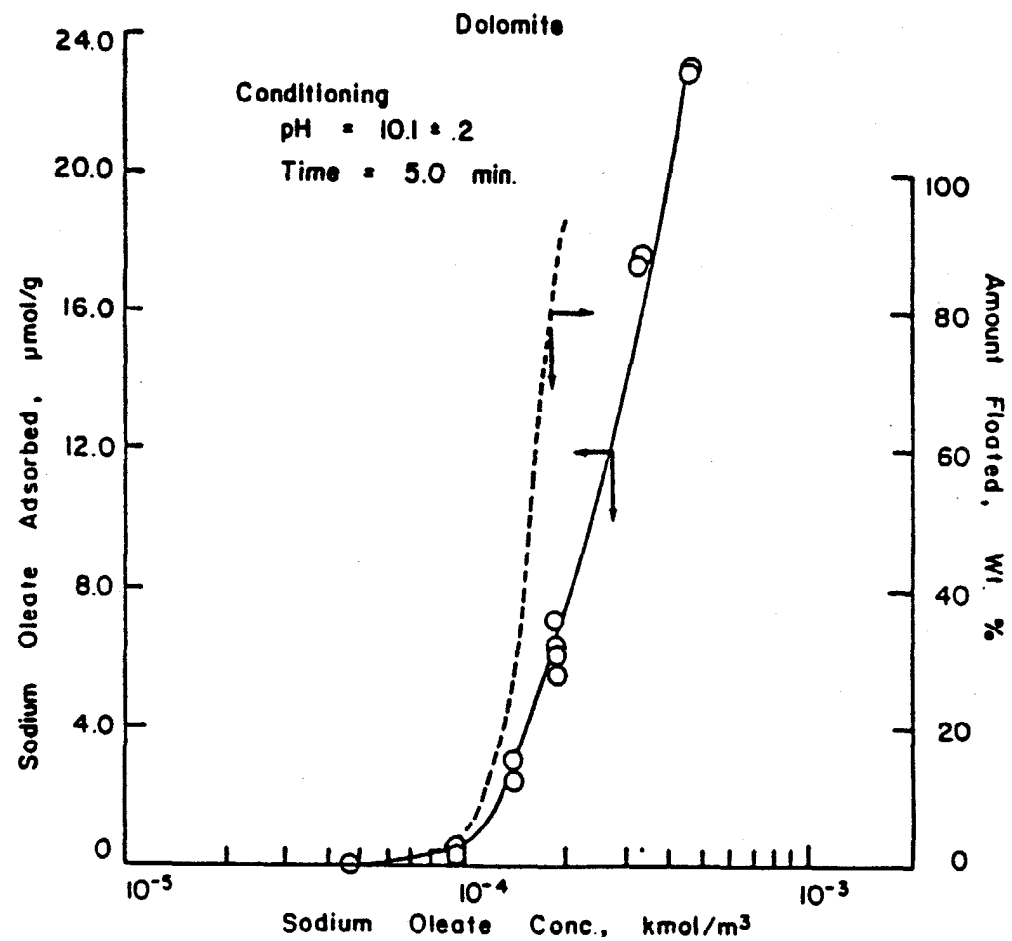


Figure 11. Correlation between amount floated and oleate adsorbed as a function of collector concentration at pH 10 for dolomite.

the major cause of nonselectivity observed in the mixed mineral system. The effect of dissolved ions was investigated next. This is discussed below.

Effect of dissolved ions: Effect of Ca^{+2} ions on the flotation recovery of apatite is presented in Figure 12. It can be observed that, whereas Ca^{+2} and Mg^{+2} ions cause a significant reduction in the apatite flotation, the effect of CO_3^{-2} ions is negligible. To isolate the effect of ionic strength on the apatite flotation, tests were conducted using up to $2.0 \times 10^{-3} \text{ kmol/m}^3$ KNO_3 . It is evident from the flotation results in Figure 12 that no significant reduction in the apatite flotation occurs as a result of KNO_3 addition. The depression of apatite flotation in the presence of Ca^{+2} and Mg^{+2} ions becomes significant only above $1.0 \times 10^{-5} \text{ kmol/m}^3$, which is the concentration range of the dissolved Ca^{+2} and Mg^{+2} ions from 1:1 mixture of apatite and dolomite at pH 10. In 1:1 mixed mineral system, the additional Ca^{+2} and Mg^{+2} ions dissolved from dolomite are believed to be the major cause of reduced apatite flotation in the alkaline pH range.

Dissolved cations could possibly depress the apatite flotation by either adsorbing and altering the electrokinetic behavior of the mineral or by depleting the oleate ions in the bulk solution by forming a soluble or insoluble complex. The effect of Ca^{+2} , Mg^{+2} and CO_3^{-2} ions on the zeta potential of apatite are reported in Figures 13, 14 and 15. Zeta potential of apatite in the presence of Ca^{+2} and Mg^{+2} ions was found to vary, but no significant effect of CO_3^{-2} ions was observed. However, the concentrations of the species required to influence the electrokinetic behavior were much higher than those that solubilized under present flotation conditions.

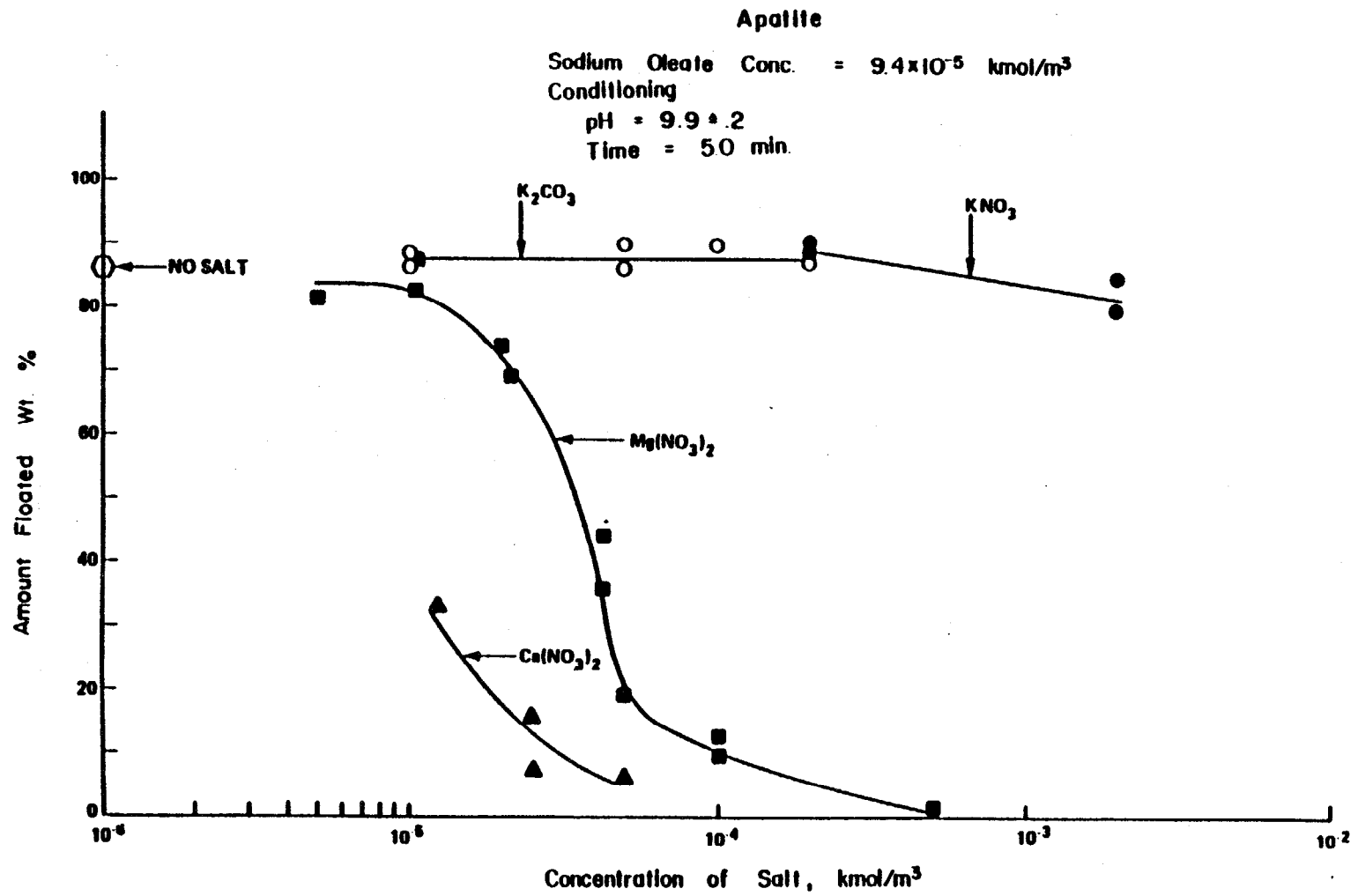


Figure 12. Flotation of apatite as a function of dissolved ion concentration at pH 10.

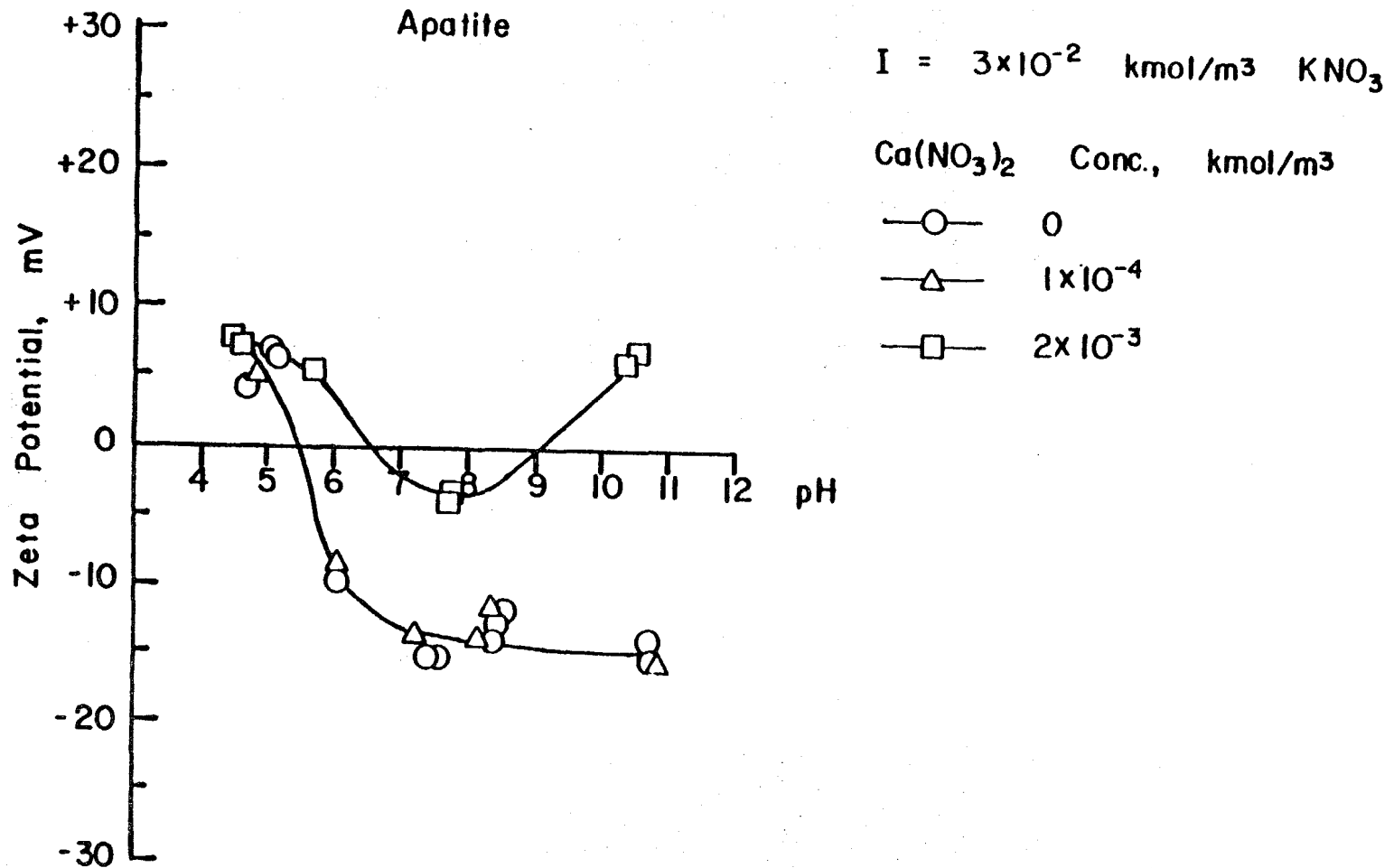


Figure 13. Effect of calcium on the zeta potential of apatite.

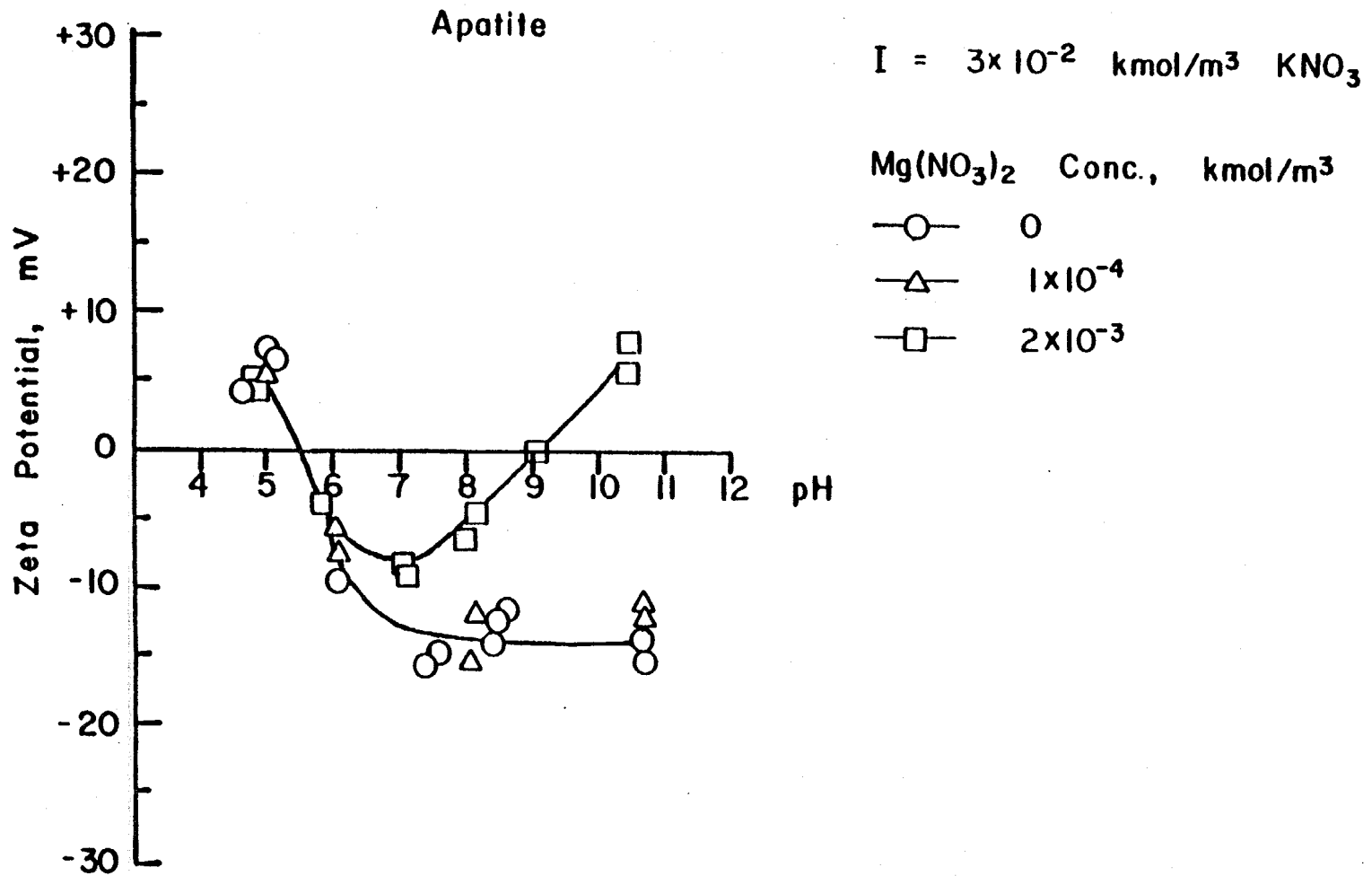


Figure 14. Effect of magnesium ions on the zeta potential of apatite.

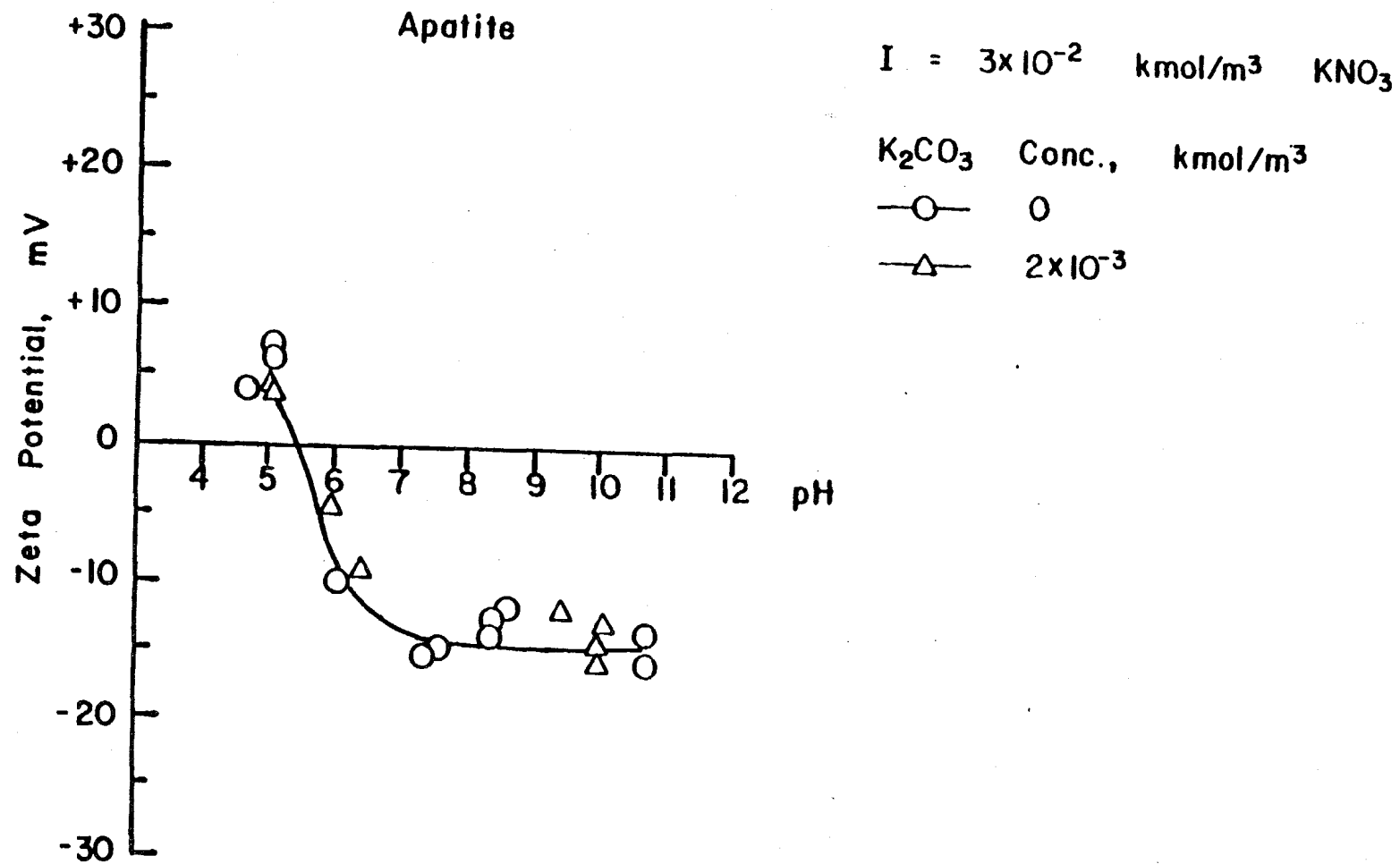


Figure 15. Effect of carbonate ions on the zeta potential of apatite.

Depletion of oleate by precipitation: It is established that the presence of Ca^{+2} and Mg^{+2} ions under alkaline pH conditions will cause precipitation of the oleate ions as Ca or Mg oleate. In the present study, precipitation of oleate soaps is confirmed by the depletion of free Ca^{+2} , Mg^{+2} and oleate ions in the bulk solution. These tests involved adding a known amount of oleate to the supernatant of 1:1 mixture, followed by centrifuging the precipitate (see Table 3). At pH 10, the cation to anion ratio in the precipitate was determined to be approximately 1:2, suggesting that the precipitate formed is Ca or Mg oleate. Depletion of calcium, magnesium and oleate ions was also reported at pH 7. At pH 4.5, however, no change in the concentration of any of the ions was observed. This is expected, since neutral oleic acid molecules present at lower pH values will not complex with Ca^{+2} and Mg^{+2} ions.

Oleate depletion was determined to be the cause of reduction in the apatite flotation, and consequently of the observed loss in selectivity. At a pH below 10, the amount of dissolved ions from dolomite increases, thus causing a higher depletion of oleate ions, which will further reduce the apatite flotation. On the other hand, if Ca^{+2} and Mg^{+2} concentrations are reduced, the amount of available oleate ions should increase due to lesser depletion. The smaller increase in dolomite flotation in mixed mineral system could be attributed to this phenomena. As seen in Table 2, the dissolved cations are less in the supernatant of the mixture, as compared to that from dolomite alone. It is to be noted that at the acidic pH where neutral oleic acid molecules are the stable specie, no depletion of oleate ions due to precipitation is observed, in spite of large amounts of dissolved Ca^{+2} and Mg^{+2} ions in the solution. Consequently, the flotation behavior of single and mixed minerals is similar under acidic pH conditions.

Table 3

Depletion of Oleate Ions Due to Ca^{+2} , Mg^{+2} Complexation

	pH	Ca^{+2} (kmol/m^3)	Mg^{+2} (kmol/m^3)	Oleate (kmol/m^3)
Supernatant Without Oleate	10.0	2.30×10^{-5}	1.23×10^{-5}	---
Depletion of Ions Upon Oleate Addition	10.0	1.00×10^{-5}	0.82×10^{-5}	3.80×10^{-5}
Supernatant Without Oleate	7.0	8.30×10^{-5}	7.40×10^{-5}	---
Depletion of Ions Upon Oleate Addition	7.0	3.00×10^{-5}	8.22×10^{-6}	precipitate observed
Supernatant Without Oleate	4.5	1.30×10^{-3}	6.20×10^{-4}	---
Depletion of Ions Upon Oleate Addition	4.5	0.00	0.00	no precipitate observed

In the case of the 95:5 apatite:dolomite mixture, the loss of selectivity can also be attributed to the amount of dissolved ions present in the system. At pH 10, cation concentration in the 95:5 mixture is mostly due to apatite and thus, flotation behavior of the mixture should be similar to that of apatite alone. On the other hand, availability of more oleate ions for dolomite flotation in the mixture, due to lower oleate ion depletion, would result in higher dolomite flotation.

It should be further noted that in the presence of foreign ions oleate adsorption on apatite is considerably reduced (see Figures 16 and 17). These results are consistent with the flotation results.

Flotation at pH 11: The flotation recovery of apatite in the 1:1 mixture at pH 11 is higher than what is predicted by the single mineral flotation data (see Figure 1). To explain the higher apatite recovery in the mixture, apatite flotation in the dolomite supernatant was conducted. The recovery under these conditions was about 15 percent lower than in the mixture, which is similar to the trend observed at pH 10. It can therefore be concluded that the higher flotation of apatite at pH 11 is obtained only when both the minerals are floated together. The role of surface charge characteristics of the two minerals is discussed next.

Zeta potential measurements of apatite and dolomite as a function of pH, presented in Figures 18 and 19, indicate the major differences in the surface chemistry of the two minerals. The isoelectric point (IEP) of apatite was determined to be at pH 5.5. For dolomite, however, two isoelectric points at pH 5.5 and pH 10.5 were observed. Of particular interest is the IEP at pH 10.5, above which the surface is positively charged. The second IEP is attributed to the hydroxylation of Mg ions to $\text{Mg}(\text{OH})^+$ and $\text{Mg}(\text{OH})_2$ (s) dolomite

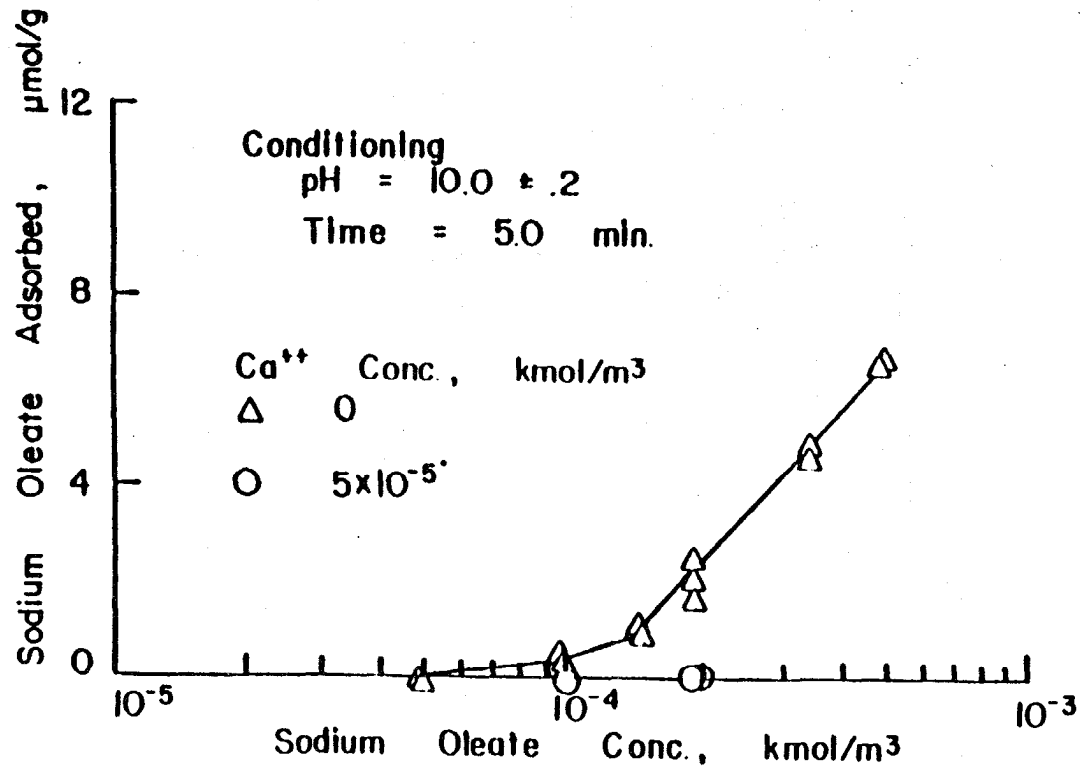


Figure 16. Effect of Ca⁺² ions on the amount of oleate adsorbed on apatite as a function of collector concentration.

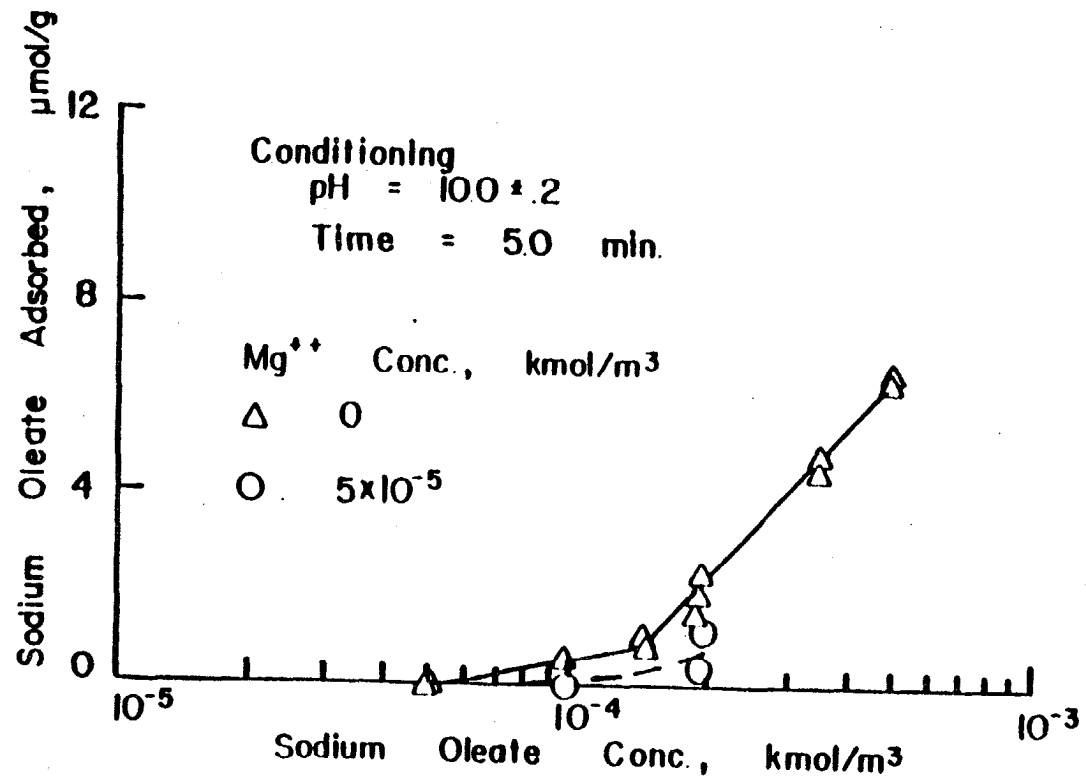


Figure 17. Effect of Mg⁺² ions on the amount of oleate adsorbed on apatite as a function of collector concentration.

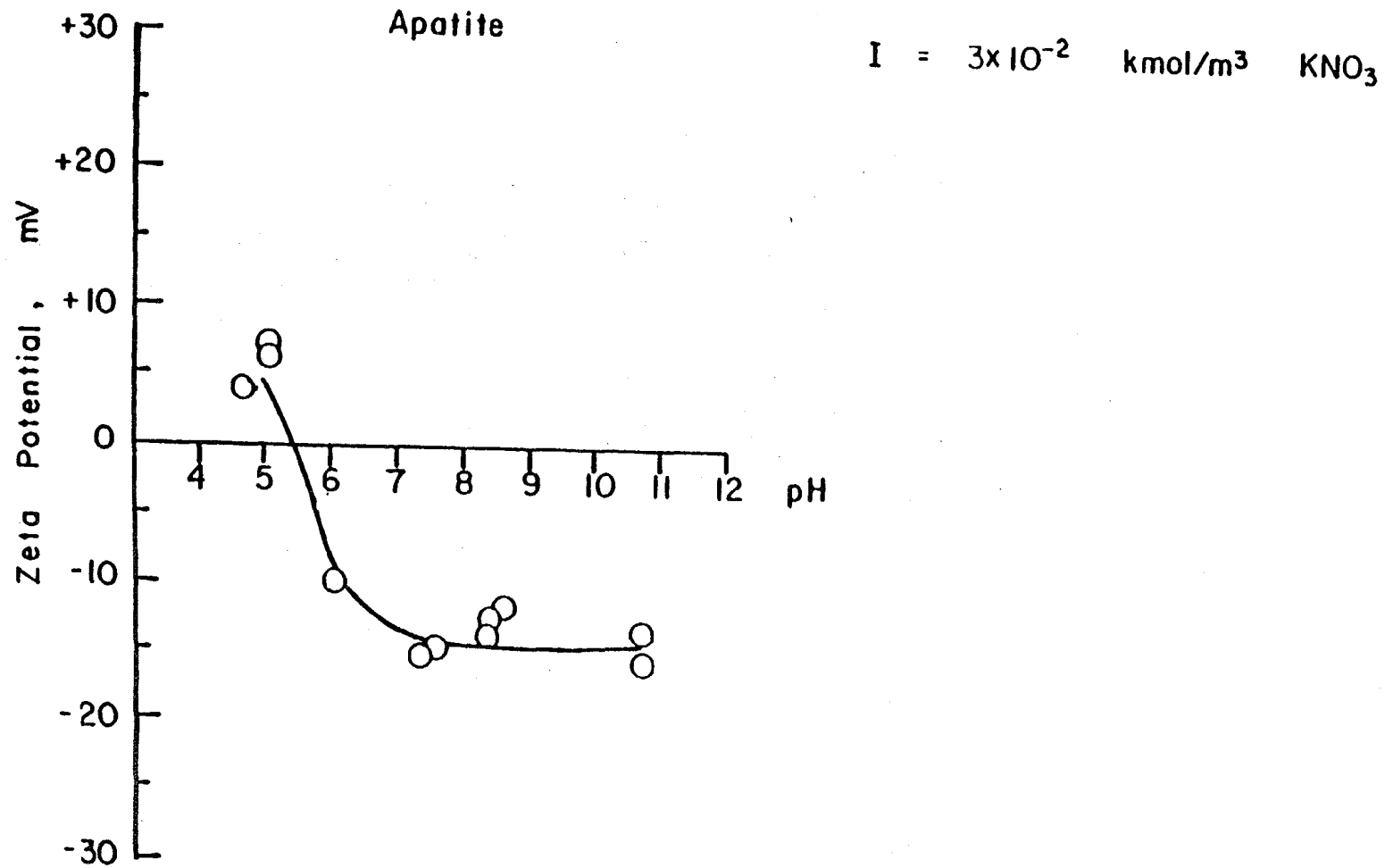


Figure 18. Zeta potential of apatite as a function of pH.

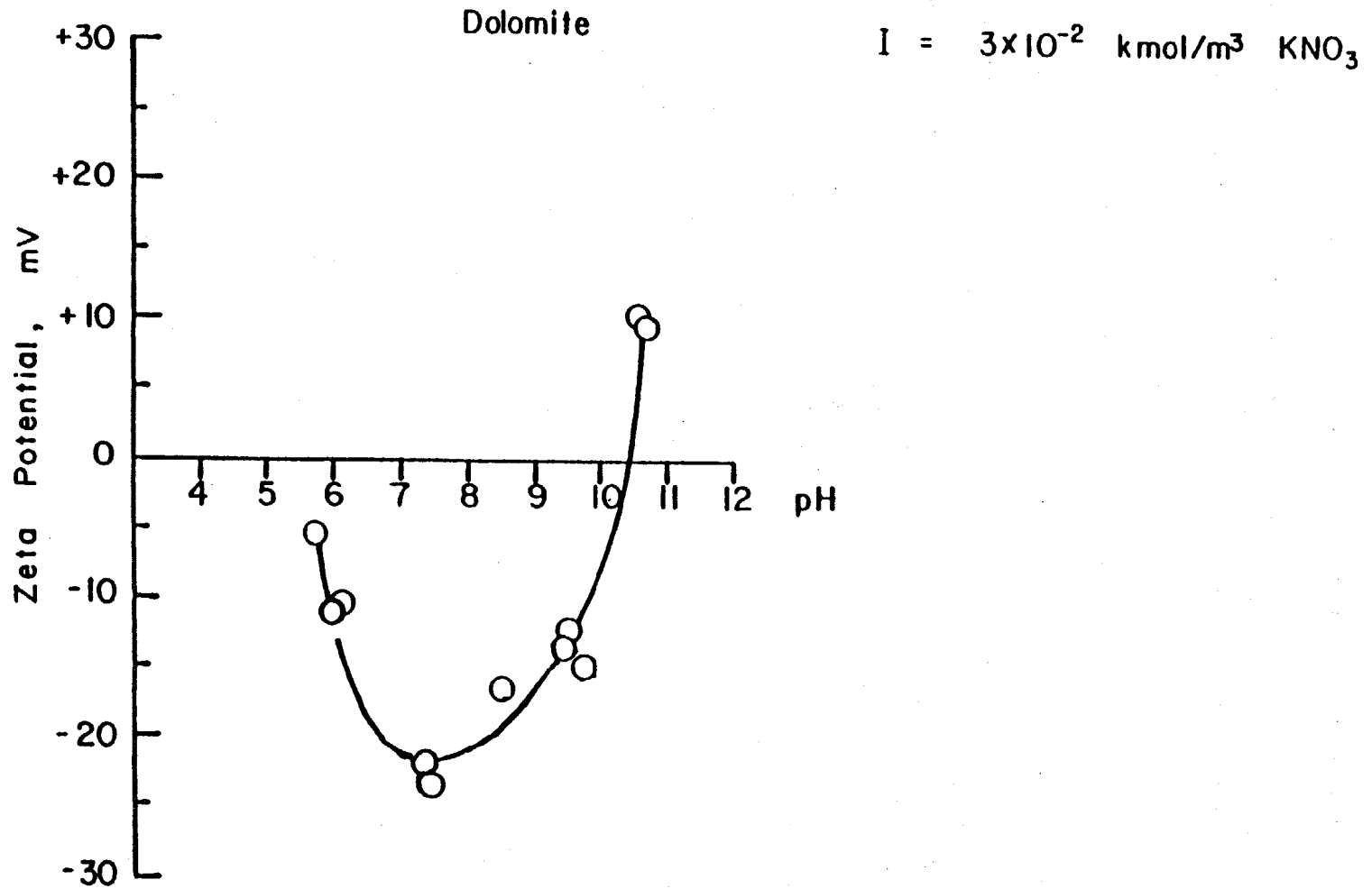


Figure 19. Zeta potential of dolomite as a function of pH.

surface. It is known that the $\text{Mg}(\text{OH})_2$ has an IEP at about pH 13, and therefore, the surface is positively charged at pH 11. Heterocoagulation between the minerals and transfer of hydroxylated surface species from dolomite to apatite under these conditions cannot be ruled out.

In the 95:5 apatite:dolomite mixture, apatite flotation is similar, but dolomite flotation is reduced by 15 percent from their respective single mineral flotation results. In this case, dolomite is not present in sufficient amount to alter the apatite surface. The smaller dolomite recovery value could be attributed to the presence of a large number of non-floating apatite particles in the suspension.

SUMMARY

Flotation behavior of single and mixed mineral systems was investigated as a function of the collector concentration over a pH range varying from 3 to 11. Selectivity, predicted by single mineral flotation test at pH 7 to 10 was not observed in mixed minerals. This is attributed to the depletion of oleate by precipitation with cations dissolved from dolomite. At pH 11, the loss of selectivity in mixed mineral systems is due to possible modification of the apatite surface when in contact with dolomite.

Chapter VII

THE TWO STAGE CONDITIONING PROCESS

INTRODUCTION

A two stage conditioning process was developed to separate dolomite from apatite. In this new process the mineral is conditioned first at an alkaline pH with a conventional fatty acid collector, then reconditioned in a second stage at acidic pH with the same collector solution before flotation. Separation of dolomite from apatite, which is recovered in the sink fraction, is achieved without adding any depressant or other modifying agent.

In this chapter, the basic study carried out in order to elucidate the mechanisms that explain the separation of dolomite from apatite by selective flotation after two stage conditioning with fatty acids is discussed. Also, the results of flotation tests performed at bench scale using this new process with different samples of dolomite and apatite are presented.

BASIC STUDIES

Experimental details of this study including minerals, chemicals and methods, have been described in the previous chapter. A complete analysis of dolomite and apatite samples used in this study is given in Table 1. Solubility of both minerals and mixtures of them in the pH range of 4.0 to 11.0 are presented in Figure 1 and Table 2.

Table 1
Chemical Analysis

Mineral	P ₂ O ₅ %	Fe ₂ O ₃ %	Al ₂ O ₃ %	Acid Insolubles	MgO %	CaO %	CO ₂ %	F %	Organic Matter, Carbon %
Apatite	36.78	0.42	0.93	3.34	0.12	50.35	1.68	3.82	0.19
Dolomite	1.67	0.94	0.96	5.11	17.58	32.33	42.16 (loss on ignition)	0.21	0.06

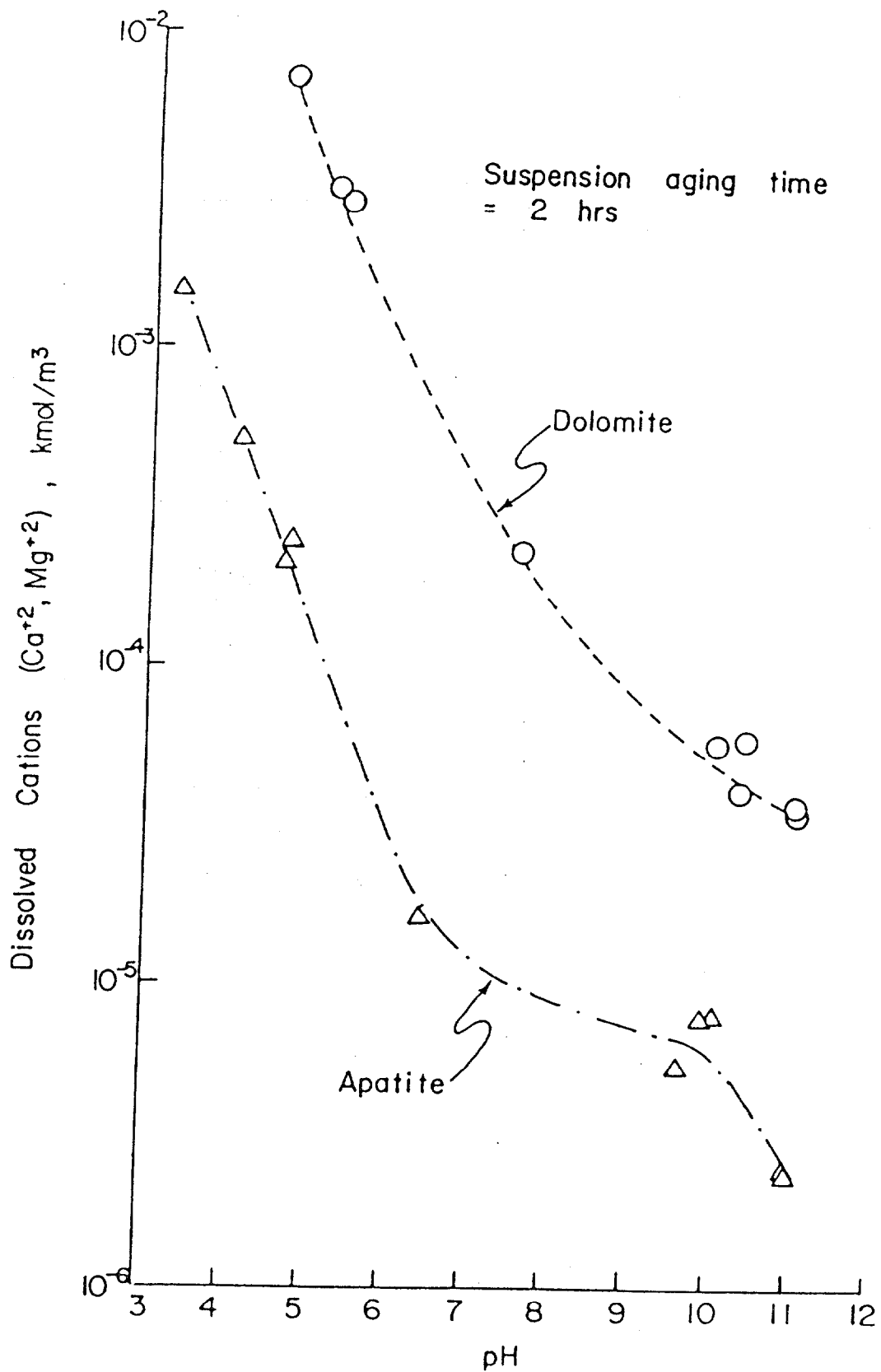


Figure 1. Effect of pH on the amount of cations dissolved from apatite and dolomite (65 X 100 mesh) 1 wt % slurry.

Table 2
Amount of Dissolved Calcium and Magnesium Ions

pH	Mineral	Ca ⁺² (ppm)	Mg ⁺² (ppm)
11.0	Apatite	0.1	0.0
	Dolomite	1.4	0.0
10.0 ± 0.3	Apatite	0.3	0.0
	Dolomite	1.2	0.4
	1:1 Mixture	0.9	0.3
	95:5 Mixture	0.3	0.0
7.0 ± 7.0	Apatite	0.6	0.2
	Dolomite	5.0	2.4
	1:1 Mixture	3.3	1.8
	95:5 Mixture	0.7	0.3
4.8 ± 0.3	Apatite	8.0	0.7
	Dolomite	70.0	32.0
	1:1 Mixture	50.0	15.0
	95:5 Mixture	10.0	1.4

1 ppm Ca⁺² = 2.5 x 10⁻⁵ kmol/m³

1 ppm Mg⁺² = 4.1 x 10⁻⁵ kmol/m³

Results and Discussion

Flotation After Reconditioning Without Changing Collector Concentration

In these tests, oleate concentration during conditioning and reconditioning was maintained constant. The variables tested were the initial collector concentration, reconditioning pH, reconditioning time and flotation time. The effect of initial collector concentration on flotation is plotted in Figure 2. The effect of reconditioning pH at a collector concentration of $1.87 \times 10^{-4} \text{ kmol/m}^3$, is illustrated in Figure 3. These results indicate that dolomite can be selectively floated out at a reconditioning pH below 5.5. It should be noted that selectivity observed for the 1:1 mixed mineral system is higher than that predicted by single mineral flotation behavior. To confirm the separation of the ore containing dolomite as a minor mineral, 95:5 apatite:dolomite mixture flotation tests were conducted. The results reported in Figure 4 indicate that effective separation of dolomite from apatite is possible. Reconditioning time was also tested to further optimize the separation of the two minerals. The results comparing the single mineral data to 1:1 and 95:5 mixtures are presented in Figures 5 and 6, respectively. It is observed that increased reconditioning time did not improve the selectivity significantly. The effect of flotation time on apatite recovery was also examined. Increasing flotation time from 1 minute to 4 minutes also did not improve the flotation recovery, indicating that complete flotation had occurred within the first minute.

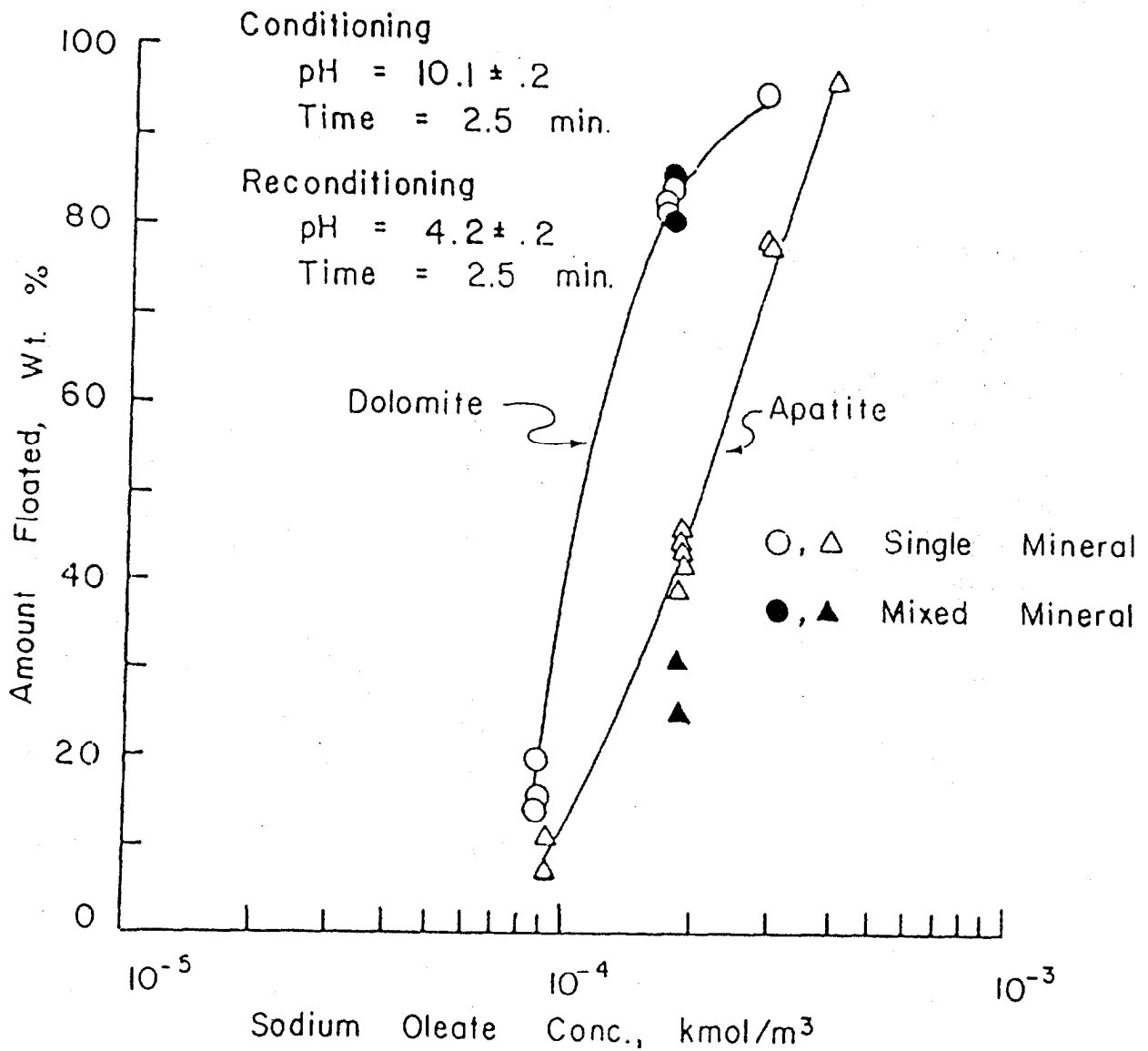


Figure 2. Flotation of apatite and dolomite after reconditioning at pH 4.2 as a function of initial collector concentration.

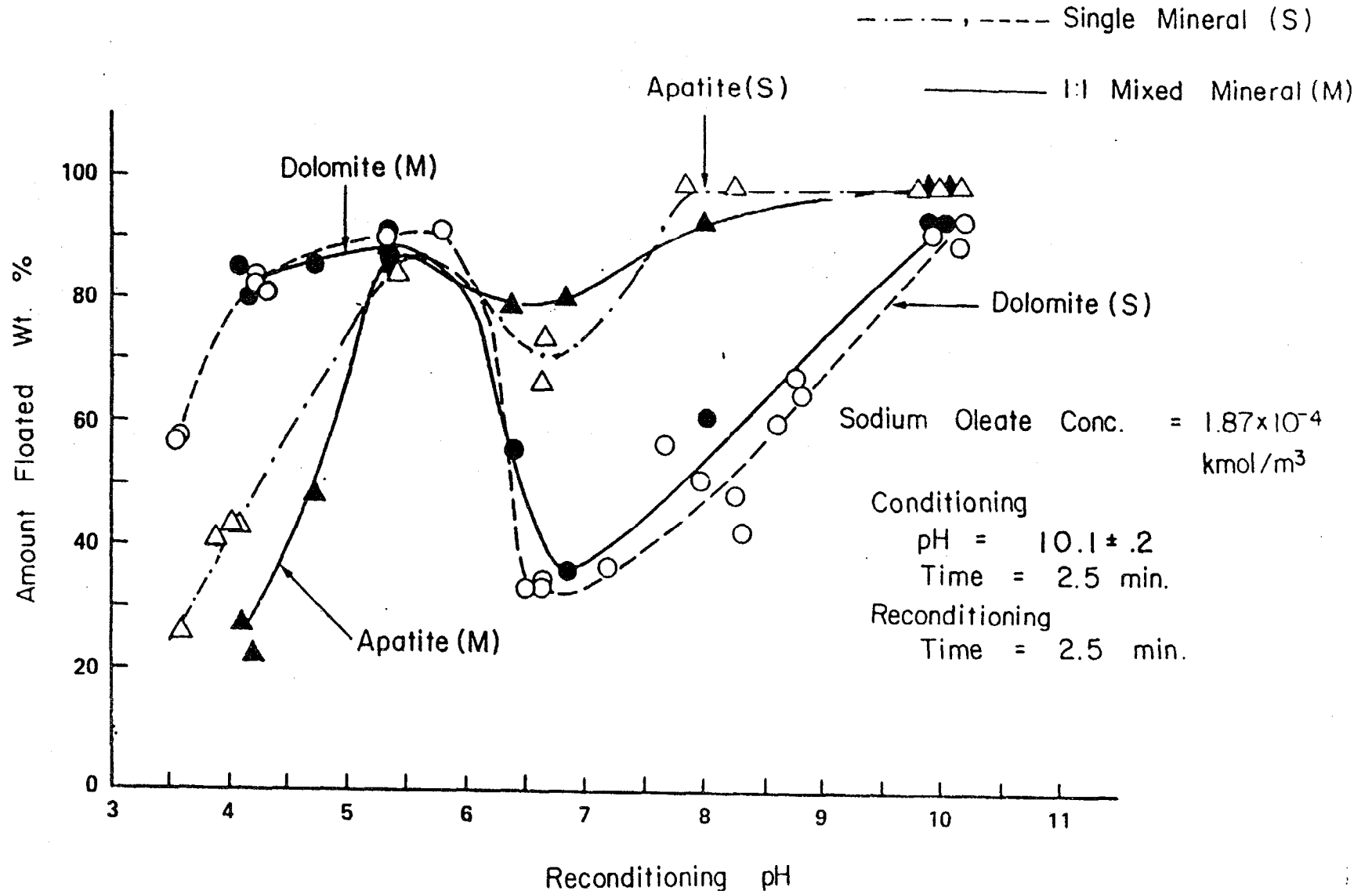


Figure 3. Flotation of apatite and dolomite as a function of reconditioning pH using 1.87×10^{-4} kmol/m³ sodium oleate concentration.

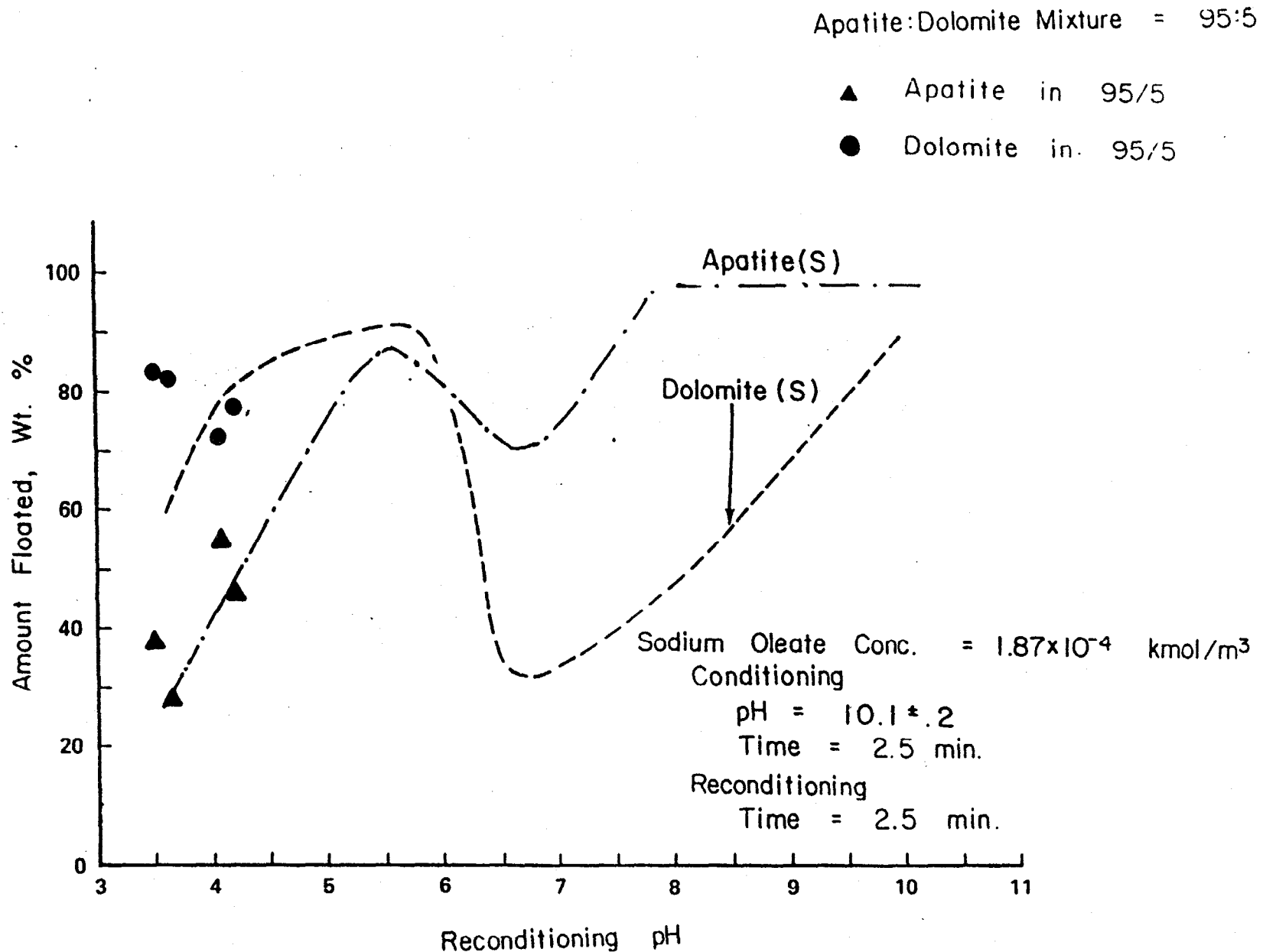


Figure 4. Flotation of 95:5 apatite:dolomite mixture as a function of reconditioning pH using 1.87×10^{-4} kmol/m³ sodium oleate concentration.

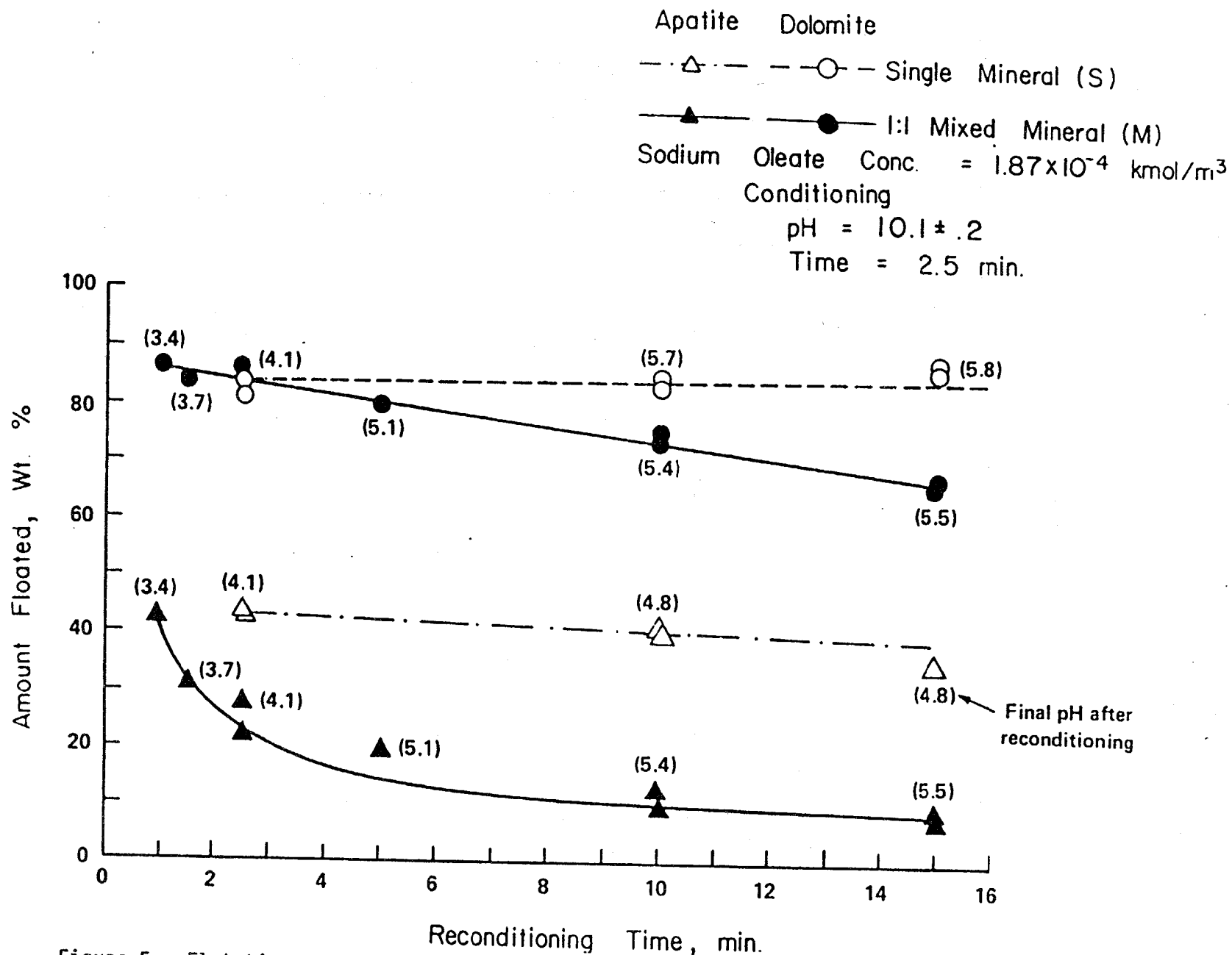


Figure 5. Flotation of apatite and dolomite as a function of reconditioning time (single and 1:1 mineral mixture).

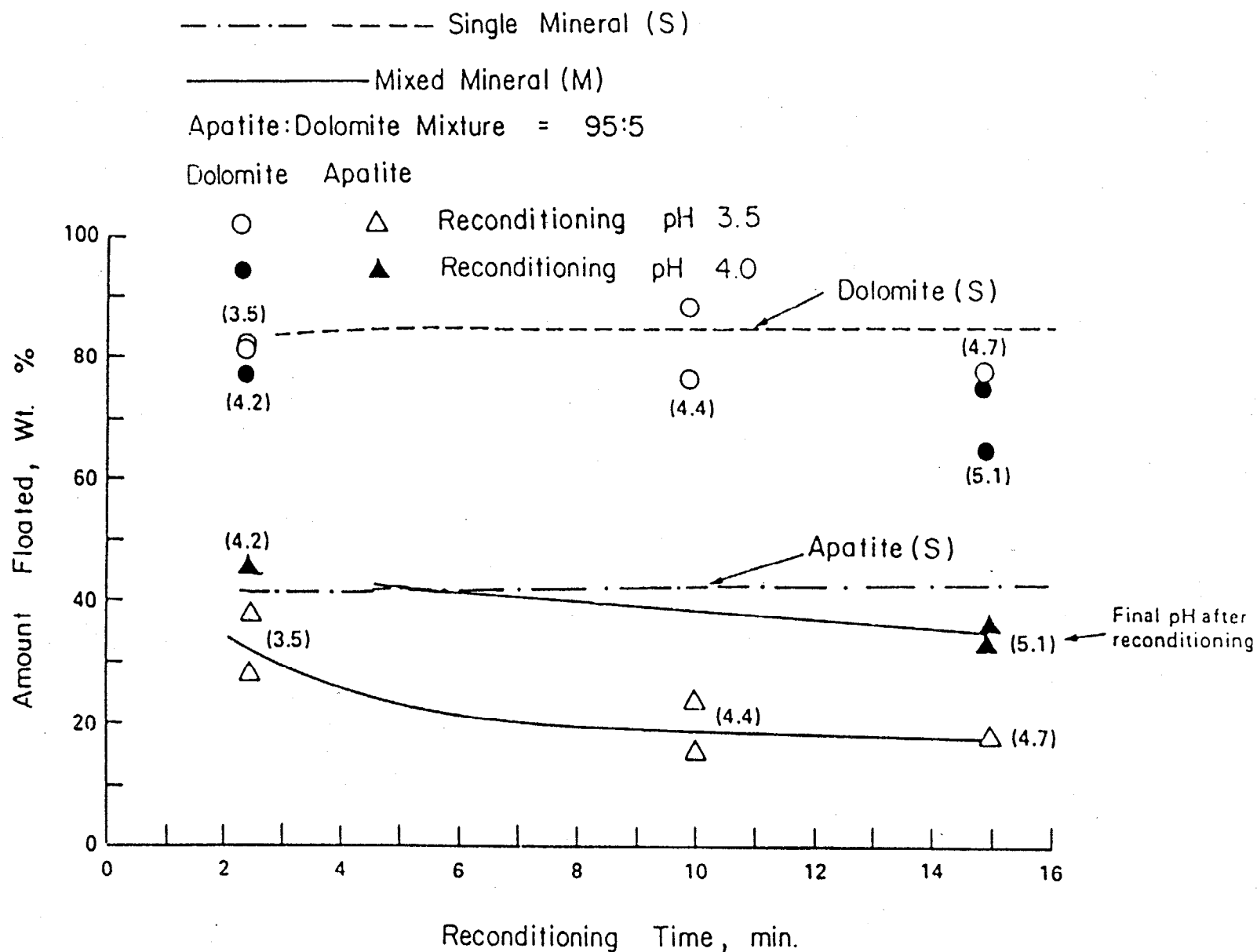


Figure 6. Flotation of 95:5 apatite:dolomite mixture as a function of reconditioning time.

Flotation After Reconditioning With Reduced Collector Concentration

In these tests the collector concentration during reconditioning was reduced by replacing 70 percent of the supernatant with water at different pH values. The effect of reconditioning pH on the flotation recoveries is illustrated in Figures 7 and 8. As in the previous case, the selective flotation of dolomite was observed at a reconditioning pH below 5.5.

Mechanism of Selective Flotation by Two-Stage Conditioning

Possible reasons for selective flotation of dolomite from apatite upon acid reconditioning are:

- (a) Selective desorption of collector molecules during reconditioning.**
- (b) Modifications in the effectiveness of the adsorbed collector upon reconditioning.**
- (c) Selective flotation of dolomite by CO₂ gas evolution under acidic pH conditions,**

Selective Desorption of Oleate Ions: This possibility was examined by measuring the amount of oleate adsorbed after reconditioning. No significant difference in the amount of oleate adsorbed after conditioning and reconditioning the minerals was observed (see Figures 9, 10, 11 and 12). It is therefore concluded that the selective desorption of the collector species from the apatite surface is not the major mechanism of the observed selective flotation.

It should be noted that the amount of oleate adsorbed on dolomite at pH 10.0 is higher than on apatite. Since the oleate adsorption did not change significantly upon reconditioning, the amount of oleate adsorbed on dolomite remained higher than on apatite after the reconditioning steps.

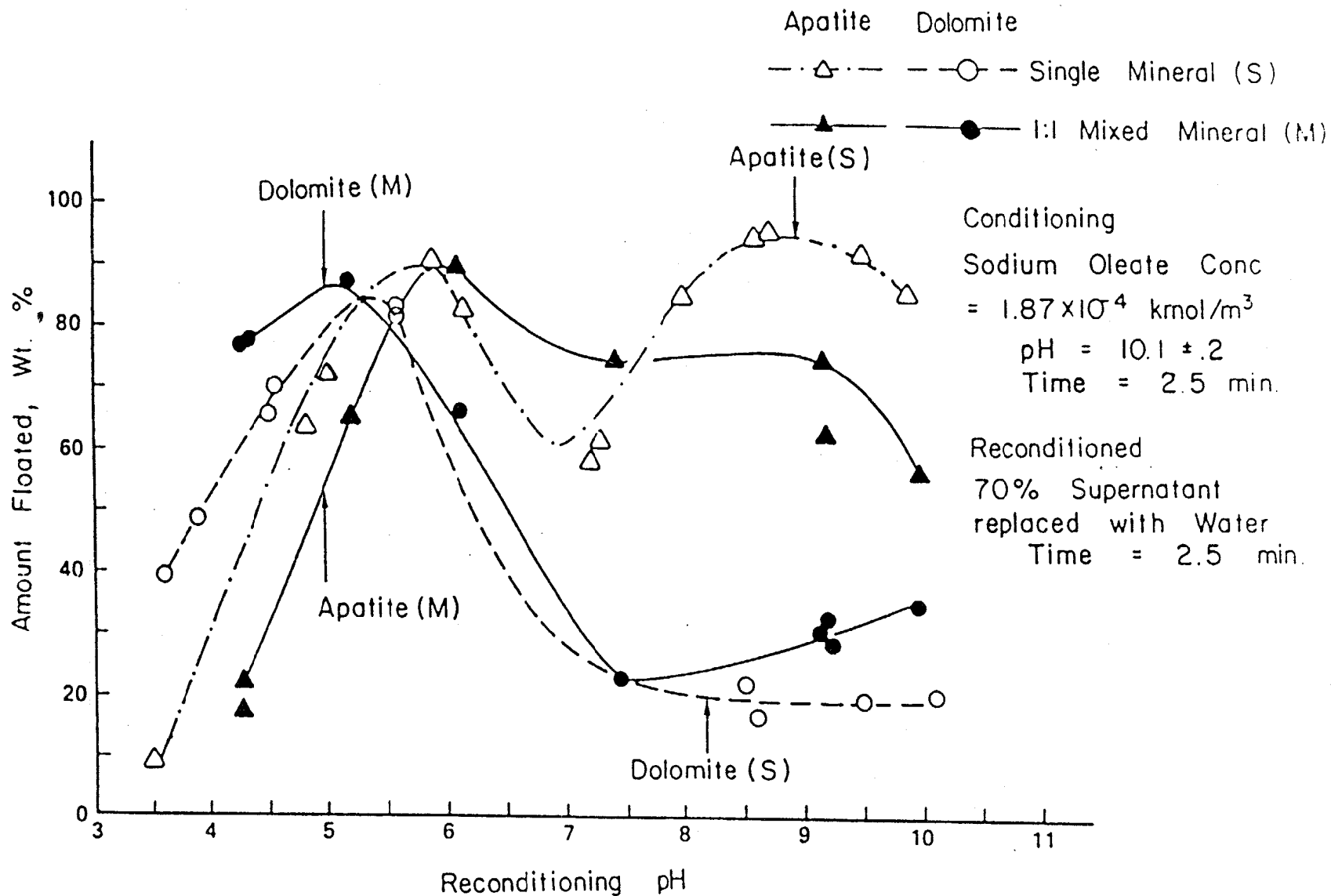


Figure 7. Flotation of apatite and dolomite as a function of reconditioning pH, with supernatant replaced with water.

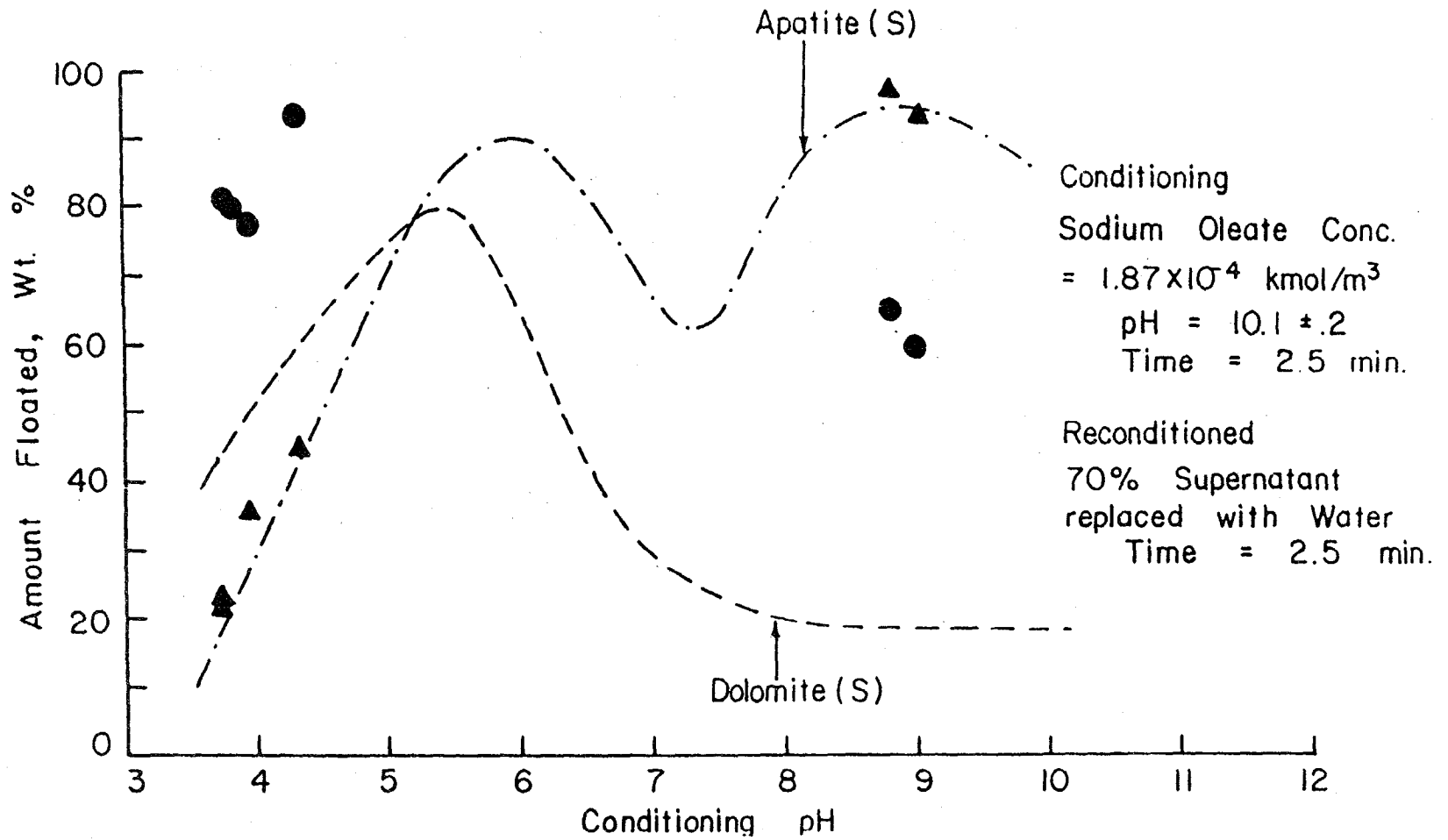


Figure 8. Flotation of 95:5 apatite:dolomite mixture as a function of reconditioning pH, with 70% supernatant replaced with water.

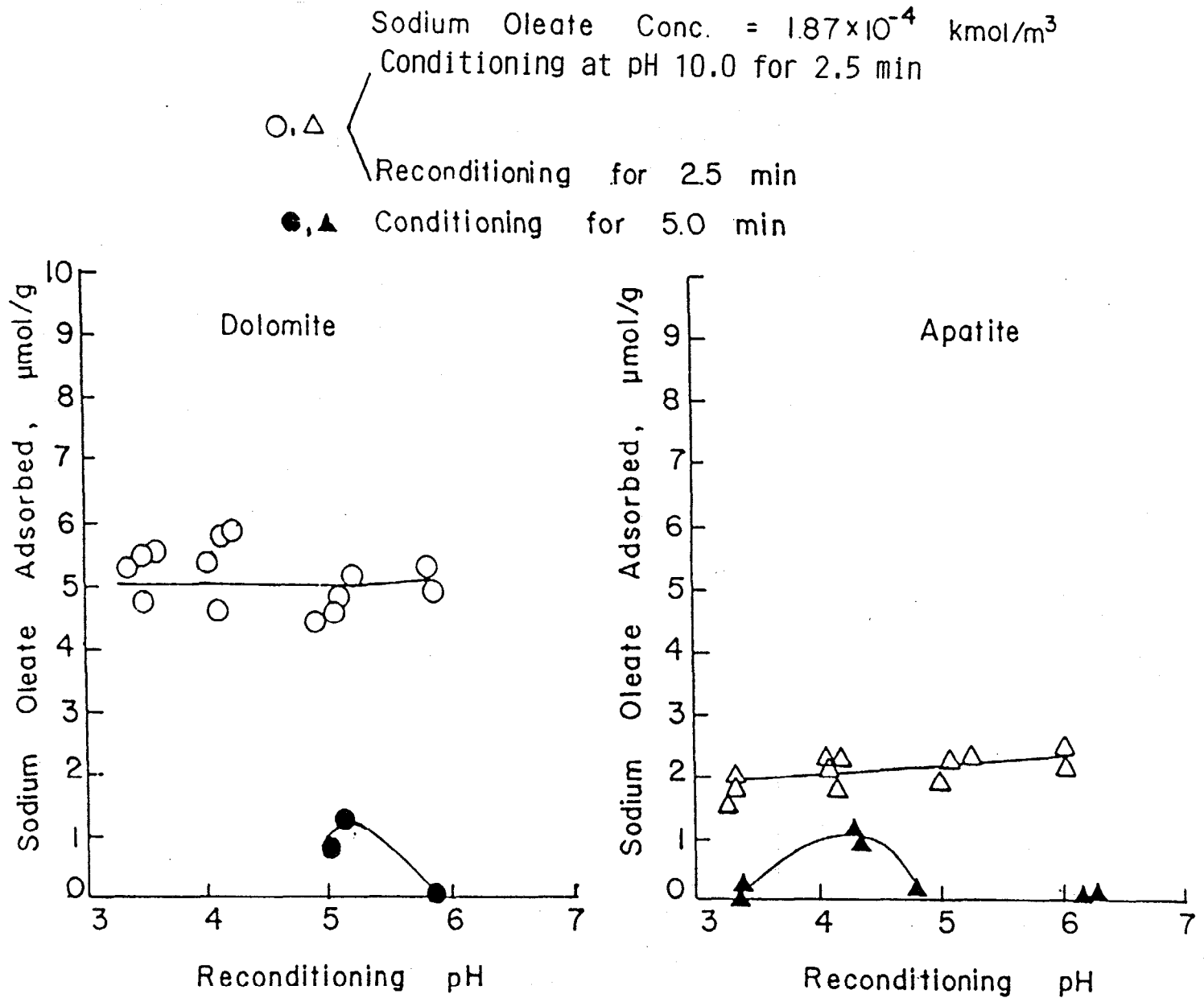


Figure 9. Amount of oleate adsorbed on apatite and dolomite as a function of reconditioning and conditioning pH.

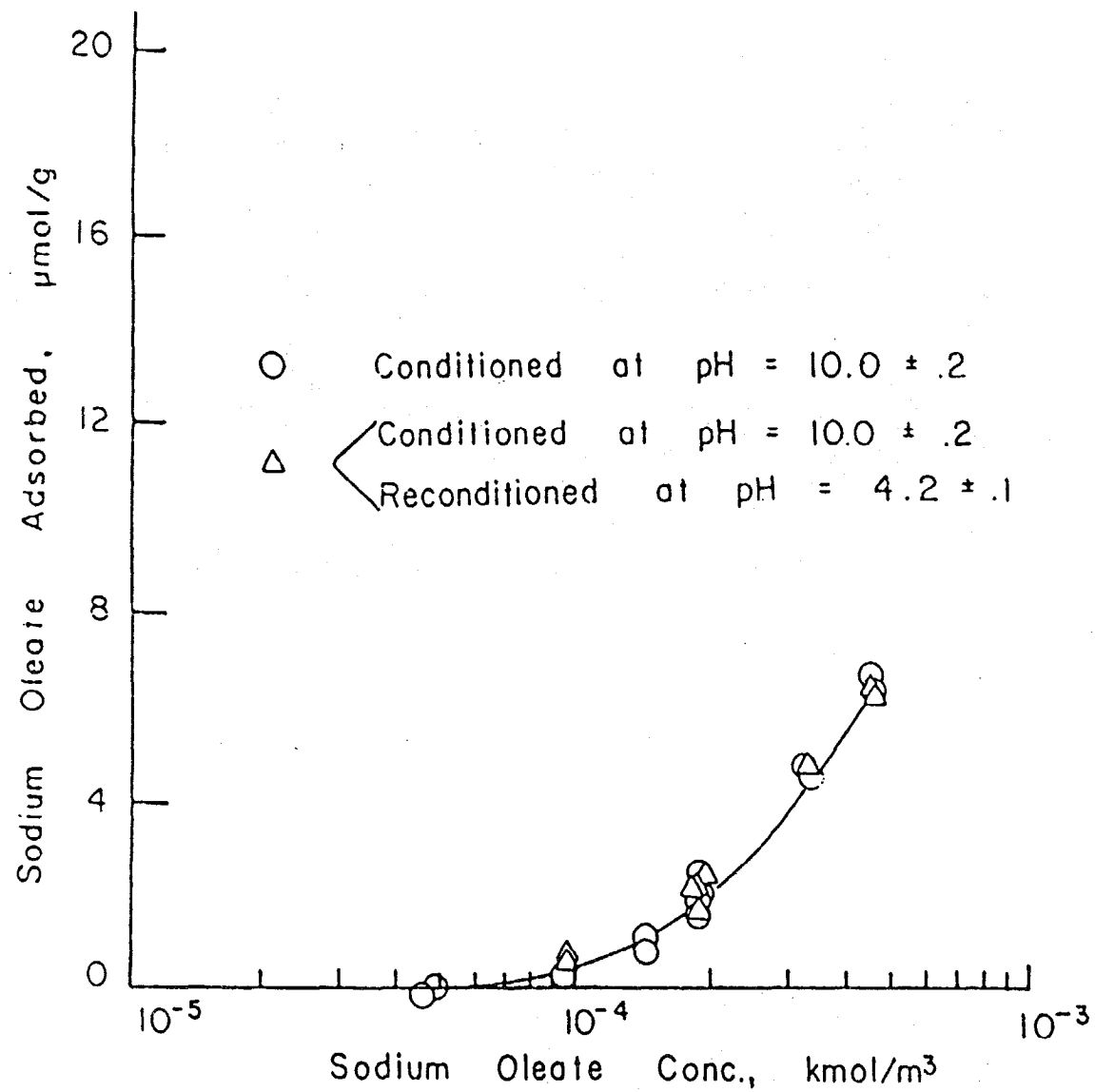


Figure 10. Amount of oleate adsorbed on apatite as a function of collector concentration after conditioning at pH 10.0 and reconditioning at pH 4.2.

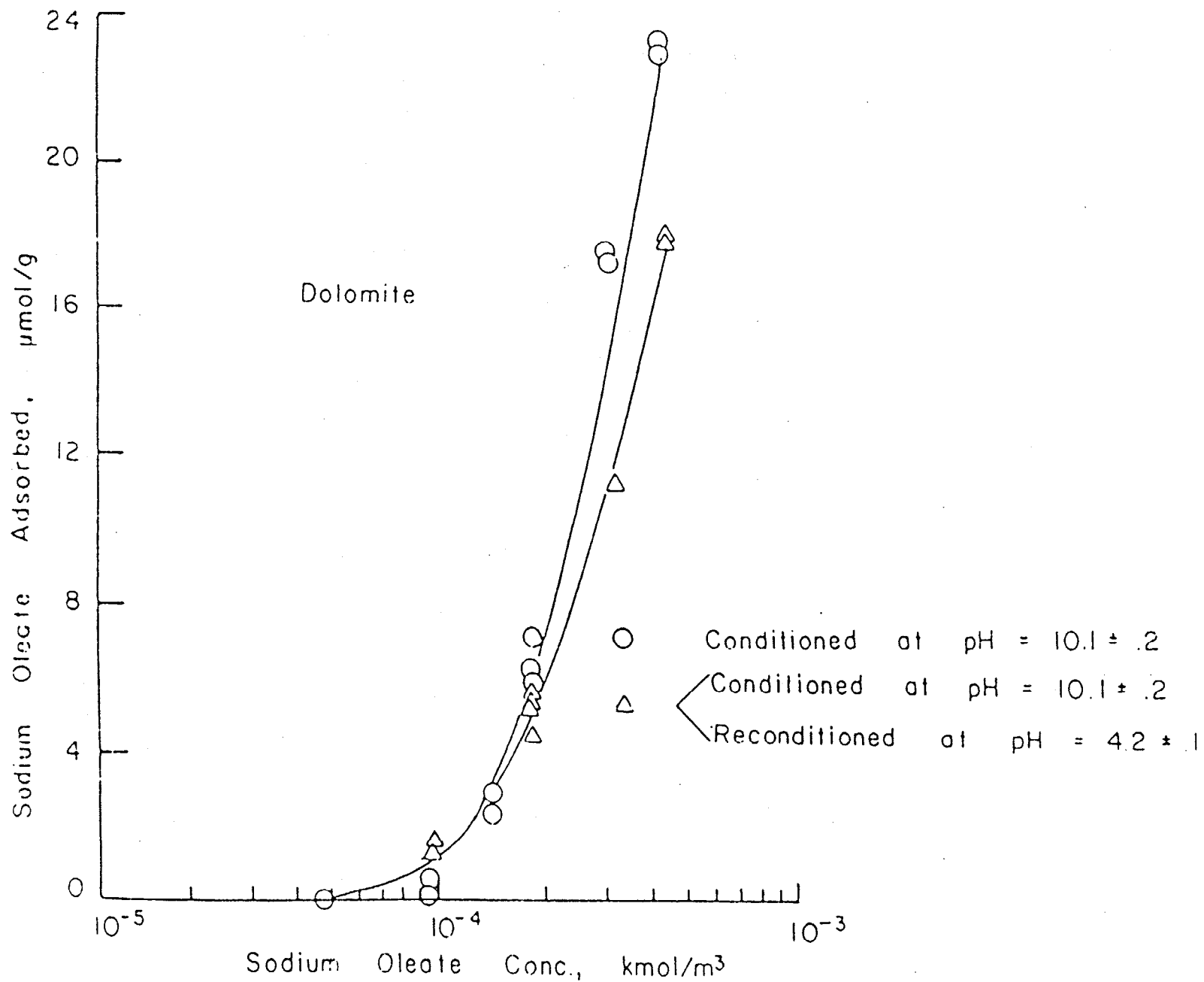


Figure 11. Amount of oleate adsorbed on dolomite as a function of collector concentration after conditioning at pH 10 and reconditioning at pH 4.2.

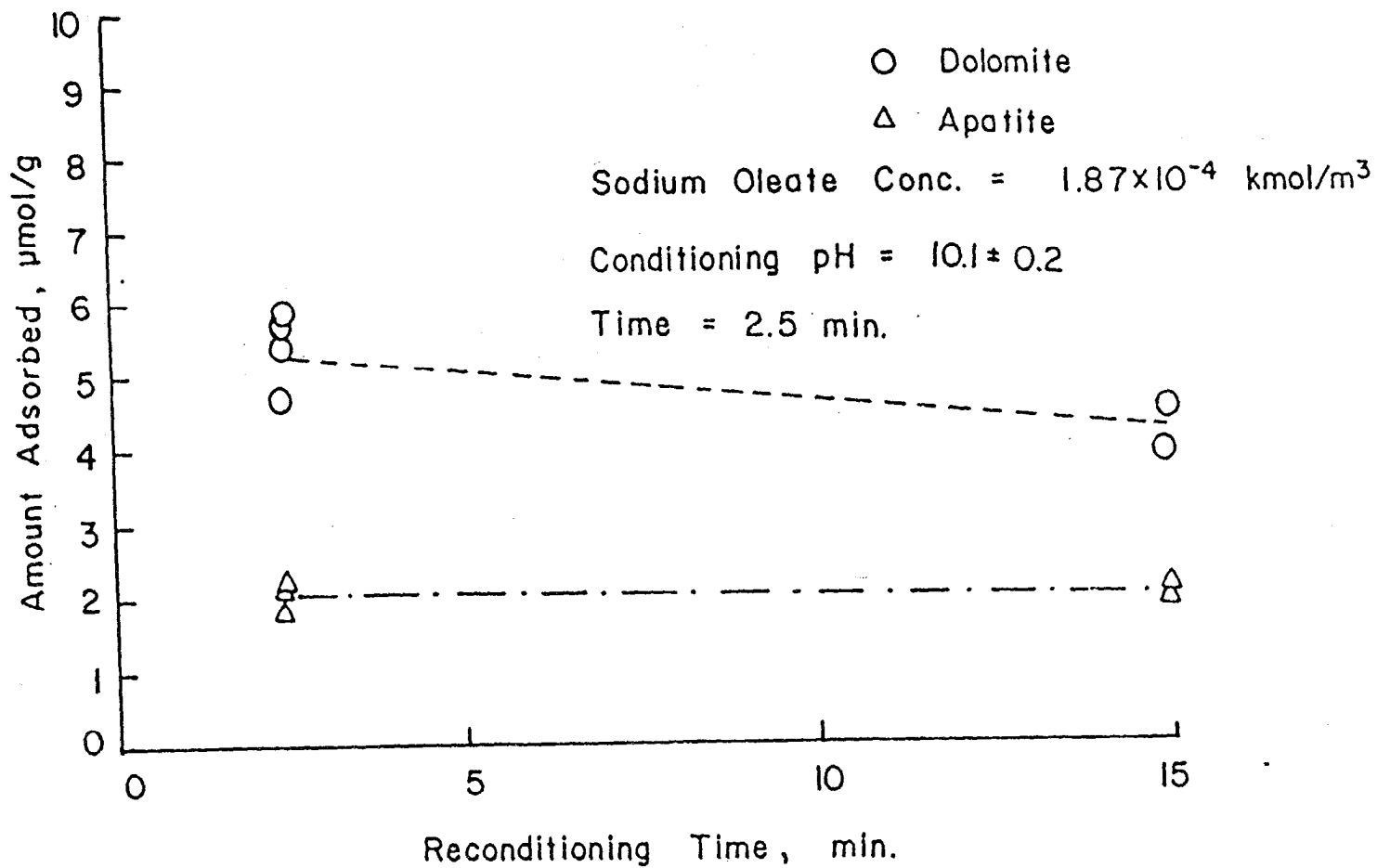


Figure 12. Amount of oleate adsorbed on apatite and dolomite as a function of reconditioning time.

Effectiveness of Adsorbed Species: The flotation response of apatite was considerably lower after reconditioning at pH 4.2, but the amount of oleate adsorbed was the same as at pH 10.0 (see Figure 13). On the other hand, the flotation response of dolomite did not change upon reconditioning (see Figure 14).

Transmission IR spectra, shown in Figure 15 and Figure 16, have confirmed the transformation of the adsorbed species on the apatite surface from oleate at pH 10.0 to oleic acid at pH 4.2. Similar information on the nature of the adsorbed specie could not be obtained for dolomite because of a strong carbonate peak located at the same frequency as the oleate peaks.

It has already been discussed (see section on conventional conditioning) that the effectiveness of neutral oleic acid in flotation as compared to the ionic oleate species is poor. Thus, after reconditioning at pH 4.2, the loss of apatite flotation recovery can be attributed to the nature of collector species present in the system

Similar collector response is expected in the case of dolomite. However, the experimental results do not show a significant difference between the flotation recovery after conditioning at pH 10 and after reconditioning at pH 4.2. This possibly could be attributed to the larger amount of the collector adsorbed initially at pH 10 on the dolomite surface.

CO₂ Gas Evolution on Dolomite: Dolomite, being a carbonaceous mineral, would react with acid to form CO₂ gaseous product. The evolved CO₂ gas should aid the flotation of dolomite by facilitating particle bubble attachment. It was, however, observed that evolution of CO₂ gas from the dolomite surface was not significant at pH 3.5. Furthermore, at lower pH values more CO₂ gas evolution is expected, which should result in higher dolomite flotation. On the

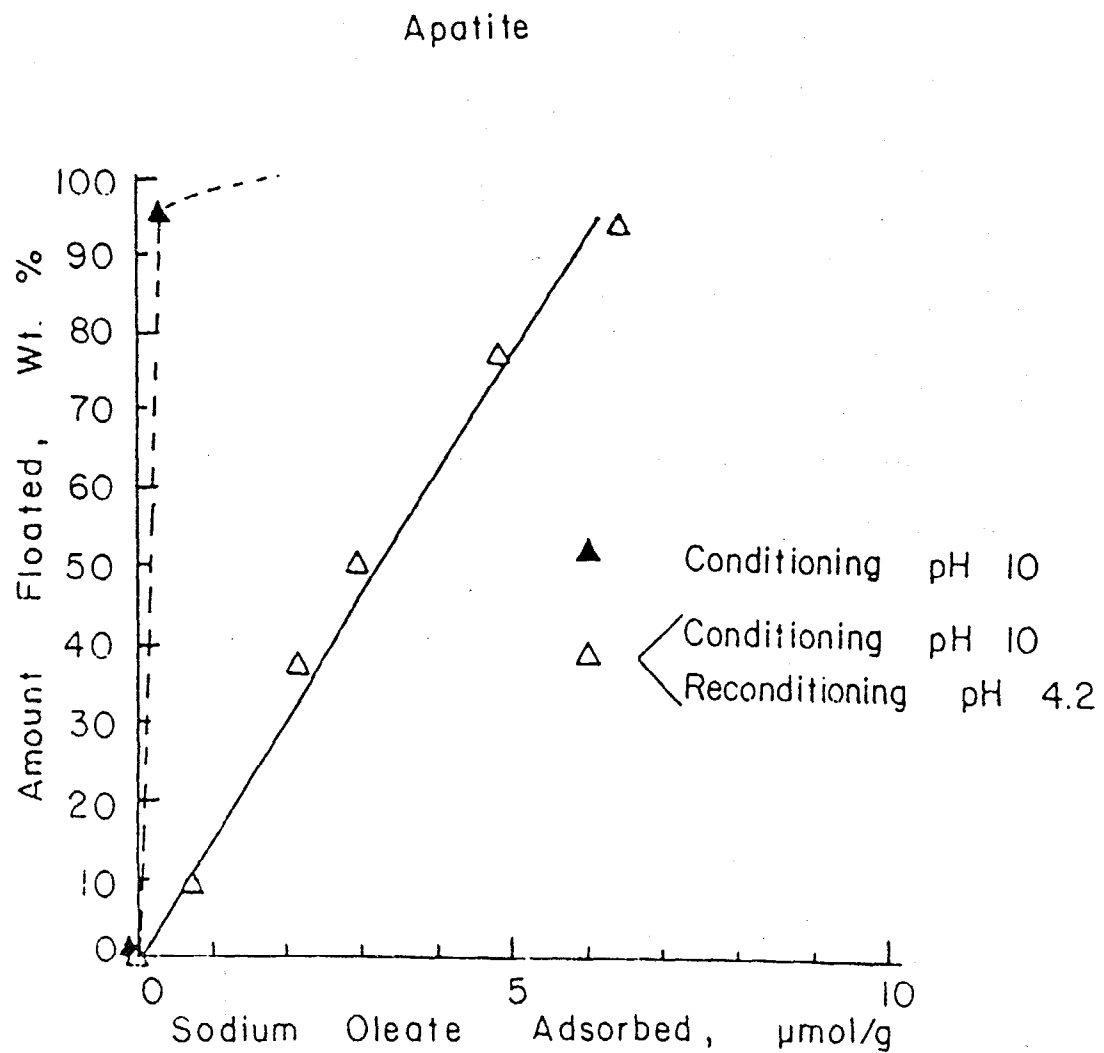


Figure 13. Flotation of apatite as a function of amount of oleate adsorbed after conditioning at pH 10 and reconditioning at pH 4.2.

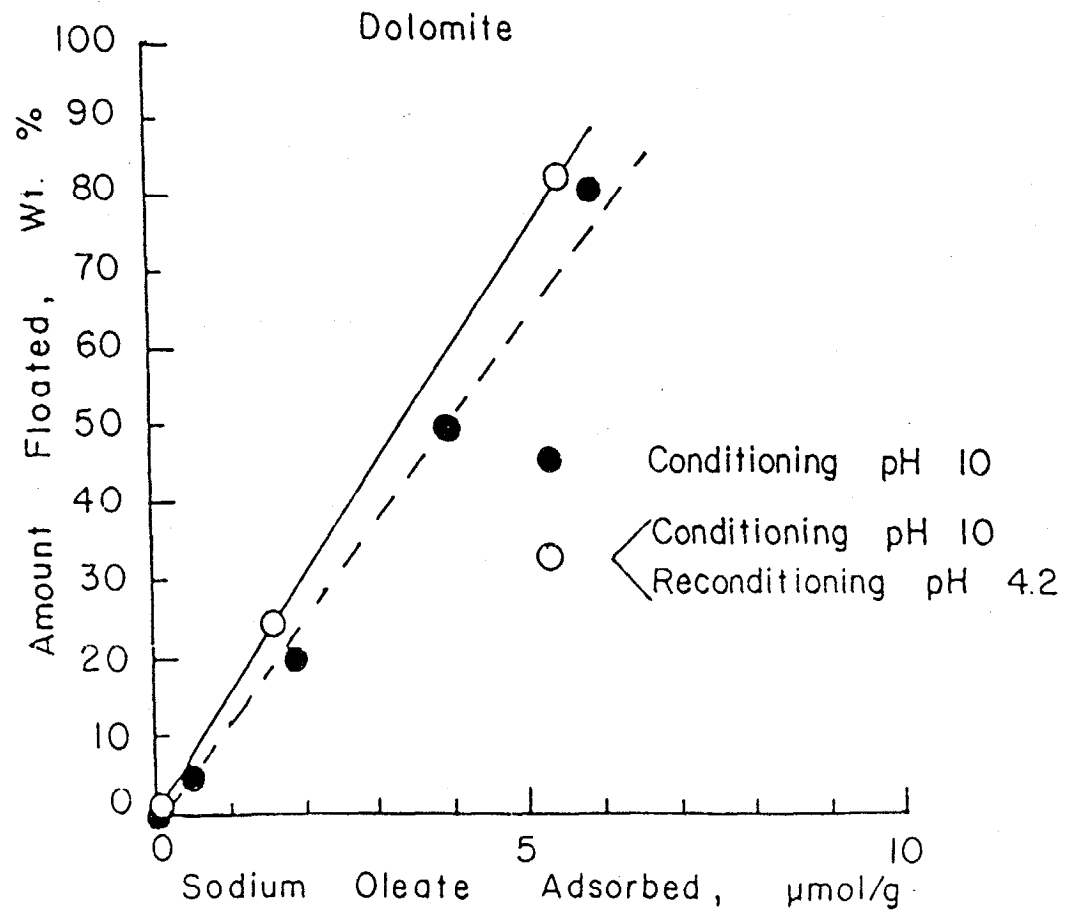


Figure 14. Flotation of dolomite as a function of amount of oleate adsorbed after conditioning at pH 10 and reconditioning at pH 4.2.

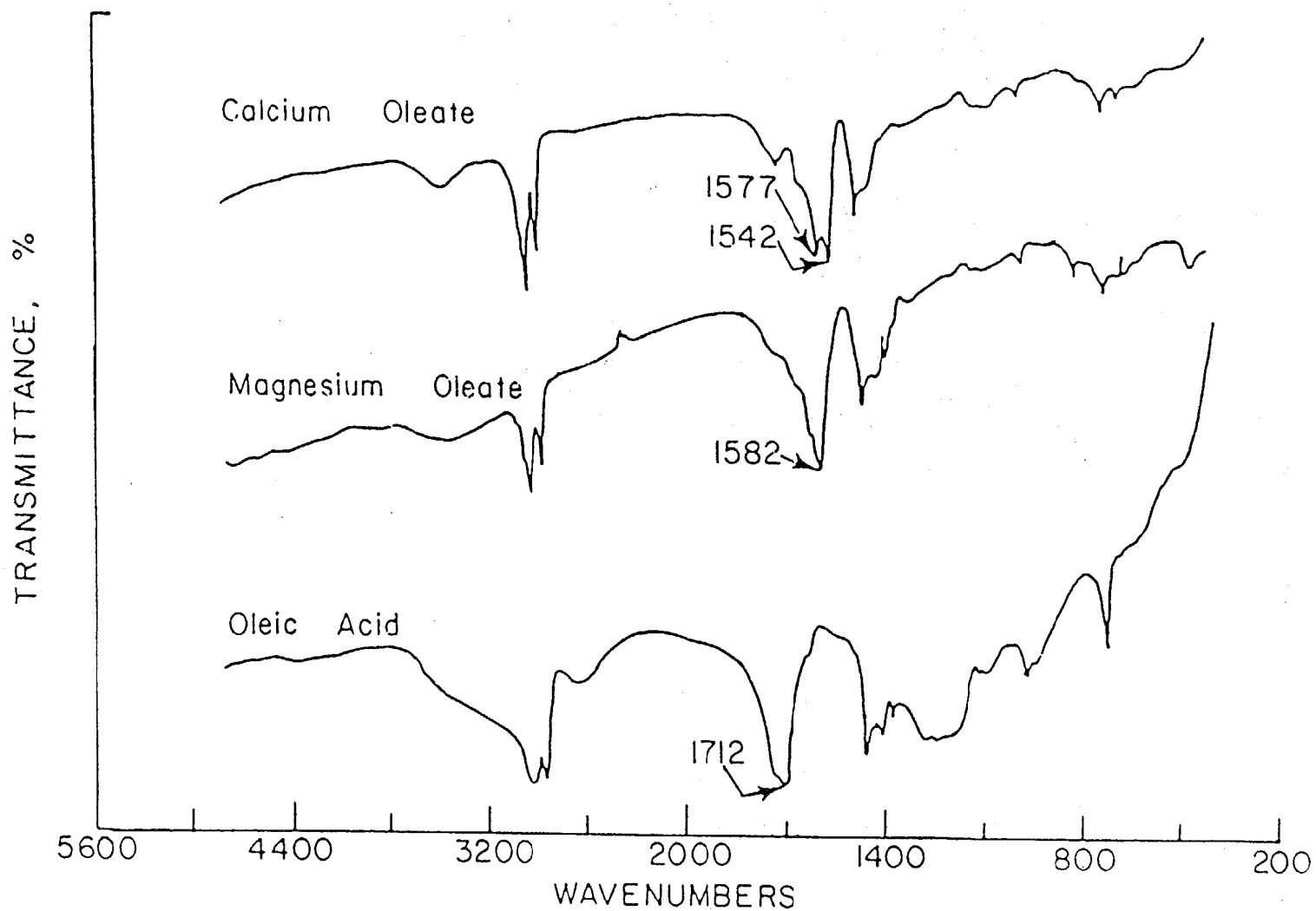


Figure 15. Transmission IR spectra of calcium oleate, magnesium oleate and oleic acid.

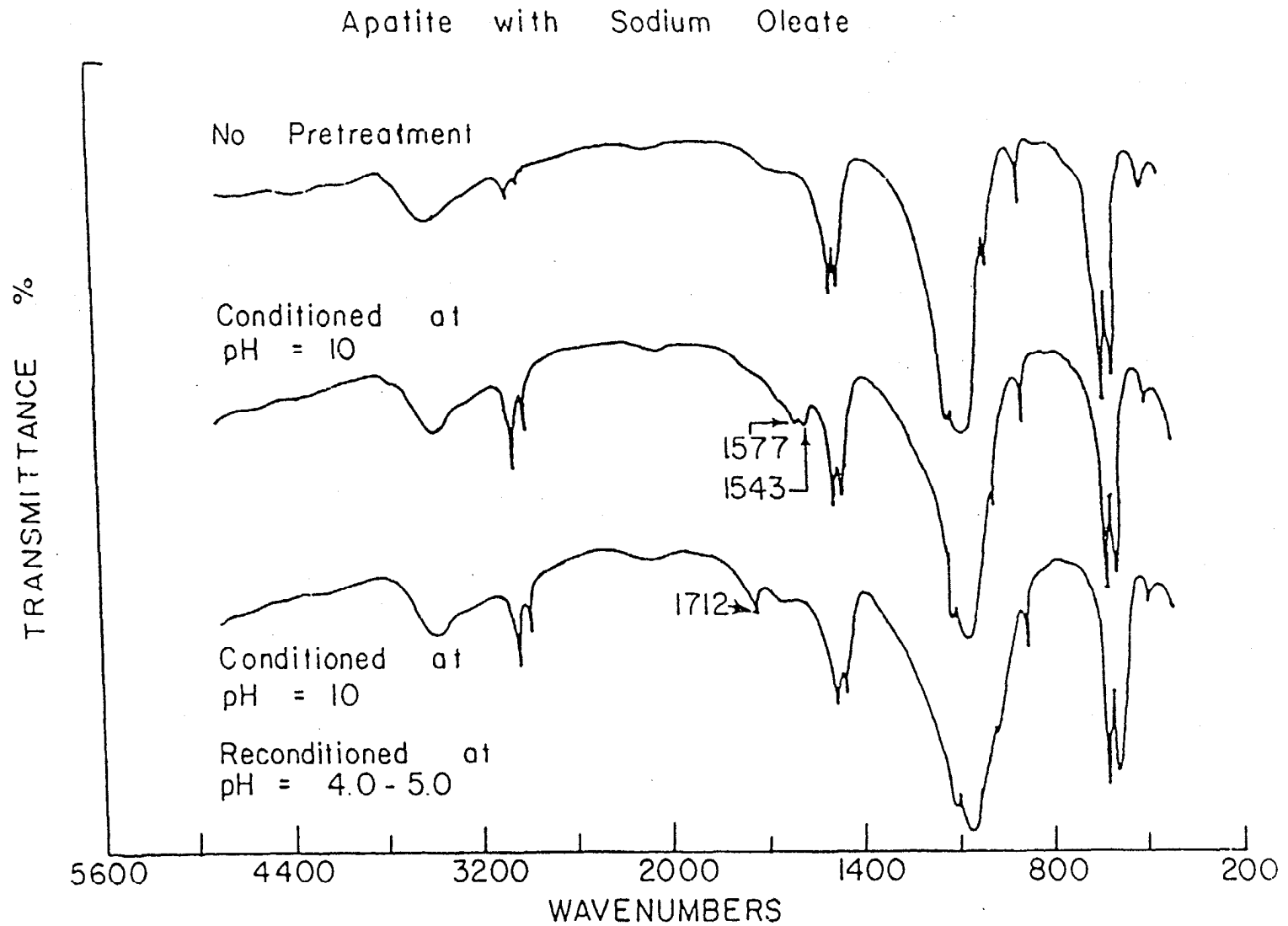


Figure 16. Transmission IR spectra of apatite, after conditioning at pH 10 and after two-stage conditioning.

contrary, flotation of dolomite was found to be lower after reconditioning at pH values below 4.

From the above discussion it can be concluded that the major mechanism of the adsorbed selectivity is the difference in the flotation response of the two minerals upon reconditioning. During conditioning at pH 10.0, there is a higher oleate adsorption on dolomite than on apatite. Upon reconditioning at pH below 6, no significant changes in the amount of collector adsorbed were observed for either of the two minerals. The nature of the adsorbed collector molecules does change, from ionic at pH 10 to neutral oleic acid molecules under acidic pH conditions. As an auxiliary effect, flotation of dolomite could be further aided by CO₂ gas evolution. This could explain the selective flotation of dolomite after acid reconditioning and higher separation in the mixed minerals system

According to this mechanism the amount adsorbed during the conditioning stage at pH 10.0 governs the flotation after the reconditioning stage. In the presence of additional Ca⁺² and Mg⁺², dissolved from dolomite in a 1:1 mixed mineral system oleate adsorption on apatite would be reduced (refer to Figures 17 and 18). Consequently, apatite flotation after acid reconditioning would be lower, resulting in higher separation of the minerals in the mixed mineral systems as compared to that predicted on the basis of single mineral flotation behavior.

Relevance of Two-Stage Conditioning Process to Current Processing Schemes

In the entire reconditioning pH range studied, the maximum separation was obtained by reconditioning the minerals at a pH below 4.5. In view of the objective of this study to separate dolomite from South Florida phosphate

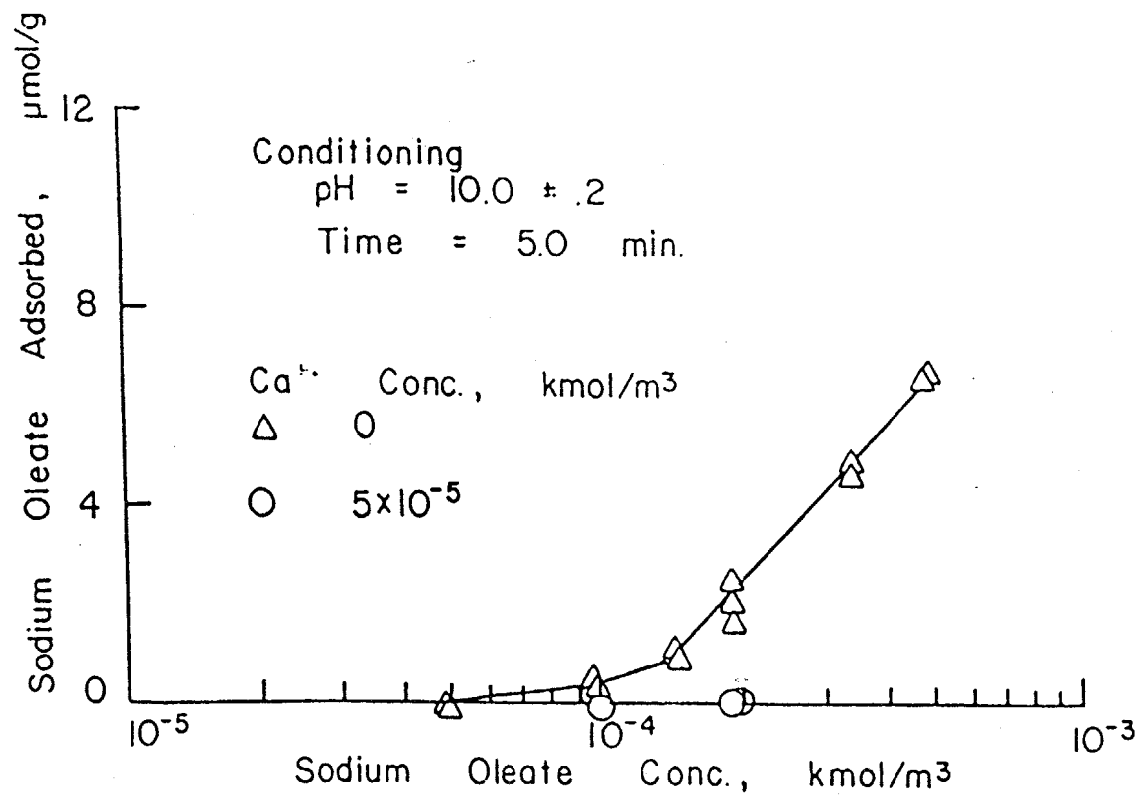


Figure 17. Effect of Ca²⁺ ions on the amount of oleate adsorbed on apatite as a function of collector concentration.

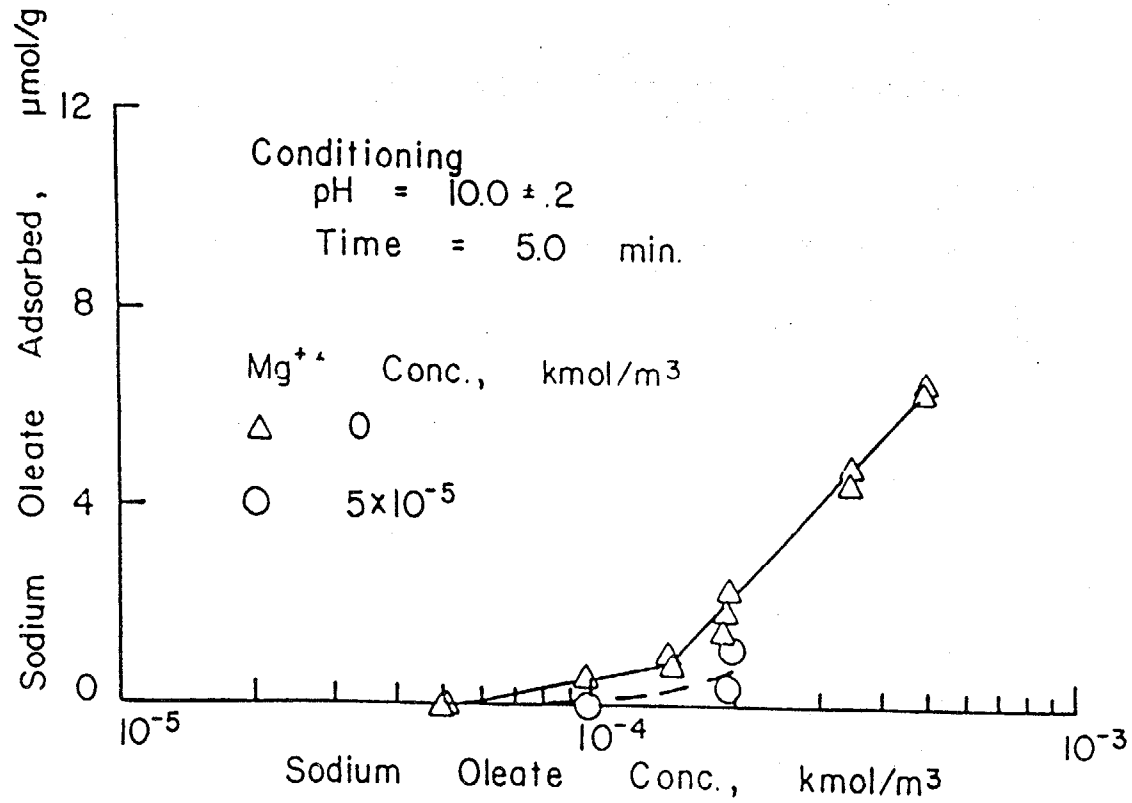


Figure 18. Effect of Mg^{+2} ions on the amount of oleate adsorbed on apatite as a function of collector concentration.

rock, the two-stage conditioning process, if proven to be effective on large scale, offers unique benefits, some of which are:

- (a) Overall separation of the minerals is higher than that obtained by conventional conditioning.
- (b) Observed selectivity for mixed minerals is better than predicted by single mineral flotation tests.
- (c) Dolomite, the minor mineral in the mixture, is floated. This is preferred for higher process efficiency.
- (d) Separation of dolomite from apatite has been achieved without adding any other surface active or surface modifying agents.
- (e) The currently practised flotation scheme in a phosphate processing plant does allow for acid scrubbing at a pH lower than 4. Therefore, no additional reagent should be involved in incorporating the second conditioning step in the current process.

Further studies were conducted to examine the feasibility of the two-stage conditioning method at bench scale. The results obtained are discussed in the following sections.

BENCH SCALE FLOTATION TESTS

The objective of these tests was to determine if the trends observed in the flotation tests in the Hallimond cell using two stage conditioning could be verified at the bench scale.

Several dolomite and apatite samples of different origin and two natural ore samples from the Florida field were used in this phase of the study.

Materials

Apatite

Two different apatite samples were used in the bench scale flotation tests. An amine concentrate, 16 x 150 mesh, from the AMX Phosphate Co. was used in some of the earlier tests, but most of the study was performed with a high grade product from Agrico Chemical Co.

The high grade product from the Agrico Chemical Co. was screened to provide 35 x 65, 65 x 100, 100 x 150, and for later tests, 35 x 150 mesh. These samples were then leached, deslimed 10 times, dried at 50°C, and stored in glass bottles. The BPL content of the composite sample was 74.6%, with an MgO content of 0.37%.

Dolomite

A total of four different samples of dolomite were used in the bench scale testing of the two stage conditioning process.

New Jersey Crystalline Dolomite: The 16 x 150 mesh size fraction of New Jersey crystalline dolomite from Wards Scientific Co. was prepared by first reducing the dolomite pieces using a circular saw, followed by passing them through a Bico-Braun Chipmunk Crusher, and finally, through a Bico-Braun UA Pulverizer. The required size was obtained by sieving the ground material. After washing ten times to remove excess fines produced during the size reduction process, the material was dried at 50°C and stored in a glass jar.

Agrico Dolomite: Large size pieces of hand picked bottom dolomite from the Agrico Chemical Co. were dried in an oven at 50°C and reduced in size with a hammer before grinding in a rod mill. Batch samples of one kg were ground in the rod mill for 12 seconds and then the material was dry screened on a Ro-Tap Siever to separate the 35 x 150 mesh and the oversize recycled to the mill.

After using a hand magnet to remove iron impurities, the 35 x 150 mesh dolomite was wet sieved to remove the coating of fines on the particles, and then dried in an oven. Finally a high tension separator from CarpcO, Inc., Jacksonville, Florida, was used to remove the quartz thus reducing the acid insoluble content to 3.1%.

IMC Four-Corners Dolomite: This dolomite was a much harder type than the Agrico dolomite, and was reduced with the Chipmunk Crusher without excessive material loss through fines production. Following size reduction, the material was washed with deionized water, then dried at 50°C. A hand magnet was used to remove iron impurities and silica grains were removed using the electrostatic separator.

Perry Dolomite: A pure dolomite sample obtained from Cabbage Grove in Perry, Florida, was ground in a Bico-Braun Chipmunk crusher, pulverized in a Bico Pulverizer, and screened to the same size fractions as the apatite samples. The various size fractions were passed through a CarpcO Magnetic Separator to remove any iron impurity. The samples were then deslimed 10 times, dried at 50°C, and stored in glass bottles. The MgO assay of the composite material was 19%.

Natural Phosphate Ore: A natural high MgO feed was obtained from the Agrico Chemical Co. The sample was dried at 50°C and screened to eliminate the +35 mesh material and stored. During testing, the samples were deslimed in deionized water one time prior to use. The assay of the sample was 52.7% Insols, 28.84% BPL, (13.2% P₂O₅) and 2.4% MgO.

A different natural ore sample described as "Hawthorne brown feed" was provided by Brewster Phosphates. Chemical analysis of this sample indicated 8.3% P₂O₅, 61% Insolubles, and 20% MgO. This sample was used as received except that the +35 mesh material, about 10% of the total, was screened out.

Chemicals

Collectors: Purified sodium oleate from Fisher Scientific, and fatty acid (M28), and fuel oil, supplied by Westvaco Co., were used in this study.

Frother: Aerofroth 65 from American Cyanamid Co. was used in this study.

pH modifiers: ACS certified grade potassium hydroxide and sulfuric or nitric acid were used for pH adjustments.

Water: Deionized water was used for all tests.

Methods

Chemical Analysis

Analysis for BPL content was performed with a Bausch and Lomb Spectronic 2000 spectrometer. MgO content was determined by either an Instrumentation Laboratory Model 200 inductivity coupled plasma spectrometer, a Perkin Elmer 6000 atomic adsorption spectrometer, or in the case of synthetic mixtures, by calculations based on the BPL content of the sink fraction. Details of the various procedures are given in Chapter II.

Flotation

Flotation tests were carried out using a Denver D-2 flotation cell at 1100 rpm. The pH during conditioning and flotation was adjusted either manually or with a Brinkman Metrohm Herisau Multi Dosimat titrator. Three different conditioning procedures were used: in earlier tests the pulp was conditioned by tumbling, but this method was eventually discarded because control of pH in the closed container was impossible, therefore the conditioning was carried out directly in the flotation cell at 1100 rpm or in a beaker stirred at 200-400 rpm with a paddle type stirrer. A detailed description of the three procedures is given below.

Two Stage Conditioning by Tumbling: Samples were aged for 2 hours in deionized water at pH 10.0 and at varying pulp densities. The slurry was then transferred to a one liter bottle and tumbled at 24 rpm for 2.5 minutes. Nine hundred ml of the supernatant was removed, and the pH was lowered to 2.6 using sulfuric acid. The supernatant was returned to the one liter bottle and the mineral suspension was tumbled for an additional 2.5 minutes. The slurry was next transferred to the Denver cell, frother was added, and floated until completion. The impeller speed was 1100 rpm during flotation. The various fractions were filtered, dried, and weighed.

Two Stage Conditioning in the Denver Cell: Samples (65 x 100 mesh) were aged for 2 hours in deionized water at pH 10.0 and at a pulp density of 4.0%. The slurry was then transferred to the Denver cell and conditioned at 1100 rpm for 2.5 minutes after adding the required amount of the collector. Then, 1000 ml of the supernatant was removed. The pH of the supernatant was lowered to a value that would yield a final pH of about 4 after returning to the cell. Next, frother was added and the suspension was further conditioned for 2.5 minutes at 1100 rpm. The solution pH was maintained at 4 during conditioning. Due to the high agitation intensity it was difficult to keep a constant acidic pH. The air valve was turned on and floated to completion. The float and sink fractions were filtered, dried, and weighed.

Two Stage Conditioning with Paddle Type Stirrer: In order to more closely simulate present plant conditions, and also to maintain closer control over pH, it was decided to condition the slurry by agitating in a separate vessel with a paddle type stirrer. It was determined that agitation for 30 minutes between 200 and 400 rpm depending on pulp density, gave optimum results.

Solution pH was maintained at pH 10.0 using the Brinkman titrator. At the end of the aging period, the collector was added, and the suspension conditioned for an additional 2.5 minutes. Frother was added during this step. Then the pH was lowered to a value below 4.0, and further conditioned for 2.5 minutes. The slurry was next transferred to the Denver cell, and floated until completion. During flotation, solution pH was kept constant by adding appropriate amounts of 0.1N H₂SO₄.

Results and Discussion

Single Minerals

The flotation results from single mineral tests for Anax apatite and New Jersey dolomite are presented in Table 3. It is observed that apatite did not float while under the same conditions more than 80% of the dolomite floated. Other apatite and dolomite samples exhibited similar flotation behavior. For example, flotation after two-stage conditioning of Agrico apatite and Perry dolomite yielded negligible flotation of apatite whereas about 87% of dolomite was recovered in the float fractions (see Table 4). Also, a new fatty acid type collector, a sulfonated oleic acid (OA-5) yielded very high recoveries of dolomite after two stage conditioning while apatite showed a very limited flotability (see Table 5). These results confirmed selectivity observed using the Hallimond cell at the bench scale. However, the Agrico dolomite yielded poor flotation results. In Table 6 it is shown that the dolomite yielded recoveries of only about 40% even when large amounts of collector were added. Since this dolomite was found to be softer than other samples, it was thought that the lower recoveries could be due to the generation of slimes during conditioning. Also, removal of the reagent coating due to attritioning during conditioning could not be ruled out (as shown in Table 7). This was

corroborated by the increased recoveries obtained when conditioning was carried out at lower agitation intensity. However, even under these favorable conditions, recoveries of dolomite were in the range of 50-60% significantly lower than recoveries obtained with the other dolomite samples tested.

Table 3

**Flotation of Apatite and Dolomite
after Two-Stage Conditioning**

Feed: Apatite (Amine Concentrate)
Dolomite (New Jersey crystalline)
Collector: M 28, 2.0 lb/t
Extender: IMC fuel oil, 4.0 lb/t
Conditioning: 2 min at pH 10.0
Reconditioning: 5 min at pH 4.0

Feed	Amount Floated, wt. %
Amax Apatite	0.2
New Jersey Dolomite	86.3, 83.6

Table 4

**Flotation of Apatite and Dolomite after
Two Stage Conditioning**

Collector: M 28, 1.6 lb/t
Extender: IMC fuel oil, 1.6 lb/t
Conditioning: 2 min at pH 10.0
Reconditioning and Flotation: at pH 4.0

Feed	Amount Floated, wt. %
Agrico Apatite	1.0 - 1.7
Perry Dolomite	86.6 - 87.9

Table 5

**Flotation of Apatite and Dolomite after Two-Stage
Conditioning Using OA-5 as the Collector**

Feed: Apatite (Amine Concentrate)
Dolomite (New Jersey crystalline)
Collector: OA-5, 3.0 lb/t
Extender: IMC fuel oil, 6.0 lb/t
Conditioning: 2 min at pH 10.0
Reconditioning: 2 min at pH 10.0

Feed	Amount Floated, wt. %
Anax Apatite	7.7
New Jersey Dolomite	89.7, 89.5

Table 6

**Flotation of Agrico Apatite and Dolomite
after Two Stage Conditioning**

Feed: Apatite (Agrico High Grade Product)
Dolomite (Agrico)
Collector: M 28
Extender: IMC fuel oil
Frother: Aerofroth 73 (Dolomite: .12 lb/t,
Apatite: .05 lb/t)
Conditioning: 2 min at pH 10
Reconditioning: 5 min at pH 4.

	Amount Floated Wt %	Collector Concentration* lb/t
Feed	6.0	10.0
Agrico Apatite	5.1	19.0
Agrico Dolomite	18.7	39.6

* 1:1, M 28: fuel oil ratio.

Table 7

Flotation of Agrico Apatite and Dolomite After
Conditioning at Lower Agitation Intensity

Feed: Apatite (Agrico High Grade Product)
Dolomite (Agrico)
Collector: M-28
Extender: IMC fuel oil
Frother: Aerofroth 73 (Dolomite: .12 lb/t,
Apatite: .05 lb/t)
Conditioning: 6 min at pH 10.0
Reconditioning: 5 min at pH 4.0

Feed	Amount Floated, wt%	
	Collector Concentration*, lb/t	
	6.0	10.0
Agrico Apatite	12.6, 4.7	--
Agrico Dolomite	51.8, 46.1, 34.3	63.3, 58.5

* 1:1, M-28:fuel oil ratio.

Agrico Dolomite-Agrico Apatite Mixture

A limited reduction in MgO content of mixtures of Agrico dolomite and apatite was obtained by flotation after two stage conditioning. The MgO content of the feed, as shown in Table 8, was reduced from 6.4 to 4.6% MgO at a recovery of 70% of the phosphate values. This performance can be attributed partially to the soft character of this dolomite sample and also to the presence of interlocked apatite in the dolomite grains.

Quantifying the relative amounts of each type of particle in the feed versus the float and sink fractions was accomplished by taking representative samples of each fraction and counting the individual particles as they were observed under the microscope. The results obtained are summarized in Table 9. It can be clearly seen from the data that the majority of the pure dolomite particles reported in the float fraction, while those particles containing dolomite in an apatite matrix and the pure apatite grains reported to the sink fraction. Thus, a separation of the pure dolomite from the pure apatite grains had taken place after two stage conditioning.

Characterization of the Dolomite Particle Surface Using the SEM with EDS:

Examination of the data presented in Table 9 indicated that those particles which are comprised of dolomite embedded in an apatite matrix tend to report to the sink fraction along with the pure apatite grains. This would suggest that the surface composition of these particles primarily consists of apatite. In an effort to confirm the presence or absence of apatite mineral on the surface of particles reporting to the sink fraction, specimens of representative samples of the float and sink fractions were prepared for examination under the SEM utilizing the energy dispersive X-ray spectrometer (EDS) to map the location of the various elements.

Table 8

Flotation of 1:1 Agrico Apatite and Dolomite
Mixture After Two Stage Conditioning

Feed: Agrico apatite
Agrico dolomite
Collector: M-28, 6.0 lb/t
Extender: IMC fuel oil, 6.0 lb/t
Frother: Aerofroth 73, .12 lb/t
Conditioning: 6 min at pH 10.0
Reconditioning: pH 4.0

	BPL, %	MgO, %	BPL Recovery, %
Feed	46.26	6.41	100
Concentrate (Sink Fraction)	48.73	4.56	70.12

Table 9**Comparison of Feed, Float and Sink Fractions from a
Two Stage Conditioning Test Using Agrico Dolomite (-65 mesh)**

Sample	Total Number of Grains Counted	Percent of Grains in Each Category					Quartz
		Pure Apatite	Apatite with Small Dolomite Content	Apatite with Mderate Dolomite Content	Apatite with Large Dolomite Content	Pure Dolomite	
Feed	232	10.0	18.0	8.0	2.0	59.0	3.0
Float	464	2.0	4.0	0.5	0.5	93.0	0.0
Sink	188	11.0	55.0	9.0	6.0	14.0	5.0

Initial efforts involved examination of individual grains of apatite and dolomite to study the different topography of the two minerals. X-ray scans were then run on these particles to obtain their characteristic spectral data. At this point, particles which were known to contain interlocked apatite and dolomite were examined under different levels of electron beam voltage, X-ray rate, dwell time of beam on specimen, and particle dispersion on specimen stage. This methodology maximized data acquisition and efficiency while at the same time minimized interference from both elements within the particles or from adjacent particles.

The grains from each fraction were mapped for P, Ca, Mg and Si by selecting the appropriate energy levels to be counted by the detector, and then creating an image based on the pulses received by the detector as it scans the sample. The black and white images displayed on the CRT as a result will be composed of dots of varying density, with areas of high density appearing light and areas of low density appearing dark. By assigning colors to the grey (intensity) scale, it is possible to further highlight the areas of high element concentration.

A series of color photographs of images produced in this manner are presented in Figures 19 and 20, along with their corresponding black and white back-scattered electron image. In the color photographs, blue shades represent areas of low intensity (or background). Areas of high intensity, and hence high element concentration, are represented by the red-yellow hues.

In Figure 19, an apatite (smooth) particle and a dolomite (granular) particle were isolated and the image area magnified to include only these particles. The mapping scan revealed the smooth particle to have a high concentration of P on its surface, with some small scattered spots of Mg. On

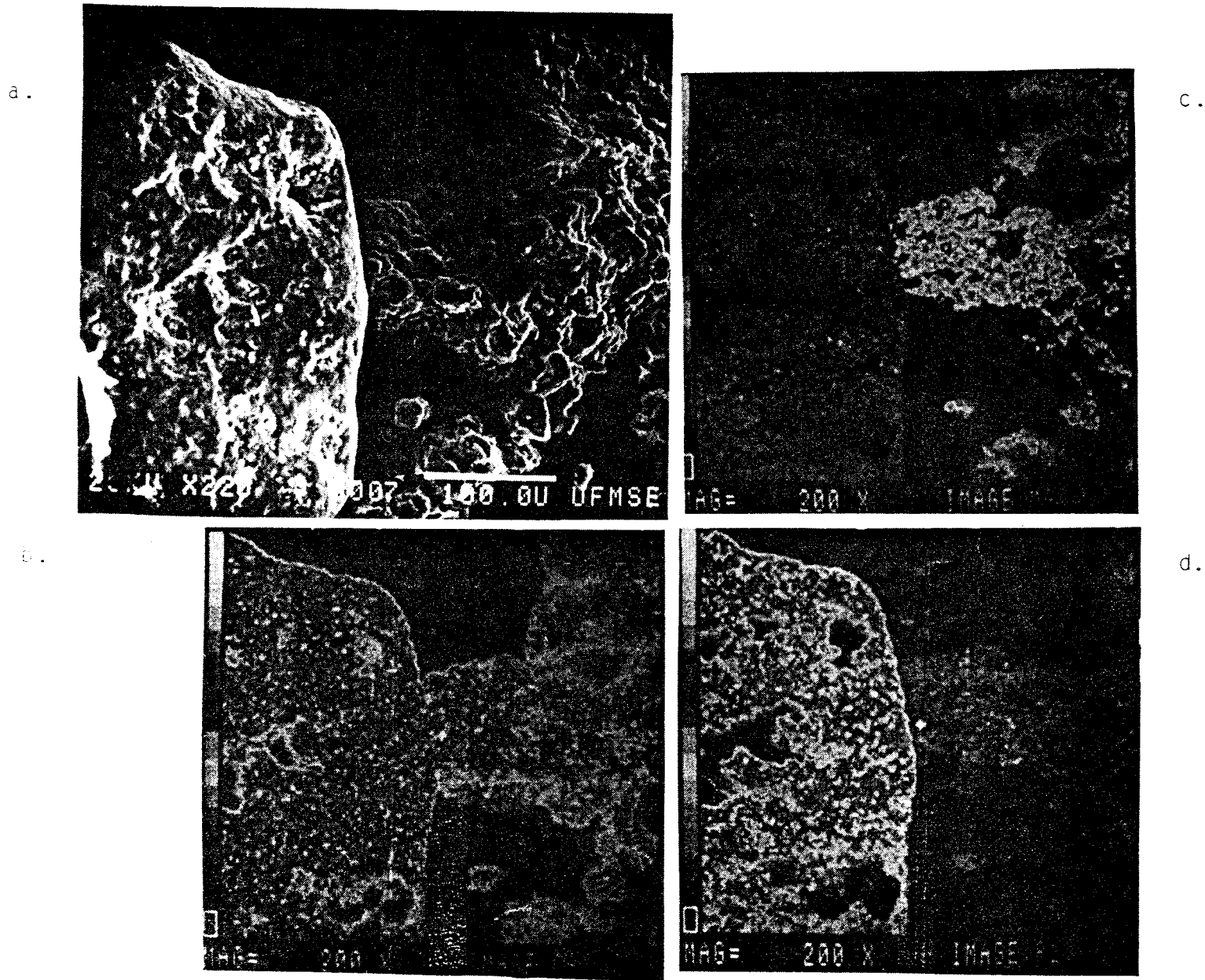


Figure 19. Apatite (left) and dolomite (right) particles from Agrico dolomite feed (65 x 150 mesh). (a) Backscattered electron image. (b) Calcium distribution map. (c) Magnesium distribution map. (d) Phosphorous distribution map.

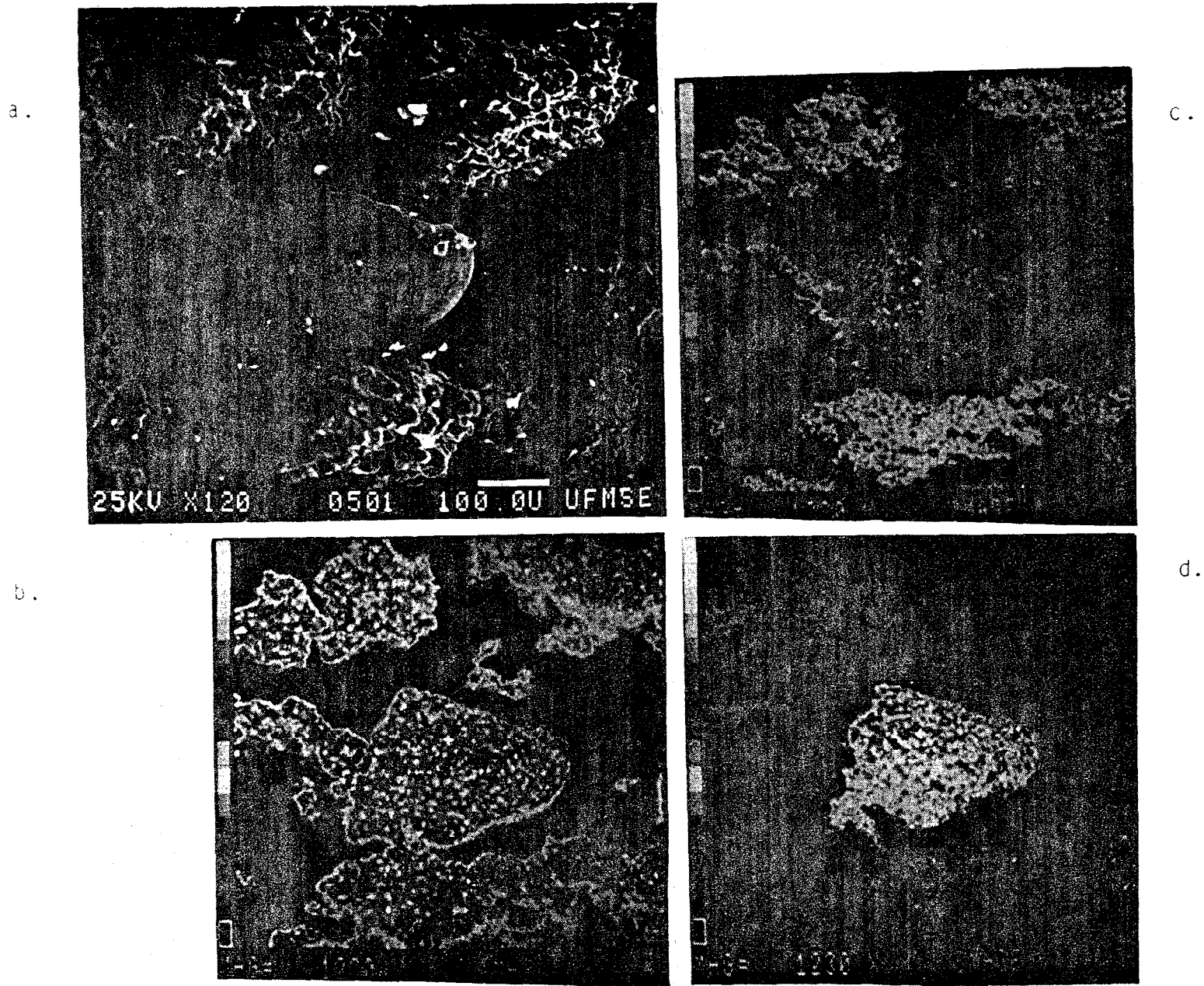


Figure 20. Agrico dolomite, 65 x 150 mesh float fraction (apatite particle is in center). (a) Backscattered electron image. (b) Calcium distribution map. (c) Magnesium distribution map. (d) Phosphorous distribution map.

the other hand, the granular particle showed high Mg concentration, as expected, with very little P present.

Images of particles from the float fraction and sink fraction after two stage conditioning are presented in Figures 20 and 21, respectively. It is clear that more particles in the sink fraction contain a significant amount of P than in the float fraction. Also, it appears from the Mg mapping of the float fraction that the apatite particle in the center does contain some Mg on its surface.

Anax Apatite and New Jersey Dolomite Mixture

The two stage conditioning process was very successful when tried on a mixture of the Anax apatite and New Jersey dolomite. The MgO content of the feed material, using M28 as the collector, was reduced from 1.5% MgO to 1.1% MgO in the sink fraction with a recovery of 99% of the P₂O₅ (see Table 10). Similarly when a sulfonated fatty acid (OA-5) was used as collector the flotation concentrate assayed 1.0% MgO at a P₂O₅ recovery of about 92% (see Table 11).

Agrico Apatite and IMC Four Corners Dolomite Mixture

A few flotation tests were performed with a mixture of Agrico apatite and IMC Four Corners dolomite. As shown in Table 12, the MgO content of the mixture was reduced from 1.85% to about 1%. The recovery of P₂O₅ in the sink fraction was in the range 67-74%.

No attempts to optimize the two stage conditioning process with this or the previous mixtures of minerals were made. Instead, a limited optimization of the process and a study of the effect of different flotation parameters

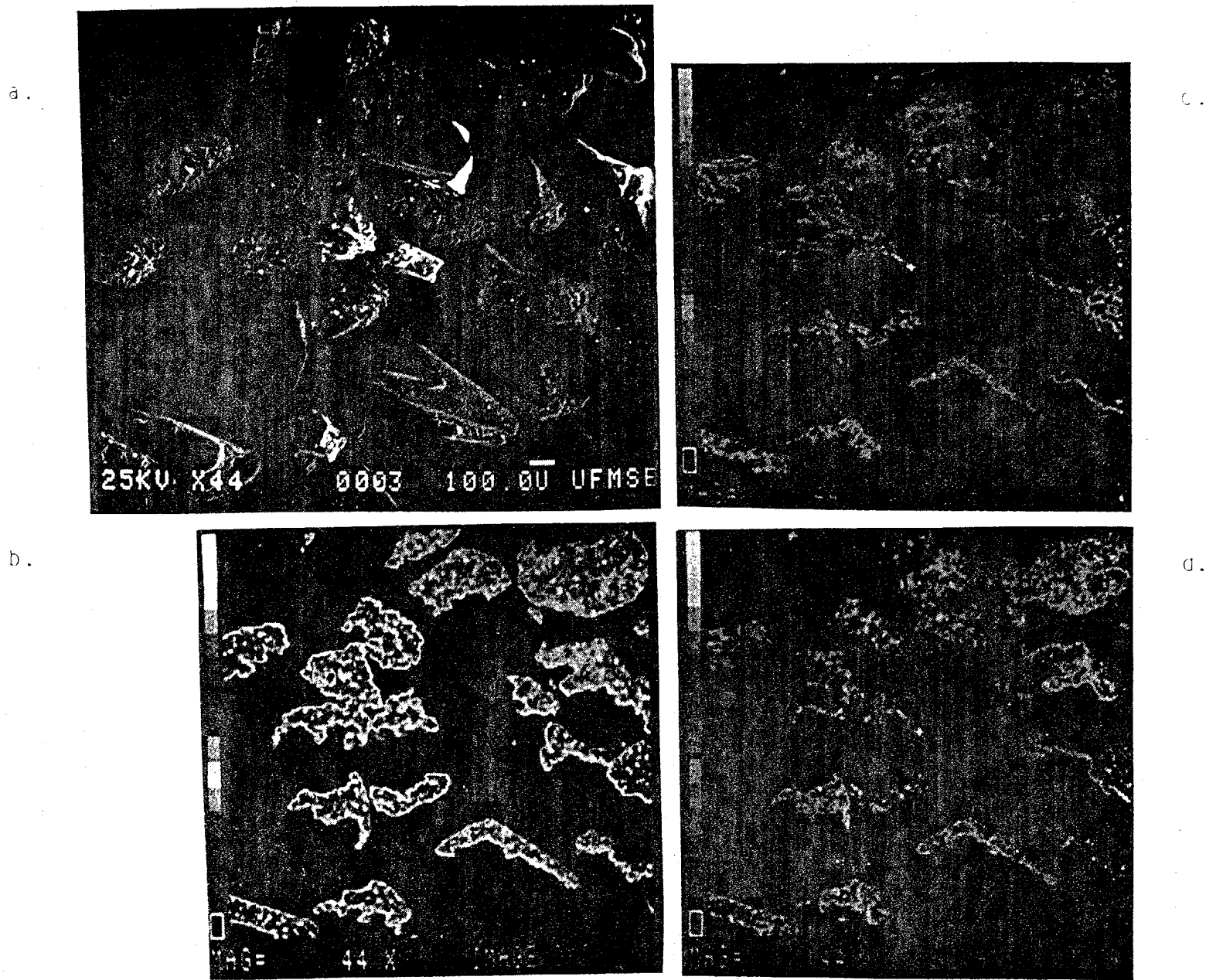


Figure 21. Agrico dolomite, 65 x 150 mesh sink fraction. (a) Backscattered electron image. (b) Calcium distribution map. (c) Magnesium distribution map. (d) Phosphorous distribution map.

Table 10

Flotation of 95:5 Apatite and Dolomite Mixture
after Two-Stage Conditioning

Feed: Apatite (Amine Concentrate Amx)
Dolomite (New Jersey crystalline)
Collector: M 28, 2.0 lb/t
Extender: IMC Fuel oil, 4.0 lb/t
Conditioning: 2 min at pH 10.0
Reconditioning: 5 min at pH 4.0

	BPL %	MgO, %	BPL Recovery, %
Feed	66.0	1.5	100.0
Concentrate (Sink Fraction)	67.0, 67.0	1.1, 1.1	99.2, 99.3

Table 11

**Flotation of 95:5 Apatite and Dolomite Mixture after
Two-Stage Conditioning Using OA-5 as the Collector**

Feed: Apatite (Amine Concentrate Amx)
Dolomite (New Jersey crystalline)
Collector: M28, 2.0 lb/t
Extender: IMC Fuel oil, 4.0 lb/t
Conditioning: 2 min at pH 10.0
Reconditioning: 5 min at pH 4.0

	BPL %	MgO, %	BPL Recovery, %
Feed	65.0	1.5	100.0
Concentrate (Sink Fraction)	67.2	1.0, 1.0	92.0, 92.8

Table 12

**Flotation of a Synthetic Mixture of Agrico Apatite and
IMC Four-Corners Dolomite After Two Stage Conditioning**

Feed: Apatite apatite
 IMC Four-Corners dolomite
Collector: M 28, 6.0 lb/t
Extender: IMC fuel oil, 6.0 lb/t
Frother: Aerofroth 73, .12 lb/t
Conditioning: 6 min at pH 10.0
Reconditioning: 5 min at pH 4.0

	BPL %	MgO, %	BPL Recovery, %
Feed	67.19	1.85	100.0
Concentrate (Sink Fraction)	67.84, 67.04	0.85, 1.26	67.16, 74.31

was carried out with a mixture of Agrico apatite and Perry dolomite. This sample was chosen because it was better characterized, did not present problems of excessive softness or interlocked apatite particles and it was available in the large amounts required for bench scale study.

Agrico Apatite-Perry Dolomite Mixture

Tests were conducted with an Agrico apatite-Perry dolomite mixture to establish the influence of parameters such as pulp density, particle size, pH, and collector concentration as they were varied from the values prevalent during Hallimond tube testing up to values similar to those prevalent in the industrial practice of phosphate flotation.

Effect of pulp density: The influence of increasing the pulp density during two stage conditioning and flotation from 0.8% solids (equivalent to Hallimond tube tests) up to 32% solids (which is a pulp density similar to that currently used in most phosphate flotation plants) was studied.

As shown in Tables 13, 14, and 15 increasing the pulp density during conditioning and flotation had a very minor effect on the efficiency of the two stage conditioning process. Excellent recoveries and grades were obtained even at 32% solids. Recoveries in excess of 95% with a MgO grade below 1.0% were obtained with relatively high pulp densities. It is necessary to point out, however, that during the flotation test at high pulp densities, pH control was difficult and also a larger amount of acid was required to maintain pH within the prescribed limit.

Table 13

Effect of Pulp Density on Flotation of 80:20 Agrico Apatite
and Perry Dolomite 65 x 100 mesh

Feed: Agrico Apatite, 65 x 100 mesh
Perry Dolomite, 65 x 100 mesh
Collector: Sodium Oleate
Frother: Aerofroth 65
Reconditioning pH: 2.6-4.3

Collector conc., mg/l	Frother mg/l	Pulp Density %	BPL, %	MgO, %	BPL Recovery, %
--	90	--	59.69	4.0	--
410	90	4.0	71.27	0.9	99.0
370	90	8.0	70.79	1.0	100.0
274	90	8.0	73.26	0.6	97.8
410	90	0.8	73.20	0.6	95.3

Table 14

Effect of Pulp Density on Flotation of 80:20 Agrico Apatite
and Perry Dolomite 35 x 65 mesh

Feed: 35 x 65 mesh, 4.0% MgO, 59.7% BPL
 Collector: Sodium Oleate
 Frother: Aerofroth 65, 90 mg/l
 Reconditioning: By Tumbling at pH 2.3-4.3

Collector conc., mg/l	Pulp Density %	BPL, %	MgO %	BPL Recovery, %
274	0.8	74.71	0.4	97.1
2740	8.0	70.97, 71.32	1.0, 0.9	98.5, 98.9
2740	8.0	70.60	1.2	89.8
4120	16.0	73.61	0.6	94.4
4813	32.0	70.10	1.1	94.0

Table 15

Effect of Pulp Density on Flotation of 80:20 Agrico Apatite
and Perry Dolomite 35 x 150 mesh

Feed: Agrico Apatite, 35 x 150 mesh
 Perry Dolomite, 35 x 150 mesh
 Collector: Sodium Oleate, 410-2740 mg/l
 Frother: Aerofroth 65, 90 mg/l
 Reconditioning pH: 2.3-4.3

Pulp Density %	BPL, %	MgO, %	BPL Recovery, %
--	59.69	4.0	100.0
4.0	70.53, 69.22	1.2, 1.6	96.6, 95.0
4.0	71.93	0.8	96.5
8.0	72.83	0.8	96.5
16.0	71.95	0.8	97.0
16.0	70.77	1.0	98.9

Effect of particle size: Three different particle sizes were studied: 65 x 100 mesh, like the one used in Hallimond cell test, a coarse 35 x 65, and a size distribution 35 x 150 mesh similar to the industrial practice. By comparing Table 13 which shows data for the fine 65 x 100 mesh feed with Table 14 which shows data for 35 x 65 and Table 15 which shows data for 35 x 150 mesh fractions, it is observed that the particle size had very little, if any, effect on the recoveries and selectivity obtained by the two stage conditioning process. With all these size fractions, recoveries approaching 100% P_2O_5 were obtained while the MgO content of the concentrate was below 1.0% MgO. This would be an important advantage of the two stage conditioning process because other flotation schemes have been reported not to be efficient in floating dolomite particles larger than about 48 mesh. Probably the large amount of collector that dolomite can adsorb during the alkaline conditioning remains on the dolomite sample during the final conditioning and explains the good recoveries of this mineral. Flotation schemes that rely upon acidic flotation alone are unable to float large dolomite particles because under acidic conditions not enough collector is adsorbed on dolomite and therefore large particles cannot be hydrophobized to the extent required for their flotation.

Effect of collector concentration: As seen in Table 16, apatite did not float even when more than double the concentration of collector needed for dolomite flotation was used. These results indicate that the two stage conditioning is very effective in depressing the apatite.

Table 16

Effect of Collector Concentration on Flotation of 80:20
Agrico Apatite and Perry Dolomite

Feed: 65 x 100 mesh, 4.0% MgO,
59.7% BPL
Collector: Sodium Oleate
Frother: Aerofroth 65, 90 mg/l
Reconditioning pH: 2.6-4.3 by tumbling
Pulp Density: 0.8%

Collector Conc., mg/l	BPL, %	MgO, % est.	BPL Recovery, %
--	59.69	4.0	100.00
109	70.95	1.0	90.7
205	83.07, 69.20	0.6, 1.8	92.6, 87.7
205	72.83, 73.74	0.5, 0.4	93.1
274	73.24	0.6	95.3

Effect of reconditioning pH: Flotation results presented in Tables 17 and 18 indicate that pH during reconditioning has an extraordinary influence on the selectivity of dolomite flotation. The role of reconditioning pH has to be more thoroughly investigated. As can be seen in Table 17 and 18, for this particular mixture the best results were obtained when the reconditioning pH is maintained at 3.5-3.6. However, other minerals or ores can have a different optimum pH, and this has to be determined experimentally in each case.

Natural Agrico Feed

In the previous section, synthetic mixtures of apatite and dolomite were used to establish the influence of the various parameters such as pulp density, particle size, pH, and collector concentration on the separation of dolomite from apatite using two stage conditioning. As it was learned that reconditioning pH and collector concentration are the major parameters contributing to the effectiveness of the method, it was decided to test natural ores, varying these parameters. As can be seen from results presented in Tables 19, 20, 21, and 22, the % MgO of the feed was reduced from 1.7% to less than 0.7% in all cases, with P₂O₅ recoveries of more than 85% at Sodium oleate concentrations from 2.4 to 3.0 lb/t.

Natural Brewster Feed

From Table 23, it can be seen that the % MgO was reduced from 2.0% to 1.2%, with P₂O₅ recoveries of >85.0% using sodium oleate concentration's of 4.8 lb/t total.

Table 17

Flotation of 80:20 Agrico Apatite and Perry Dolomite
After Two Stage Conditioning

Feed: 35 x 150 mesh, BPL = 55.69%
MgO = 4.0%
Collector: Sodium Oleate
Frother: Aerofroth 65, 1.0 lb/t
Pulp Density: 16.0%

Reconditioning, pH	BPL, %	MgO, %	BPL Recovery, %
3.2	64.1	3.0	94.0
3.4	73.4	0.6	100.0
3.5	69.5	1.5	99.0

Table 18

Flotation of 80:20 Agrico Apatite and Perry Dolomite
After Two Stage Conditioning by Agitation

Feed: 35 x 150 mesh, BPL = 59.69%, MgO = 4.0%
 Collector: Sodium Oleate, 7.1 lb/t
 Frother: Aerofroth 65, 2.0 lb/t
 Pulp Density: 8.0%

Reconditioning pH	BPL, %	MgO, %	BPL Recovery, %
3.2	64.0	3.0	94.0
3.5	74.2	0.4	100.0
3.7	44.3	7.8	48.0

Table 19

Flotation of Natural Agrico Feed
After Two Stage Conditioning

Feed: 48 x 150 mesh Agrico Feed
 Collector: Sodium Oleate, 3.0 lb/t
 (1.2 lb/t float #1, 1.8 lb/t float #2)
 Frother: Aerofroth 65, 1.0 lb/t
 Pulp Density: 6.0%
 Reconditioning pH = 3.6

	BPL, %	MgO, %	BPL Recovery, %
Feed	28.84	1.70	100.00
Concentrate	66.05	0.68	84.10
Dolomitic Float	43.93	--	--

Table 20

Flotation of Natural Agrico Feed
After Two Stage Conditioning

Feed: 48 x 150 mesh Agrico Feed
 Collector: Sodium Oleate, 2.4 lb/t
 (1.2 lb/t float #1, 1.2 lb/t float #2)
 Frother: Aerofroth 65, 1.0 lb/t
 Pulp Density: 16.0%
 Reconditioning pH = 3.6

	BPL, %	MgO, %	BPL Recovery, %
Feed	28.84	1.70	100.00
Concentrate	66.93	0.57	95.60
Dolomitic Float	20.30	--	--

Table 21

Flotation of Natural Agrico Feed
After Two Stage Conditioning

Feed: 35 x 150 mesh Agrico Feed
 Collector: Sodium Oleate, 2.7 lb/t
 (1.2 lb/t float #1, 1.5 lb/t float #2)
 Frother: Aerofroth 65, 2.0 lb/t
 Pulp Density: 8.0%
 Reconditioning pH = 3.4

	BPL, %	MgO, %	Insols, %	BPL Recovery, %
Feed	26.96	1.70	60.05	--
Concentrate	68.78	0.30	5.68	86.60
Dolomitic Float	54.63	--	2.51	--
Quartz Sink	0.92	--	97.71	--

Table 22

Flotation of Natural Agrico Feed
After Two Stage Conditioning

Feed: 35 x 150 mesh Agrico Feed
 Collector: Sodium Oleate, 2.7 lb/t
 (1.2 lb/t float #1, 1.5 lb/t float #2)
 Frother: Aerofroth 65, 2.0 lb/t
 Pulp Density: 8.0%
 Reconditioning pH = 3.6

	BPL, %	MgO, %	Insols, %	BPL Recovery, %
Feed	26.96	1.70	60.05	100.00
Concentrate	68.17	0.35	6.45	87.70
Dolomitic Float	57.23	--	2.40	--
Quartz Sink	0.98	--	97.46	--

Table 23

Flotation of Natural Brewster Feed
After Two Stage Conditioning

Feed: 35 x 150 mesh Brewster Feed
 Collector: Sodium Oleate, 4.8 lb/t
 (1.8 lb/t float #1, 3.0 lb/t float #2)
 Frother: Aerofroth 65, 2.0 lb/t
 Pulp Density: 8.0%
 Reconditioning pH = 3.3

	BPL, %	MgO, %	Insols, %	BPL Recovery, %
Feed	21.98	2.00	62.97	100.00
Concentrate	57.23 61.53	1.20 1.00	16.12 10.89	90.10 85.80
Dolomitic Float	30.70 32.23	-- --	6.49 6.53	-- --
Quartz Sink	0.59 3.26	-- --	97.13 94.76	-- --

SUMMARY

A new technique involving two-stage conditioning prior to flotation has been developed. This involves conditioning the feed at pH 10 followed by reconditioning at a lower pH before flotation. Selective flotation of dolomite from apatite was observed both for single and mixed minerals by reconditioning at pH 4. To understand the mechanisms of observed selective flotation, further studies involving oleate adsorption, infrared spectroscopy, and solubility of the minerals were conducted. Selective flotation of dolomite by reconditioning at pH 4 is attributed to the combined effect of higher oleate adsorption on dolomite and hydrolysis of the adsorbed oleate molecules to oleic acid at lower pH values.

The method has been tested at bench scale level with several dolomite-apatite mixtures and several natural high magnesium phosphate samples from the Florida phosphate field.

Samples containing 1.8-4.0% MgO were upgraded to below 1% MgO with recoveries of about 90% P₂O₅.

Reconditioning pH was determined to be the most important process parameter in this new method.

Chapter VIII
SELECTIVE FLOCCULATION

INTRODUCTION

It has been observed that some of the ores obtained from South Florida are not completely liberated in the particle size range 35 x 150 mesh. The extent of interlocking between apatite and dolomite varies in samples obtained from different sources, ranging from 1.0% interlocked grains in sample K-5 to 82.5% interlocked grains in sample K-2 (see Table 26, Chapter III). Thus, the removal of pure dolomite grains alone from the ore would not always be sufficient to lower the MgO content to below 1.0%. In such cases it would be necessary to grind the ores to finer sizes to achieve liberation of the interlocked minerals before physical separation of apatite and dolomite can be attempted. However, flotation may not be efficient in fine particle size range's and an alternative method such as selective flocculation might prove to be more effective in achieving the desired separation.

Selective flocculation involves the aggregation of one of the components of the mixture of minerals in suspension in water with the aid of a polymer. The polymeric molecules adsorb on two or more particles and bind them together. The aggregates so formed are termed flocs and are separated from the unflocculated fines to achieve the desired separation. Polymer properties such as molecular weight, conformation in water, nature of charges and the chemical moieties that make it up are important variables affecting flocculation. It is possible to achieve selective flocculation either by manipulating the surface characteristics of the particles, or the nature of the polymer. A number of studies have been carried out to separate gangue

from value minerals by selective flocculation. (1-5) An attempt was made to develop a suitable selective flocculation scheme for separating apatite and dolomite.

EXPERIMENTAL

Materials

Minerals

Apatite used in this study was obtained from Agrico Chemical Company, Florida. Dolomite was received from International Minerals and Chemical Corporation, Florida. The minerals were ground in a high purity alumina mill after being dried at 110°C and dry sieved to obtain the -400 mesh fraction.

The size distribution of the particles measured with an X-ray sedigraph revealed the mean size of apatite to be 12 μm . The surface area and pore size distribution of the samples was determined with a Quantachrome Autosorb-6 unit. Both apatite and dolomite are highly porous, about 98% of the surface area being contributed by the pores.

X-ray diffraction analysis of the apatite indicated that quartz was the only impurity present. Visual observations through a microscope revealed that the entire sample consists of apatite with a few crystals of quartz, confirming the X-ray data. On the other hand, X-ray scans of the dolomite sample revealed minor amounts of quartz and apatite. Microscopic studies show that a large percentage of the dolomite is composed of individual dolomite rhombs. Apatite detected in the sample by X-ray is very small in amount; some of the apatite has a trace of dolomite interlocked with it while the rest consists of pure apatite particles.

Chemical analysis of the samples revealed apatite to be made up of 34.6% P_2O_5 , 0.2% MgO , and 2.3% insolubles, and dolomite to contain 0.7% P_2O_5 , 19.4% MgO and 4.8% insolubles.

Polymers

Poly(ethylene oxide), a partially hydrophobic polymer, was used in this study. The molecular weight of the polymer was quoted as 5 million by the manufacturer (PolySciences, Inc.).

Methods

Flocculation

Since flocculation is sensitive to the nature of agitation, a standard mixing assembly was used in the flocculation experiments. A 150 ml beaker fitted with removable plexiglass baffles served as the mixing tank. A stainless steel turbine impeller with six blades, mounted on a variable speed motor, was used to agitate the sample.

The mineral suspension of the required pulp density (usually 2.0 to 5.0 wt %) was made up with a sodium silicate solution (5.0 kg/t of solids) as dispersant and aged for 1 hour. After aging, it was conditioned for 4 minutes to stabilize the pH at 9.50 and sonicated to ensure complete dispersion of the mineral particles. The suspension was further agitated for 30 seconds to keep the solids in suspension and a predetermined amount of the polymer was added. The agitation was continued for 2 additional minutes followed by separation of the flocs from the suspension. The various fractions were dried at 110°C overnight, weighed, and analyzed.

Separation of Floccs

Two methods were used for separating the floccs and fines in this investigation. A sedimentation column with an ID of 4.5 cm and length of 73.0 cm was used to settle the floccs. After allowing 200 seconds for sedimentation, the supernatant above a fixed height was siphoned out. Since this method of separation is sensitive to the size, it can be used for monitoring floc properties as a function of the given variable.

The other method of separation utilized a 400 mesh screen submerged in a water bath. The flocculated mixture was poured on the screen and the whole assembly gently rocked for 2 minutes at a fixed frequency. Since the material used in this study is -400 mesh, all the fines passed through the screen while the floccs stayed on it.

Analysis of Floccs and Fines

The floccs and the fines consisting of mixtures of apatite and dolomite were analyzed using the spectrophotometer for the amount of P_2O_5 as noted in Chapter II. The composition of the mixtures was also confirmed by analyzing for Mg^{2+} ion concentration using the ICP method as described earlier in Chapter II.

Polymer Adsorption

PEO adsorption on the minerals was determined by the solution depletion method. The adsorption measurements were conducted under conditions identical to the flocculation tests so that meaningful correlations between the two could be established. PEO concentrations were initially determined by the turbidity method reported by Attia and Rubio (6). But ions leaching out of

the minerals interfered with the polymer analysis resulting in erroneous readings. In order to obtain reliable data, the viscosity method of PEO analysis was utilized. A Ubbelohde viscometer was used to generate a calibration curve and determine the concentration of the given sample.

RESULTS AND DISCUSSION

Single Mineral Flocculation

In selective flocculation, it is necessary to use a polymer that will flocculate only one of the minerals. Experiments conducted with different polymers showed that poly(ethylene oxide) flocculated dolomite but did not flocculate apatite. Further tests were conducted to study the flocculation behavior of the minerals as a function of the polymer dosage. It was observed that apatite was not flocculated at any polymer dosage. On the other hand, dolomite flocculated instantaneously on polymer addition even at very low polymer dosages.

The size of the dolomite flocs grew larger as the amount of polymer added increased. The amount of apatite and dolomite settled in 200 seconds in a sedimentation column after addition of various amounts of polymer is shown in Table 1. These results suggest the possibility of selectively flocculating dolomite from a mixture of apatite and dolomite.

Mixed Mineral Flocculation Studies

Mixed mineral tests were conducted with 80:20 mixtures of apatite and dolomite as a function of polymer dosage. It can be seen from Table 2 that the grade of the apatite is increased from 80.0% to 94.5% by flocculation. In fact, with critical control of experimental parameters, it is possible to

Table 1

Single Mineral Flocculation of Apatite and Dolomite

Minerals: Apatite (Agrico high grade product, Florida)
 Dolomite (International Minerals and Chemical Corporation, Florida)
 Polymer: Poly(ethylene oxide) (PolySciences Inc., Pennsylvania)

Polymer Dosage, kg/t	Amount Settled in 200 sec, wt %	
	Apatite	Dolomite
0.0	6.9	11.2
0.5	6.8	99.7
5.0	5.8	97.9
10.0	6.3	99.9

Table 2

Flocculation of Apatite-Dolomite Mixtures

Feed: 80% Apatite
20% Dolomite
Feed Analysis: 3.88% MgO
Polymer: Poly(ethylene oxide)

Polymer Dosage	Apatite, %	MgO, %	Recovery of Apatite
kg/t			%
0.2	87.7	2.39	24.1
0.4	94.5	1.07	21.6
1.0	92.6	1.44	25.7
2.0	92.9	1.38	43.0

increase the grade of apatite from 60% in the feed to 98% in the product (MgO decreased from about 7.76% to 0.39%) after flocculation. However, the recoveries obtained in these tests are low.

Reasons for Poor Recoveries

The basic reason for obtaining poor recoveries can be traced to the association of the apatite with dolomite in the flocs. The unflocculated apatite is relatively pure as reflected by the grade of the product. While the process succeeds in removing most of the dolomite by flocculation, it abstracts apatite with the dolomite. Efforts at increasing the recovery of apatite are thus aimed at understanding the reasons for the association of apatite in the dolomite flocs.

Previous studies on selective flocculation have documented causes for such association of the "inert" material in the flocs. They include heterocoagulation, ion activation, entrapment of the inert material in the flocs, and entrainment of fines between the flocs.

Charges of similar nature on both apatite and dolomite under the experimental conditions suggest that heterocoagulation is not a major cause for the association of apatite in the dolomite flocs. Experimental evidence shows that although ions leaching out of dolomite have a minor role in activating apatite, ion activation is not a major cause for the presence of apatite in the flocs. Entrapment can occur due to the engulfment of the inert particles in a growing three-dimensional structure of the floc because of the mere presence of the particles in the vicinity of the growing floc. Physical entrapment however, can be minimized by breaking the flocs. No significant reduction of the apatite content of the floc was detected even after breaking

them to smaller sizes, proving that physical entrapment is not a significant factor in the aggregation of apatite along with dolomite. Entrainment of the fines occurs when the flocs that are settling down sweep the unflocculated fines along with them. Experiments conducted with unflocculated apatite and flocculated dolomite revealed no effects of entrainment, eliminating it as a possible cause for the poor recoveries obtained in the mixed mineral flocculation experiments.

It is observed that although apatite is not flocculated with PEO, it adsorbs the polymer. Adsorption data is presented in Table 3. It can be seen that dolomite adsorbs more than four times the amount of polymer adsorbed by apatite. It is proposed that the adsorption of PEO by apatite is the main reason for its association with dolomite in the flocs. Experiments with mixtures of other minerals and dolomite show a correlation between the amount of polymer adsorbed by the minerals and the extent of their presence in the dolomite flocs.

Future work needs to concentrate on efforts to prevent adsorption of PEO on apatite which would result in higher recoveries of apatite while maintaining the excellent grades observed. Modification of the surface chemistry of apatite and the solution chemistry of the polymers are promising methods to achieve this objective. It is also possible to investigate additional polymers with special chelating groups which would permit specific adsorption on only one of the minerals.

SUMMARY

Although exhaustive data about the nature and extent of interlocking of apatite and dolomite grains in the South Florida deposit is not available,

Table 3

Saturation Adsorption of PEO on Apatite and Dolomite

Minerals: Apatite (Agrico high grade product, Florida)
 Dolomite (International Minerals and Chemical Corporation, Florida)
 Polymer: Poly(ethylene oxide) (PolySciences Inc., Pennsylvania)

Minerals	Amount Adsorbed, mg/g
Apatite	0.46
Dolomite	2.04

preliminary studies suggest that certain ores would need to be ground to fine sizes for complete liberation. Selective flocculation is a promising technique for separating the minerals existing in such fine sizes.

Preliminary results using PEO as a flocculant are very encouraging in reducing the MgO levels below 1.0%, although recoveries are low. Further experiments show that adsorption of PEO on apatite needs to be reduced or eliminated to achieve higher recoveries.

REFERENCES

Chapter I. Introduction

1. Lawver, J. E., Raulerson, J. D. and Cook, C. C., 1980, "New Techniques in Beneficiation of Phosphate Rock," Trans. SME-AIME, Vol. 268, pp. 1787-1801.
2. Dufour, P. et al., 1980, "Beneficiation of South Florida Rock with High Carbonate Content," Proceedings, 2nd Int. Congr. on Phosphorous Compounds, Boston, April, pp. 247-267.
3. Minmet Recherche, 1980, French Patent No. 80-08707, April 10.
4. Baumann, A. N. and Snow, R. E., 1980, "Processing Techniques for Separating MgO Impurities from Phosphate Products," Proceedings, 2nd Int. Congr. Phosphorous Compounds, Boston, April, pp. 269-280.
5. Cox, C. H., Lang, W. H. and Snell, H., 1980, "Beneficiation of Unaltered Western Phosphate Ore," Trans. SME-AIME, Vol. 268, pp. 1780-1783.
6. Wiegel, R. L. and Hwang, C. L., 1984, "A Predictive Model for Heavy Media Cyclone Separation of Phosphate Pebble from Dolomite," SME-AIME Annual Meeting, Los Angeles, CA, Feb.-March, SME Preprint #84-648, 8 pages.
7. Llewellyn, T. D. et al. 1982, "Beneficiation of High Magnesium Phosphate from Southern Florida," U.S. Bureau of Mines RI 8609.
8. Snow, R. F., 1979, "Beneficiation of Phosphate Ores," U.S. Patent 4 144 969, March 20.
9. Lawver, J. E. et al., 1983, "Method of Beneficiating Phosphate Ores Containing Dolomite," U.S. Patent 4 372 843, Feb. 8.
10. Soto, H. and Iwasaki, I., 1985, "Flotation of Apatite from Calciferous Ores with Primary Amines," Minerals and Metallurgical Processing, Vol. 2, pp. 160-166.
11. Llewellyn T. D. et al. 1984 "Beneficiation of Florida Dolomite-Phosphate Ores," Minerals and Metallurgical Processing, May 1984 pp. 43-48.
12. Lawver, J. E. et al., 1984, "New Techniques in Beneficiation of the Florida Phosphates of the Future," Minerals and Metallurgical Processing, Vol. 1, pp. 89-106.
13. Rule, A. R., and Dallenbach, C. B. 1985, "Beneficiation of Complex Phosphate Ores Containing Carbonate and Silica Gangue," Proceedings, XVth IMPC, Vol. 3, pp. 380-389.
14. Rule, A. R., Gruzensky, W. G. and Stickney, W. A., 1970, "Removal of Magnesium Impurities from Phosphate Rock Concentration," U.S. Bureau of Mines, RI 7362.

15. Hsieh, S. S. and Lehr, J. R., 1985a, "Beneficiation of Dolomitic Idaho Phosphate Rock by the TVA Diphosphoric Acid Depressant Process," Minerals and Metallurgical Processing, Vol. 2, pp. 10-13.
16. Hsieh, S. S. and Lehr, J. R., 1985b, "Development of Differential Desorption-Reflotation Process for Beneficiation of North Carolina Coleitic Phosphate Pebble," Ind. Eng. Chem Proc. Design Dev. Oct. 1985, pp. 937-941.
17. Fu, E. and Somsundaran, P., "Alizarin Red S as a Flotation Modifying Agent in Calcite-Apatite Systems," Accepted for publication in International J. of Mineral Processing.
18. Johnston, D. J. and Leja, J., 1978, "Flotation Behavior of Calcium Phosphates and Carbonates in Orthophosphate Solution," IMM Transactions, Vol. 87, December, pp. C237-242.
19. Rule, A. R., Gruzensky, W G. and Stickney, W A., 1970, "Removal of Magnesium Impurities from Phosphate Rock Concentration," U.S. Bureau of Mines, RI 7362.
20. Mudgil, B. M and Chanchani, R., 1985, "Selective Flotation of Dolomite from Francolite Using Two-Stage Conditioning Process," Minerals and Metallurgical Processing, Vol. 2, pp. 19-25.
21. Mudgil, B. M and Chanchani, R., 1985, "Beneficiation of Complex Phosphate Ores from South Florida by Two Stage Conditioning Process," Proceedings, XVth IMPC, Vol. 3, pp. 357-366.
22. Blanchard, F. N., Goddard, R. E., and Saffer, B., "Application of Quantitative X-ray Diffraction Combined with Other Analytical Methods to the Study of High Magnesium Phosphorites," in press, Advances in X-ray Technology.
23. Mudgil, B. M and Somsundaran, P., "Advances in Phosphate Flotation," Proc., Arbitr Symposium on Advances in Mineral Processing, AIME Annual Meeting, March 1986, New Orleans, LA, to be submitted for publication.

Chapter III. Mineralogical Studies

1. Riggs, S., 1979, "Petrology of the Tertiary Phosphorite System of Florida," Econ. Geol., 74, pp. 195-220.
2. Riggs, S., 1979, "Phosphorite Sedimentation in Florida-A Model Phosphogenic System" Econ. Geol., 74, pp. 285-314.
3. McConnell, D., 1938, "A Structural Investigation of the Isomorphism of the Apatite Group," Amer. Min., 23, pp. 1-19.
4. Smith, J. P. and J. Lehr, 1966, "An X-ray Investigation of Carbonate Apatites," J. Agr. Food Chem, 14, pp. 342-349.

5. Rooney, T.P. and P.F. Kerr, 1967, "Mineralogic Nature and Origin of Phosphorite, Beaufort County, North Carolina," Geol. Soc. Amer. Bull., 78, pp. 731-748.
6. McClellan, G.H. and J.R. Lehr, 1969, "Crystal Chemical Investigation of Natural Apatites," Amer. Min., 54, pp. 1374-1391.
7. Marlowe, J.I., 1971, "Dolomite, Phosphorite, and Carbonate Diagenesis on a Caribbean Seamount," J. Sed. Pet., 41, pp. 809-827.
8. Burnett, W.C., 1977, "Geochemistry and Origin of Phosphorite Deposits of Peru and Chile," Geol. Soc. Amer. Bull., 88, pp. 813-823.
9. Berge, J.W. and J. Jack, 1982, "The Phosphorites of West Thaniyat Turayf, Saudi Arabia," Econ. Geol., 77, pp. 1912-1922.
10. Alexander, L. and H.P. Klug, 1948, "Basic Aspects of X-ray Absorption," Anal. Chem., 20, pp. 886-889.
11. Blanchard, F.N., 1980, "A Computer Program for Calculation of Calibration Curves for Quantitative X-ray Diffraction Analysis," J. Geol. Educ., 28, pp. 135-137.
12. Bromberger, S. H., and J. B. Hayes, 1966, "Quantitative Determination of Calcite-Dolomite-Apatite Mixtures by X-ray Diffraction," Journal of Sedimentary Petrology, Volume 36, pp. 358-361.
13. Goldsmith, J. R. et al., and H. C. Heard, 1961, "Subsolidus Phase Relations in CaCO_3 - MgCO_3 ," Journal of Geology, Volume 69, pp. 45-74.
14. McClellan, G.H. 1980, "Mineralogy of Carbonate Fluorapatites," J. Geol. Soc. London, 137, pp. 675-681.
15. McClellan, G.H. and Van Kauwenbergh, 1985, private communication.
16. Van Kauwenbergh, 1985, International Fertilizer Development Center, private communication.
17. Sudarsanan, K., P. E. Mackie, and R. A. Young, 1972, "Comparison of Synthetic and Mineral Fluorapatite, $\text{Ca}_5(\text{PO}_4)_3\text{F}$, in Crystallographic Detail," Materials Research Bulletin, Volume 7, pp. 1331-1338.
18. Clark, C. M., D. K. Smith, and G. C. Johnson, 1972, "A FORTRAN IV Program for Calculating X-ray Powder Diffraction Patterns: Version r," Pennsylvania State University, University Park.
19. Althoff, P.L., 1977, "Structural Refinements of Dolomite and a Magnesium Calcite and Implications for Dolomite Formation in the Marine Environment," American Mineralogist, Volume 62, pp. 772-783.
20. Annual Report, 1983, "Separation of Dolomite from the South Florida Phosphate Rock," Florida Institute of Phosphate Research, Bartow, Florida, 141 pages.

21. Davis, B. E., T. O. Llewellyn and C. W. Smith, 1984, "Continuous Beneficiation of Dolomitic Phosphate Ores," Bureau of Mines Report of Investigations 8903, U.S. Dept. of the Interior, 14 pages.
22. Lumsden, D. N., 1983, "Determination Dolomite Character and Origin in Deep Sea Sediments," Norelco Report, 30, pp. 1-7.
23. Reeder, R. J. and C. E. Sheppard, 1984, "Variation of Lattice Parameters in Some Sedimentary Dolomites," Amer. Min., 69, pp. 520-527.
24. Randazzo, A. F. and L. G. Zachos, 1983, "Classification and Description of Dolomitic Fabrics of Rocks from the Floridan Aquifer, U. S. A.," Sed. Geol., 37, pp. 151-162.
25. Bradley, W. F., J. F. Burst and D. L. Graf, 1953, "Crystal Chemistry and Differential Thermal Effects of Dolomite," Amer. Min., 38, pp. 207-216.
26. Gavish, E. and G. M. Friedman, 1973, "Quantitative Analysis of Calcite and Mg-Calcite by X-ray Diffraction: Effect of Grinding on Peak Height and Peak Area," Sedimentology, 20, pp. 437-444.
27. Cullity, B. D., 1978, Elements of X-ray Diffraction, Addison-Wesley Publishing Company, Reading, Massachusetts, 555 pages.

Chapter VI.

1. Gregory, G., 1966, "The Determination of Residual Anionic Surface Active Reagents in Mineral Flotation Liquors," Analyst, Vol. 31, pp. 257-259.
2. Peck, A. S. et al., 1966, "An Infrared Study of the Flotation of Hematite with Oleic Acid and Sodium Oleate," Trans. AIME/SME, Sept., pp. 301-307.

Chapter VIII. Flotation in Salt Solutions

1. Soto, H. and Iwasaki, I., 1985, "Flotation of Apatite From Calcerous Ores with Primary Amines" Minerals and Metallurgical Processing, August, p. 160.
2. Ananthapadmanabhan, K. P., 1979, "Associative Intersections in Surfactant Solutions and Their Role in Flotation" Eng. Sc. D., Dissertation, Columbia University.
3. Chanchani, R., 1984, "Selective Flotation of Dolomite From Apatite Using Sodium Oleate as the Collector" Ph.D. Thesis, University of Florida.
4. Snow, R. E., 1979, "Beneficiation of Phosphate Ore" U.S. Patent 4, 144, 969.
5. Somasundaran, P. and Wang, Y. H. C., 1984, "Surface Chemical Characteristics and Adsorption Properties of Apatite" Adsorption on and Surface Chemistry of Hydroxyapatite, Edited by D. M. Misra, Plenum Press.

6. Maslow, A. D., 1971, "Flotation of Apatite in the Presence of Sodium Chloride" *Vop, Teor. Prakt. Obogashch. Rud*, pp. 159-164 (Russ).
7. Strelitsyn, G. S. et al., 1967, "Lowering the Harmful Effect of Sodium Chloride on the Flotation of Apatite-Nepheline Ore" *Obogashch. Rud* 12(3), pp. 13-14, (Russ).
8. Iwasaki, I. and Krishnan, S. V., 1983, "Heterocoagulation Versus Surface Precipitation in Quartz-Mg(OH)₂ System" SME-AIME Annual Meeting, Atlanta, Georgia, March 6-10, Preprint.
9. Zoltai, T. and Stout, J. H., 1984, "Mineralogy Concepts and Principles," Burgess Publishing Company, Minnesota, pp. 449.

Chapter IX. Selective Flocculation

1. Attia, Y. A., and Kitchener, J. A., 1975, "Development of Complexing Polymers for the Selective Flocculation of Copper Minerals," Proceedings, 11th International Mineral Processing Congress, Cagliari, pp. 123-48.
2. Read, A. D., 1971, "Selective Flocculation Separations Involving Hematite," Trans., Institution of Mining and Metallurgy (London), Vol. 80, pp. C24-C31.
3. Rubio, J., and Goldfarb, J., 1975, "Separation of Chrysocolla From Quartz by Selective Flocculation with Polyacrylamide-type Flocculants," Trans., Institute of Mining and Metallurgy (London), Vol. C84, pp. C123-C127.
4. Sadowski, Z., and Laskowski, J., 1980, "Selective Coagulation and Selective Flocculation of the Quartz-Carbonate Mineral (Calcite, Magnesite Dolomite) Binary Suspensions," Fine Particle Processing, ed. Somsundaran, P., AIME, New York, NY, Vol. 2, pp. 1083-1103.
5. Slaczka, A. S. and Paprotny, J., 1985, "Flocculation of Smithsonite and Dolomite Using Polymers Containing Nitrogen Atoms," International Journal of Mineral Processing, Vol. 14, pp. 319-325.
6. Attia, Y. A. and Rubio J., 1975, "Determination of Very Few Concentrations of Polyacrylamide and Polyethylene Oxide Flocculants by Nephelometry," British Polymer Journal, Vol. 7, pp. 135-138.